

THE SOUND PROPAGATION  
CONDITIONS IN THE BLACK SEA

---

YAVUZ ERGENGIL

LIBRARY  
NAVAL POSTGRADUATE SCHOOL  
MONTEREY, CALIF. 93940









# United States Naval Postgraduate School



LIBRARY  
NAVAL POSTGRADUATE SCHOOL  
MONTEREY, CALIF. 93940

## THESIS

THE SOUND PROPAGATION CONDITIONS  
IN THE BLACK SEA

by

Yavuz Ergengil

Thesis Advisor:

W. E. Denner

September 1971

*This document has been approved for public re-  
lease and sale; its distribution is unlimited.*





The Sound Propagation Conditions  
in the Black Sea

by

Yavuz Ergengil  
Lieutenant, Turkish Navy  
B.S., United States Naval Postgraduate School, 1970

Submitted in partial fulfillment of the  
requirements for the degree of

MASTER OF SCIENCE IN OCEANOGRAPHY

from the  
NAVAL POSTGRADUATE SCHOOL  
September 1971



## ABSTRACT

The sound propagation conditions in the central part of the Black Sea were investigated. Profiles of temperature and salinity were generated by averaging data from the U.S. National Oceanographic Data Center over monthly periods. Wilson's equation was used to compute sound velocities and a digital computer program provided plots of sound velocity versus depth and selected ray trace diagrams.

Seasonal temperature, salinity and sound velocity variations are found only in the upper layer of the Black Sea. Below 125 m, seasonal variations are insignificant.

A well defined sound channel exists in the Black Sea that is caused by a cold intermediate layer. Therefore, a seasonal convergence zone is observed during the months of May, November and December.

Finally, bottom reflectivity was calculated by Rayleigh's formula and surface backscattering strength was calculated according to Schulkin and Shaffer.



## TABLE OF CONTENTS

I.	INTRODUCTION -----	9
II.	PHYSICAL GEOGRAPHY OF THE BLACK SEA -----	11
III.	HYDROLOGY OF THE BLACK SEA -----	15
	A. VERTICAL STRUCTURE OF WATER MASSES -----	15
	1. Surface Water -----	15
	2. Cold Intermediate Layer Water -----	16
	3. Mixed Water -----	17
	4. Deep Water -----	18
	5. Bottom Water -----	18
	B. TEMPERATURE DISTRIBUTION -----	25
	C. SALINITY DISTRIBUTION -----	39
IV.	BOTTOM SEDIMENTS -----	54
	A. COASTAL SEDIMENTS -----	54
	1. Pebble Zone -----	54
	2. Boulder Zone -----	54
	3. Gravel Zone -----	55
	4. Sand Zone -----	55
	B. SHALLOW WATER SEDIMENTS -----	56
	C. DEEP WATER SEDIMENTS -----	56
V.	ACOUSTICAL CHARACTERISTICS -----	59
	A. SOUND VELOCITY STRUCTURE -----	59
	B. BOTTOM REFLECTION -----	74
	C. DUCT PROPAGATION -----	82



D. SURFACE BACKSCATTERING	-----	82
E. RAY DIAGRAMS	-----	97
VI. CONCLUSION	-----	109
APPENDIX A: Computation of Sound Velocity	-----	112
APPENDIX B: The Computer Program for Computation of Sound Velocity	-----	114
LIST OF REFERENCES	-----	116
INITIAL DISTRIBUTION LIST	-----	118
FORM DD 1473	-----	119





## LIST OF TABLES

Table		
I.	Area of the Black Sea for Several Depths -----	12
II.	Average Monthly Temperature Distribution in the Central Part of the Black Sea -----	37
III.	Annual Minimum, Maximum and Average Temperature Distribution -----	38
IV.	Average Monthly Salinity Distribution in the Central Part of the Black Sea -----	52
V.	Annual Minimum, Maximum and Average Salinity Distribution -----	53
VI.	Average Monthly Sound Velocity Distribution in the Central Part of the Black Sea -----	72
VII.	Annual Minimum, Maximum and Average Sound Velocity Distribution -----	73
VIII.	Physical Properties of Sea Water and Bottom Sediments in the Black Sea -----	77
IX.	Monthly Reflection Coefficients Distribution in the Central Part of the Black Sea -----	78
X.	Monthly Surface Backscattering Parameters in the Central Part of the Black Sea -----	85
XI.	Monthly Surface Backscattering Strength in the Central Part of the Black Sea for Cutoff Frequencies -----	86
XII.	Monthly Surface Backscattering Strength in the Central Part of the Black Sea for 10 kHz -----	87
XIII.	Monthly Surface Backscattering Strength in the Central Part of the Black Sea for 15 kHz -----	88
XIV.	Monthly Surface Backscattering Strength in the Central Part of the Black Sea for 20 kHz -----	89



## LIST OF FIGURES

### Figure

1.	Black Sea -----	13
2.	Hypsographic Curve of the Black Sea -----	14
3-7.	Temperature - Salinity Diagrams for June, July, August, November and December -----	19-23
8.	Vertical Distribution of Oxygen and Hydrogen Sulfide at Three July Stations in the Black Sea -----	24
9-16.	Average Temperature Profiles for February, March, May, June, July, August, November, and December -----	27-34
17.	Annual Minimum, Maximum and Average Temperature Profiles -----	35
18.	Annual Minimum, Maximum and Average Temperature Profiles for Upper 100 m -----	36
19.	Salinity Distribution of the Sea Surface in the Summer (July, August and September) -----	41
20-27.	Average Salinity Profiles for February, March May, June, July, August, November and December -----	42-49
28.	Annual Minimum, Maximum and Average Salinity Profiles -----	50
29.	Annual Minimum, Maximum and Average Salinity Profiles for Upper 200 m -----	51
30.	Bottom sediment distribution in the Black Sea --	58
31-38.	Average Sound Velocity Profiles for February, March, May, June, July, August, November and December -----	62-69
39.	Annual Minimum, Maximum and Average Sound Velocity Profiles -----	70
40.	Annual Minimum, Maximum and Average Sound Velocity Profiles for Upper 200 m -----	71



41-43.	Reflectivity Versus Incident Angle Diagrams for February, May and October	----- 79-81
44-50.	Surface Backscattering Strength Versus Grazing Angle Diagrams for May, June, July, August, October, November and December	----- 90-96
51-58.	Ray Diagrams in the Central Part of the Black Sea for February, March, May, June, July, August, November and December	----- 101- 108



## ACKNOWLEDGEMENTS

The author wishes to express his appreciation for the guidance and assistance given by Professor Warren W. Denner and LCDR. Charles H. Bassett of the Naval Postgraduate School. Appreciation is also expressed to LT. Margaret A. Frederick, and other personnel of the Naval Fleet Numerical Weather Central for their cooperation during the preparation of this thesis.





## I. INTRODUCTION

The propagation of sound in the sea water of much of the world's ocean area has been studied for many years. However, until recently certain areas, particularly the smaller adjacent seas have received little attention. Increasing naval operational interest in sound propagation in these adjacent seas now demands that the ground work established by oceanographic investigations be built upon to achieve a level of understanding of sonic conditions in these regions.

The propagation of sound in the sea is dependent on several environmental factors, the most important of which are the depth and configuration of the bottom, the physical properties of the bottom material, the sound velocity structure, the distribution and character of sound scatterers and the roughness of the sea surface. The purpose of this thesis is to study sound propagation conditions in the Black Sea using available environmental information.

The temperature and salinity distributions were obtained from the U.S. National Oceanographic Data Center, Washington, D.C. (NODC). NODC has about 1000 hydrocasts from the Black Sea on file collected between 1924 and 1965. In more recent years the data seasonally incomplete and insufficient to obtain yearly oceanographic features of the Black Sea. For this reason, the data collected in 1924 to 1927 surveys was used in this thesis to obtain the sound velocity profiles. The



temperature and salinity profiles were generated by averaging over monthly periods the data from NODC. The corresponding sound velocity profiles were obtained using Wilson's equation [19].

The character of the bottom topography and the bottom sediments are the most important environmental factors which bear on the problem of bottom reflected transmission. Little is known about the bathymetry, the distribution of bottom sediments, and the physical properties of bottom sediments for the Black Sea. However, the available information has been summarized and bottom reflectivity was calculated making several assumptions.

Finally, ray diagrams for several months in the central part of the Black Sea are presented and analyzed in this thesis. These were generated using advanced digital computer ray trace programs from Fleet Numerical Weather Central, Monterey, California (FNWC).



## II. PHYSICAL GEOGRAPHY OF THE BLACK SEA

The Black Sea (Figure 1) is an almost isolated body of water, bounded by U.S.S.R. on the north and east, by Rumania and Bulgaria on the west, and by Turkey on the south and southwest. It is connected with the Mediterranean Sea through the Bosphorus and the Dardanelles, and is about 3000 km from Gibraltar, the nearest point on the Atlantic Ocean.

The Black Sea is a relatively uniform deep marine basin, with long coasts, and few islands. In the north, the Crimean Peninsula extend far into the basin, and the Peninsulas of Kerch and Taman, extending west-east, separate the Sea of Azov, which is connected with the Black Sea only by the narrow Strait of Kerch.

The Black Sea extends between latitudes  $46^{\circ}32'$  and  $40^{\circ}55'$  North, and longitudes  $27^{\circ}27'$  to  $41^{\circ}42'$  East. The greatest length is 1149 km, the width 610 km [1]. The area and volume of the Black Sea were calculated by the Institute of Oceanography of the U.S.S.R. in 1965 from the results of extensive bathymetric surveys of the Black Sea. From this data, the surface area of the Black Sea is  $420,325 \text{ km}^2$ , the volume is  $547,015 \text{ km}^3$ , and the average depth is 1301 m with a maximum depth of 2212 m [2].

The bathymetric areal averages for the Black Sea are summarized in Table I and as a hypsographic curve in Figure 2.



TABLE I  
AREA OF THE BLACK SEA FOR SEVERAL DEPTHS

<u>Depth (m)</u>	<u>Area (km<sup>2</sup>)</u>	<u>Area (%)</u>
0-100	101,452	24.1
100-200	11,400	2.7
200-500	14,610	3.5
500-1000	21,220	5.0
1000-1500	33,480	8.0
1500-2000	86,571	20.6
2000-2200	135,322	32.2
2200	16,270	3.9
TOTAL	420,325	100.0





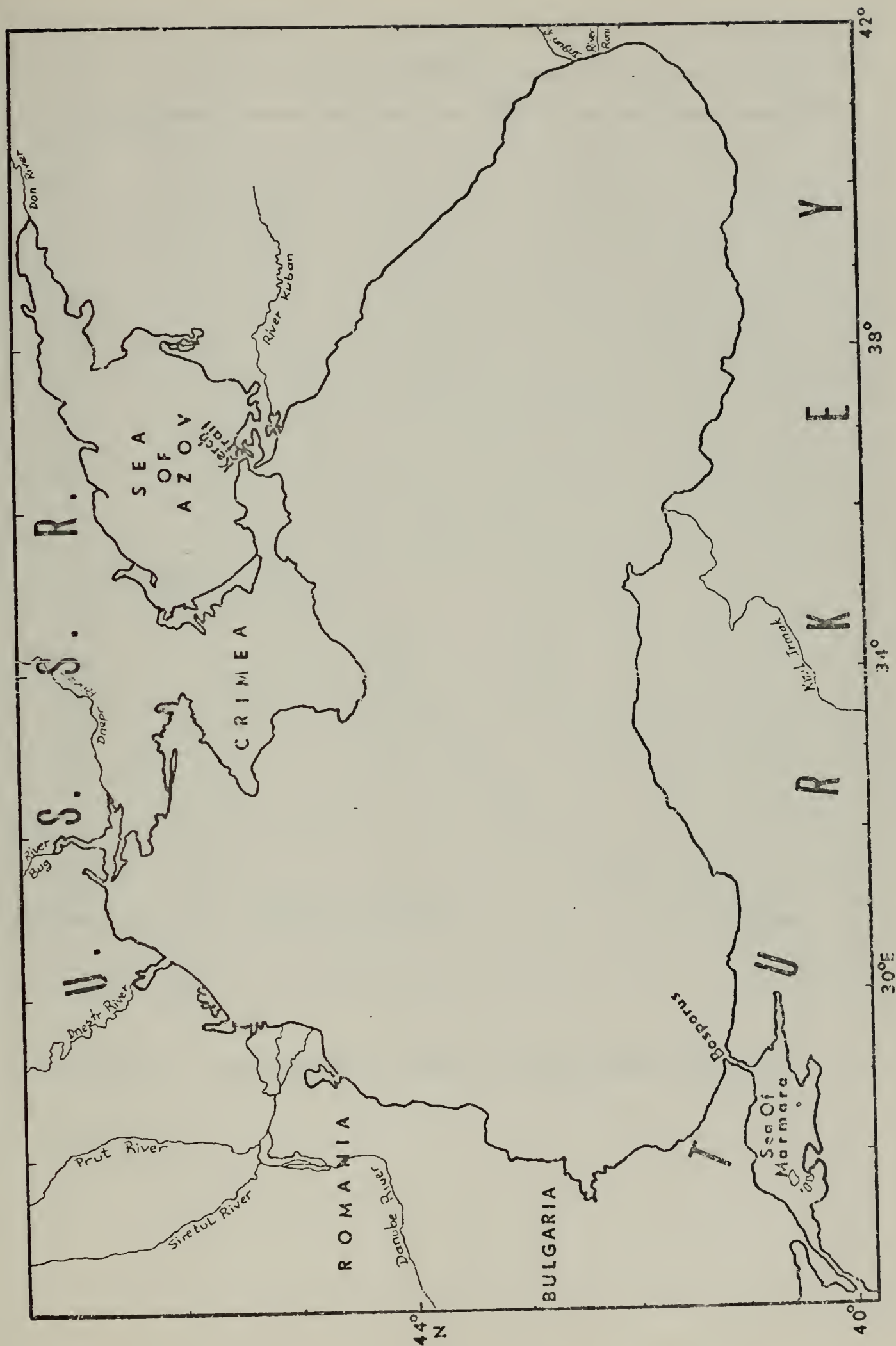


Figure 1. Black Sea.



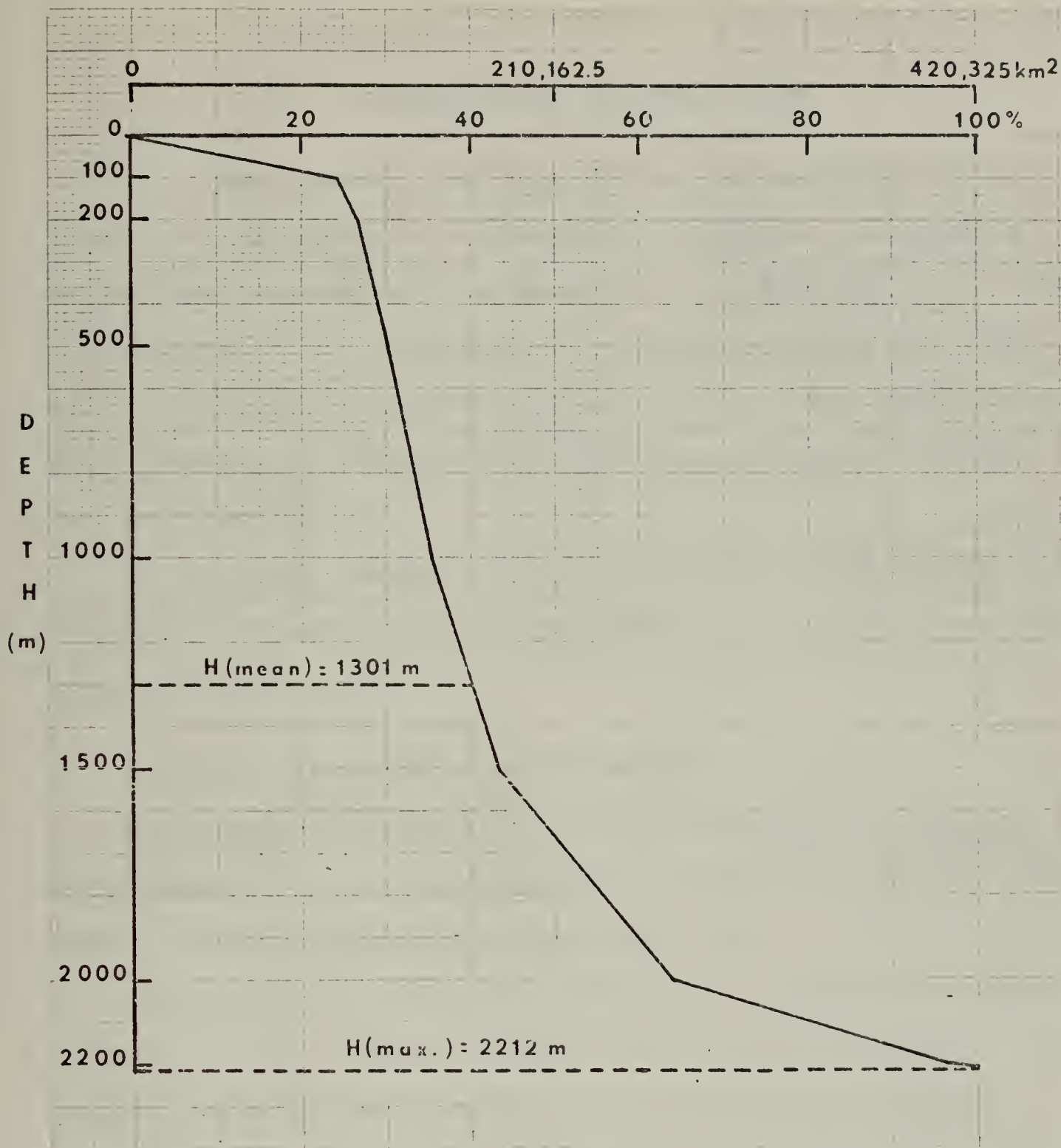


Figure 2. Hypsographic Curve of the Black Sea [2].



### III. HYDROLOGY OF THE BLACK SEA

The first general knowledge of the oceanographic structure of the Black Sea was obtained by Spindler and Wrangel during the first Black Sea Expedition in 1890-1891 [3]. From the results of this expedition, it was recognized that the Black Sea occupied a special place among all the seas of the world because it was devoid of all higher forms of life below about 200 m.

In 1923, the Russians began to explore the Black Sea in detail with measurements of the chemical, biological and physical characteristics.

#### A. VERTICAL STRUCTURE OF WATER MASSES

The temperature-salinity characteristics were analyzed by Novitskiy [4], and he suggested a scheme of vertical structure in the open portion of the Black Sea.

Figures 3, 4, 5, 6, and 7 are typical temperature-salinity diagrams in the central part of the Black Sea for June, July, August, November and December. The temperature-salinity diagrams were generated by averaging over monthly periods the data from NODC. According to Novitskiy scheme, five different water types exist for the open portion of the Black Sea.

The five water types are:

##### 1. Surface Water

The surface water of the Black Sea extends to 25 to 35 m in summer season [4], and penetrates to 15 to 80 m in





the winter months. From February to March this surface layer is almost isothermal and its temperature is lower than that of the cold intermediate layer. In summer, a very strong thermocline exists, with a minimum temperature at 50 m. Salinity increases slowly from the surface to the depth of the temperature minimum.

Along the coast this water type is often covered by a layer of runoff, and near the Kerch Strait and Crimea Coast, it is covered with water from the Sea of Azov.

The mean monthly temperature of the Black Sea surface water varies within a year from 7-8°C in winter to 24-25°C in summer but the mean monthly salinity varies only from 17.70 to 18.50 ‰.

## 2. Cold Intermediate Layer Water

The water of the cold intermediate layer lies under the Black Sea surface water. The lowest summer temperatures of the Black Sea are observed in this layer. Generally, the temperature minimum has a value of 6 to 8°C at depths of 50-75 m. Taking the upper and lower limits in the summer as the 8°C isotherms, its mean thickness is 50-70 m, being thicker along the edge of the sea than in the central regions [5]. During winter, surface temperatures decrease to below the minimum temperature of the intermediate layer and the upper limit defined by the 8°C isotherm is located at 80-90 m in January. The cold intermediate layer reaches its maximum thickness (120-130 m) in March and minimum thickness during





December and January months (around 25 m). The salinity in this layer lies in the range from 18.5 to 20.0 ‰.

According to Kolesnikov [5], the cold intermediate layer in the Black Sea is clearly produced by advection.

Kolesnikov's advection hypothesis for the formation of the cold intermediate layer in the Black Sea is as follows:

"In winter the largest layer of water affected by convection forms in the western half of the sea where there is free penetration of cold air masses from the north and northeast between Crimea and the western shores. The 50-75 m layer of water that forms here is carried to the south by the prevailing current and then to the east along to the Anatolia Coast. As they move eastwards, these waters gradually warm from the surface downwards, and are slightly freshened in the uppermost layer as a result of interaction with coastal waters."<sup>1</sup>

### 3. Mixed Water

Mixed water of the Black Sea is found between the lower limit of cold intermediate layer and 300 or 400 m. Among the dynamic factors that cause the formation of mixed water in the Black Sea, the most significant are the convergence of the surface and deep layers in the coastal belt and internal waves [4]. The mixed water is characterized by presence of both oxygen and hydrogen sulfide (Figure 8). The temperature increases gradually in the mixed layer. And reaches to 8.8°C - 8.9°C at a depth of 300 m. Salinity increase in this layer from 21.10 - 21.50 ‰ in the eastern

---

<sup>1</sup> Filippov, D. M., "The Cold Intermediate Layer in the Black Sea," Oceanology, V. 5, No. 4, p. 47-51, 1965.



Black Sea and from 21.60 - 21.90 ‰ in the western part.

#### 4. Deep Water

The deep water present between the mixed water and bottom water is found at depths of 500-1000 m in the western part of the sea, but is located at depths of 800-1400 m in the eastern part of the sea. Inflow of warm, saline water through the Bosphorus produces a temperature and salinity increase with depth in the deep water. The temperature of the layer ranges from 8.65°C to 8.95°C, the salinity is about 22.2 - 22.3 ‰.

#### 5. Bottom Water

The bottom water fills all the remaining depressions below the depths of 1000 m in the west and 1400 m in the east. The bottom water differs from the overlying layers by virtue of having very small or zero vertical temperature and salinity gradient. At the bottom, the temperature and salinity values range from 8.90 - 9.10°C and 22.39 - 22.41 ‰ over the deep basin of the Black Sea.



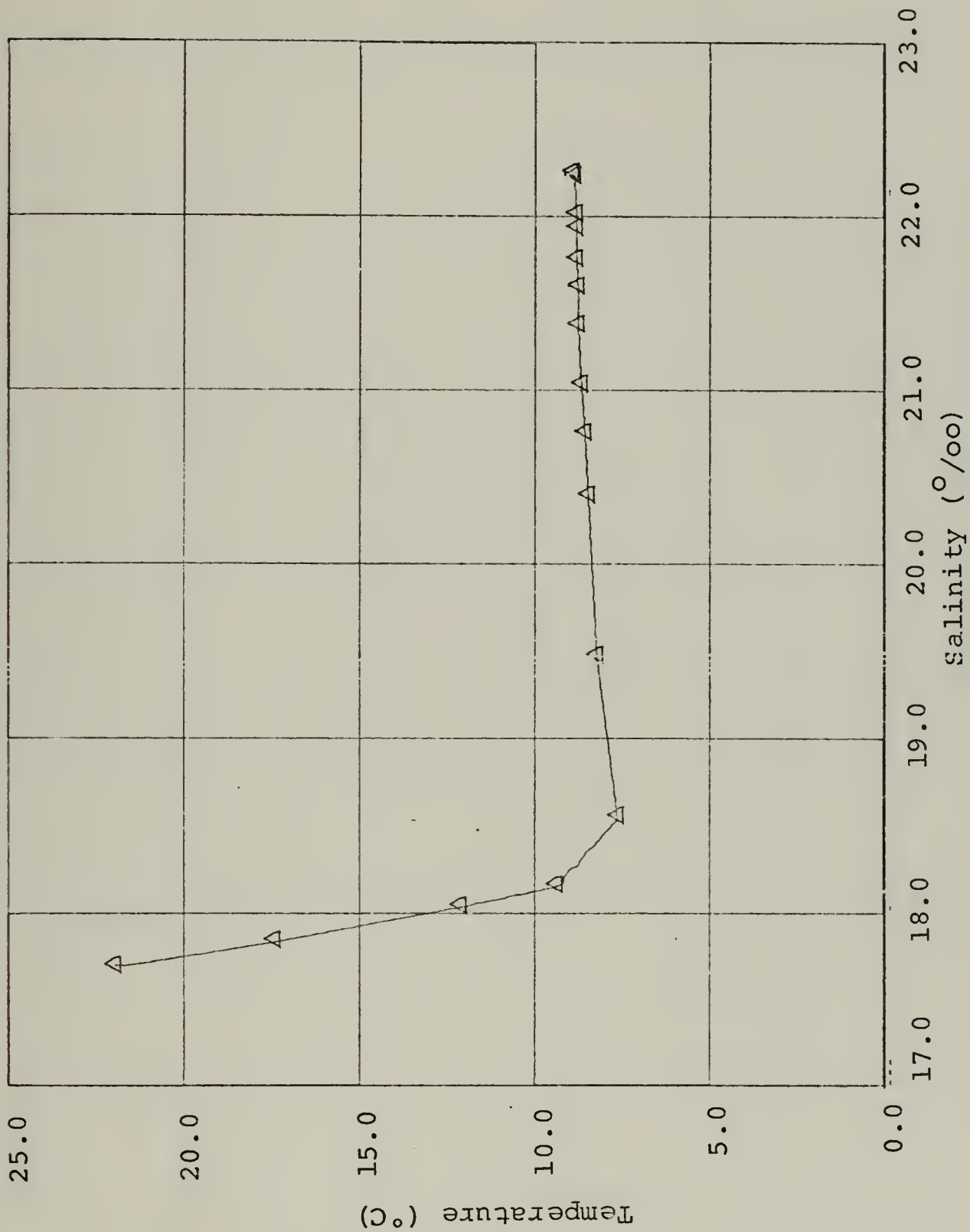


Figure 3. Temperature - Salinity Diagram for June.



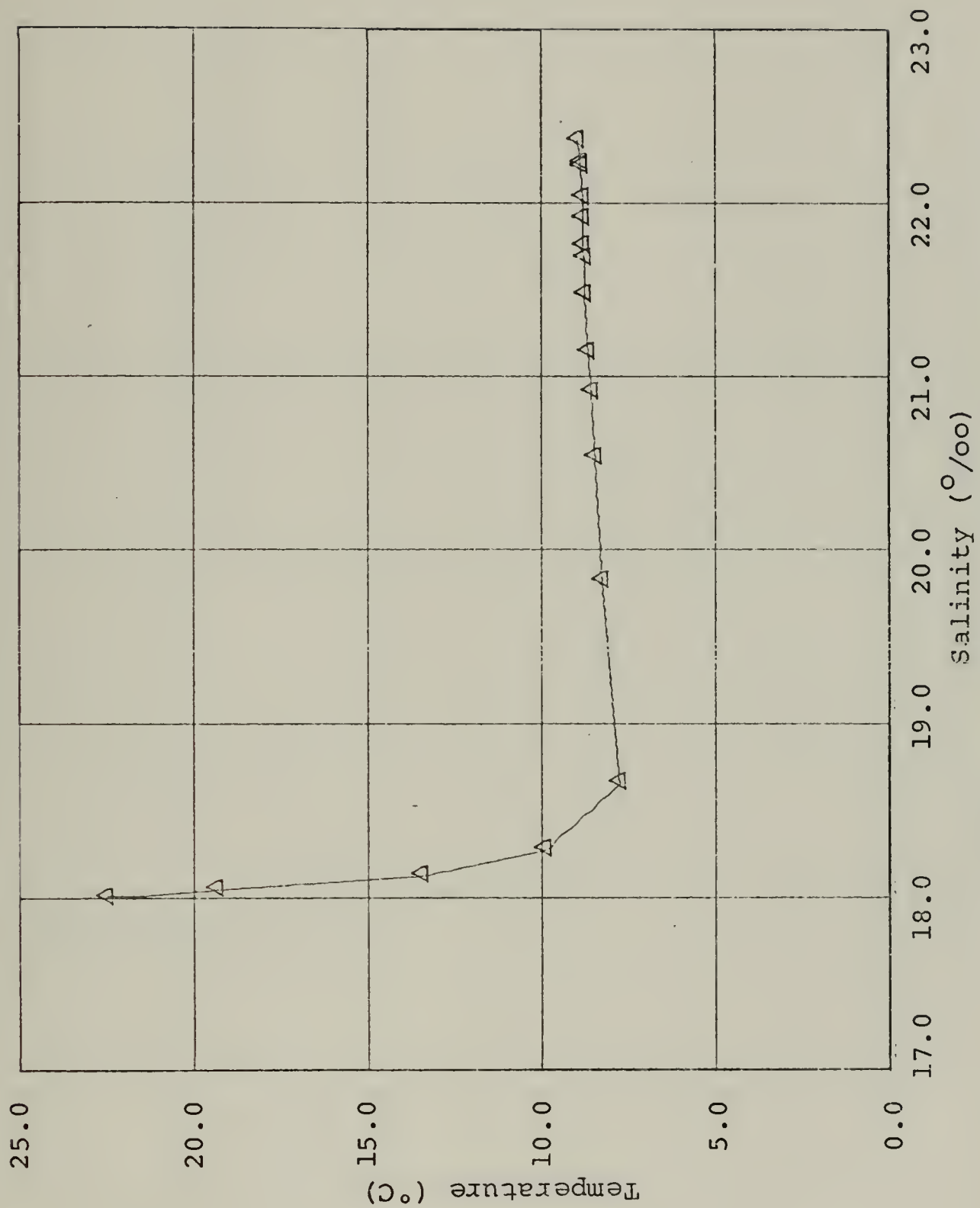


Figure 4. Temperature - Salinity Diagram for July.





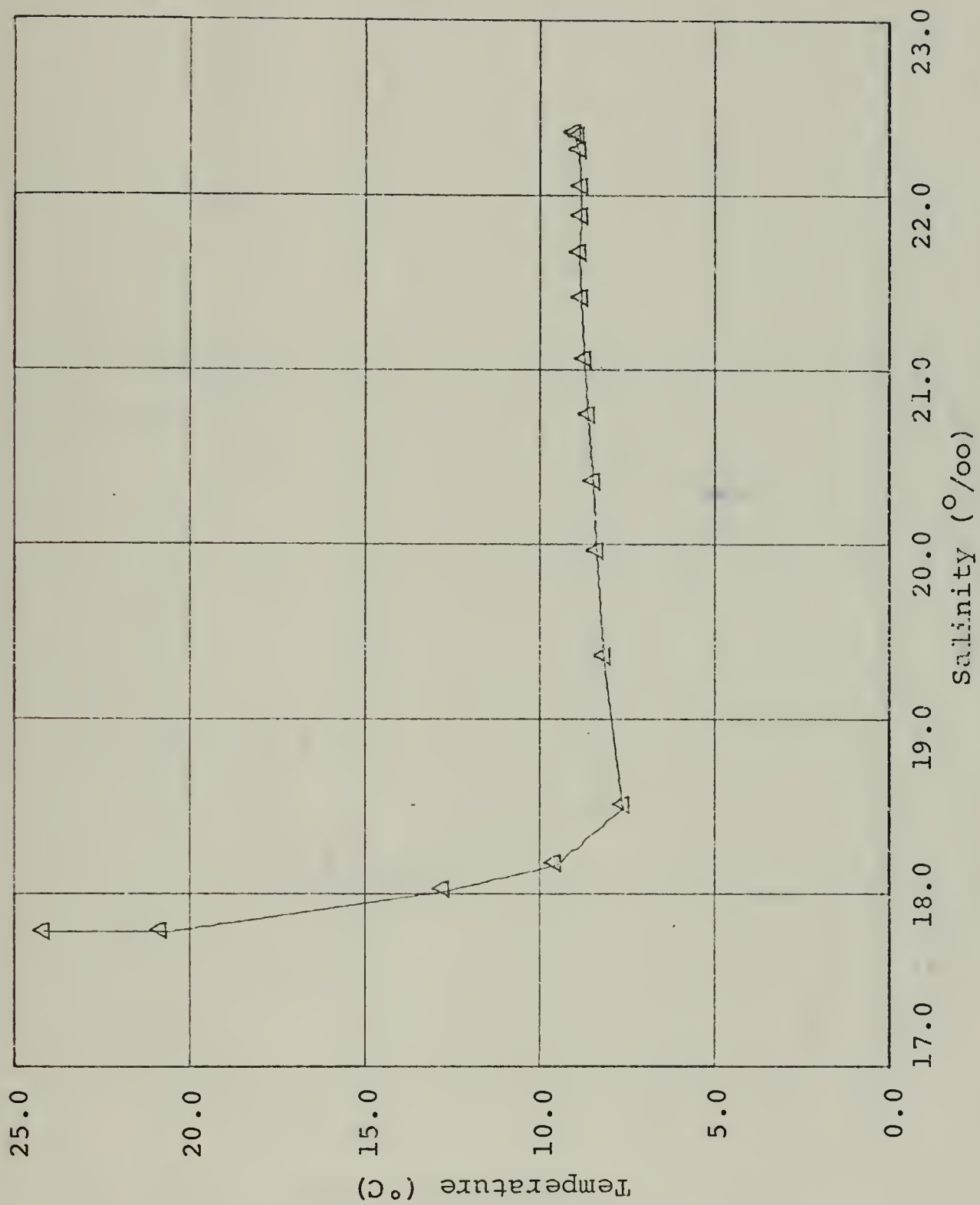


Figure 5. Temperature - Salinity Diagram for August. \*



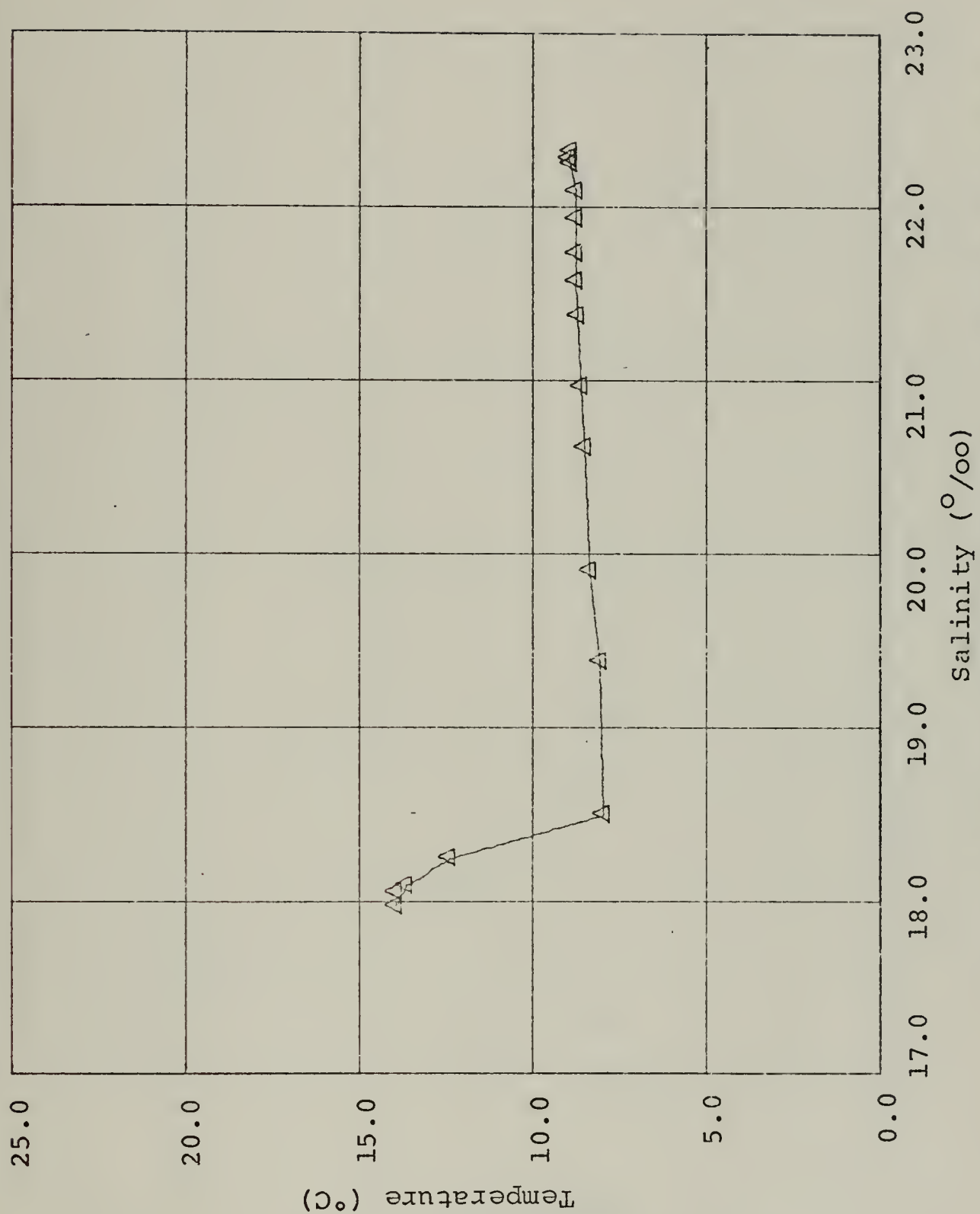


Figure 6. Temperature - Salinity Diagram for November.



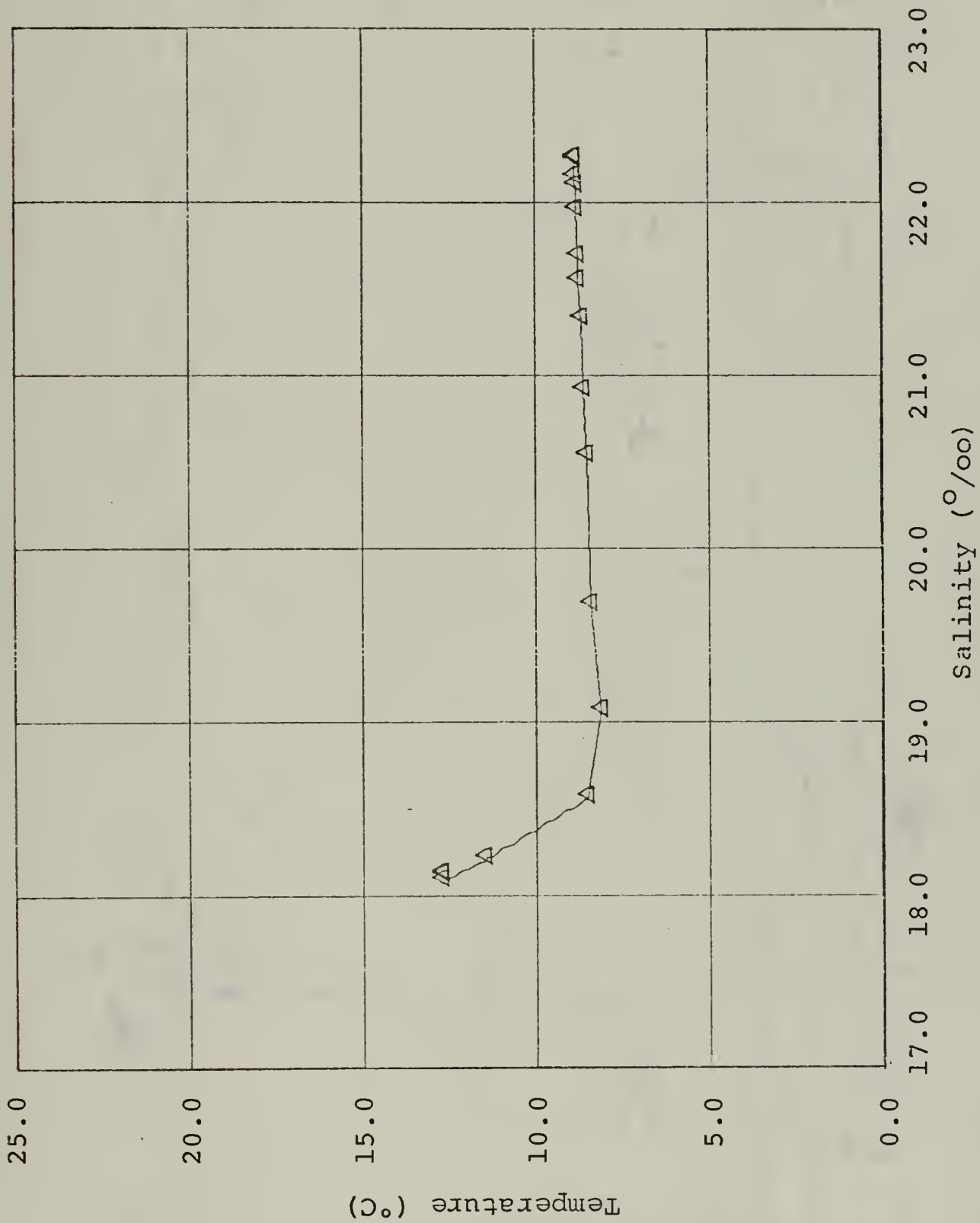


Figure 7. Temperature - Salinity Diagram for December.



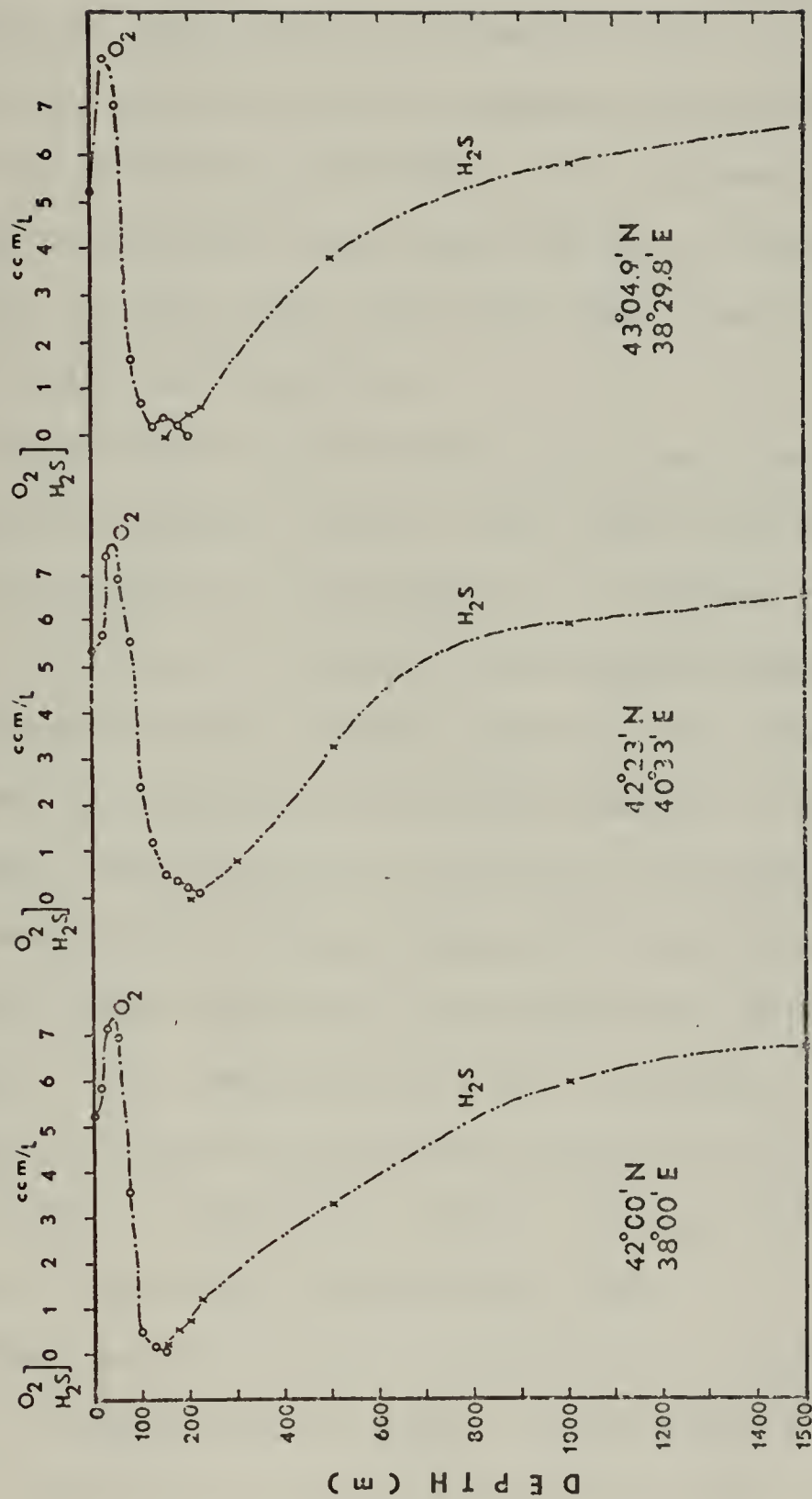


Figure 8. Vertical Distribution of Oxygen and Hydrogen Sulfide at Three July Stations in the Black Sea [Neumann Ref. 7].





## B. TEMPERATURE DISTRIBUTION

The average vertical temperature profiles in the central part of the Black Sea for several months are presented in Figures 9 to 16. These monthly average temperature distributions are summarized for selected depths in Table II, and Table III presents minimum, maximum and average temperatures. Figure 17 gives the profiles of the minimum, maximum and average temperature drawn from the data in Table III. The profiles for the upper 100 m structure are presented with expanded scale in Figure 18.

In the central part of the Black Sea, the average surface temperature changes within a year from  $7.10^{\circ}\text{C}$  in winter to  $24.17^{\circ}\text{C}$  in summer. The minimum and maximum temperatures always occurring in February and August respectively. During the period February through August, the surface temperature increases monotonically, and after August, it decreases.

Under the influence of wind and convective mixing which provides surface cooling during the winter, an isothermal layer is formed with the mixed layer depth occurring at 50 m in February. The temperature of the isothermal layer decreases gradually during the first two months of the year to its minimum ( $7.10^{\circ}\text{C}$ ) in February, which is lower than the temperature minimum of the cold intermediate layer.

After the end of the cooling season, surface heating causes a temperature increase to take place in the surface layer, resulting in the formation of a less dense layer. Consequently, a stable stratification and shallow thermocline is



developed (Figure 11). However, this shallow thermocline can be destroyed within a day either by convective mixing or by wind mixing or both.

During the summer, a well defined thermocline occurs in the central part of the Black Sea (Figures 12, 13, and 14) where the temperature may decrease with depth as much as 14 - 16°C in 50 meters.

At the end of the heating season, the surface water cools from the annual maximum (24.17°C) until it reaches its annual minimum (7.10°C) in February. As the water cools, the surface isothermal layer thickens, from its annual minimum (10  $\pm$  5 m) in August to its maximum (50 m) in February.

Below the minimum temperature zone (50-75 m), the temperature increases gradually with depth, reaching 8.90°C at a depth of 1000 m, and finally about 9.00°C near the Black Sea bottom. According to Vladimirtsev [6], the reason for the increase in water temperature with depth is related to the constant inflow of warm, saline water through the Bosphorus which mixes and sinks to form the bottom water.



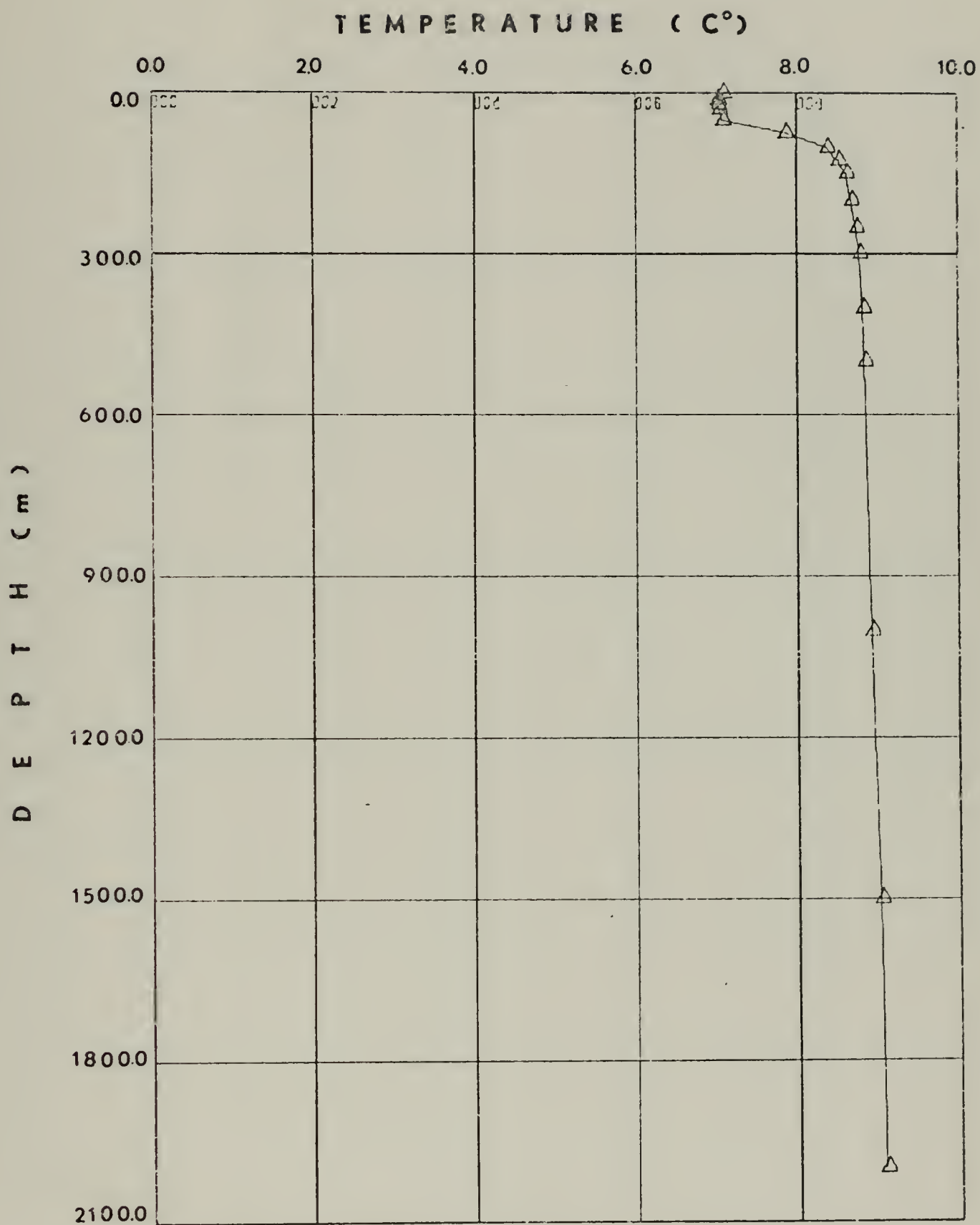


Figure 9. Average Temperature Profile for February.



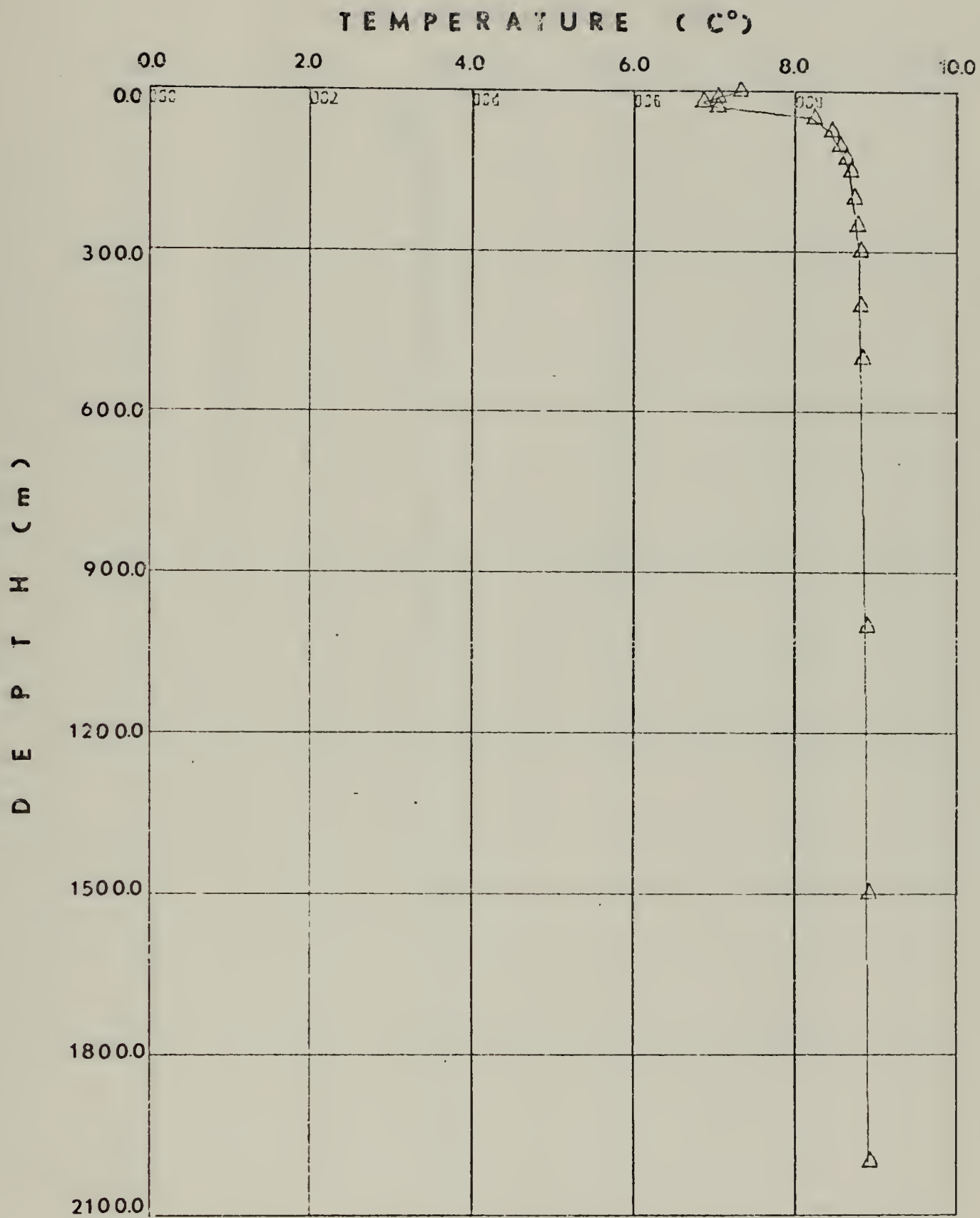


Figure 10. Average Temperature Profile for March





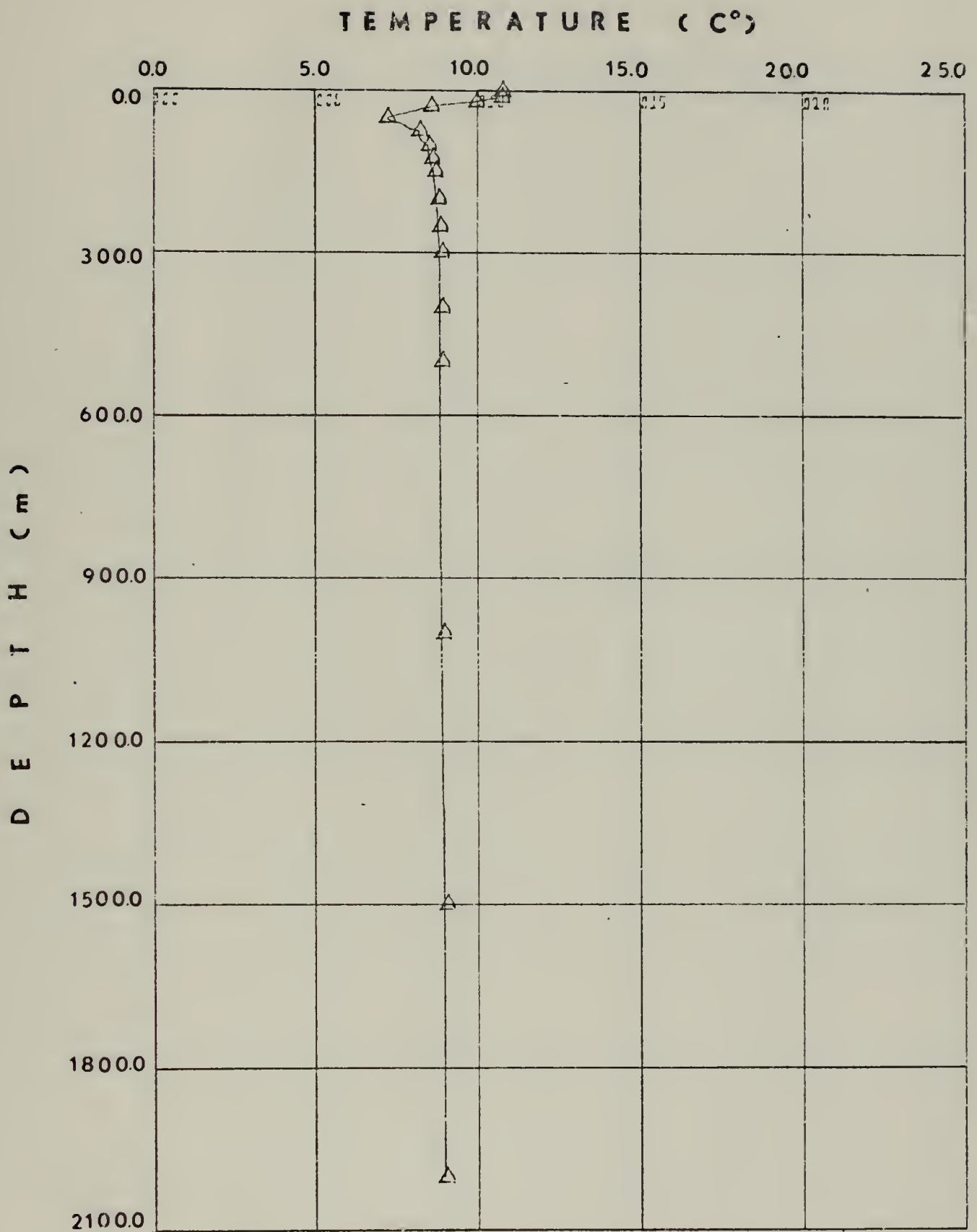


Figure 11. Average Temperature Profile for May.



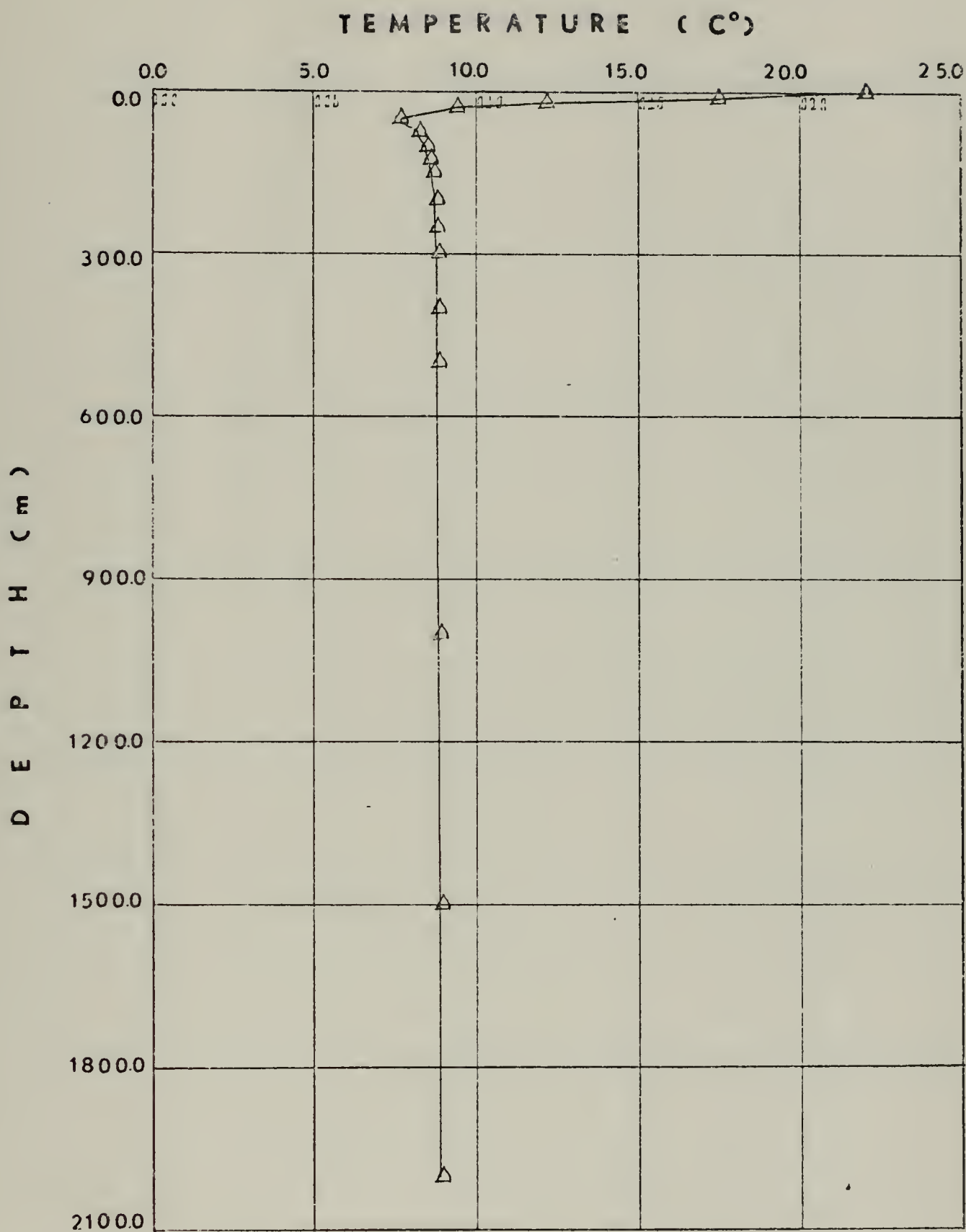


Figure 12. Average Temperature Profile for June.



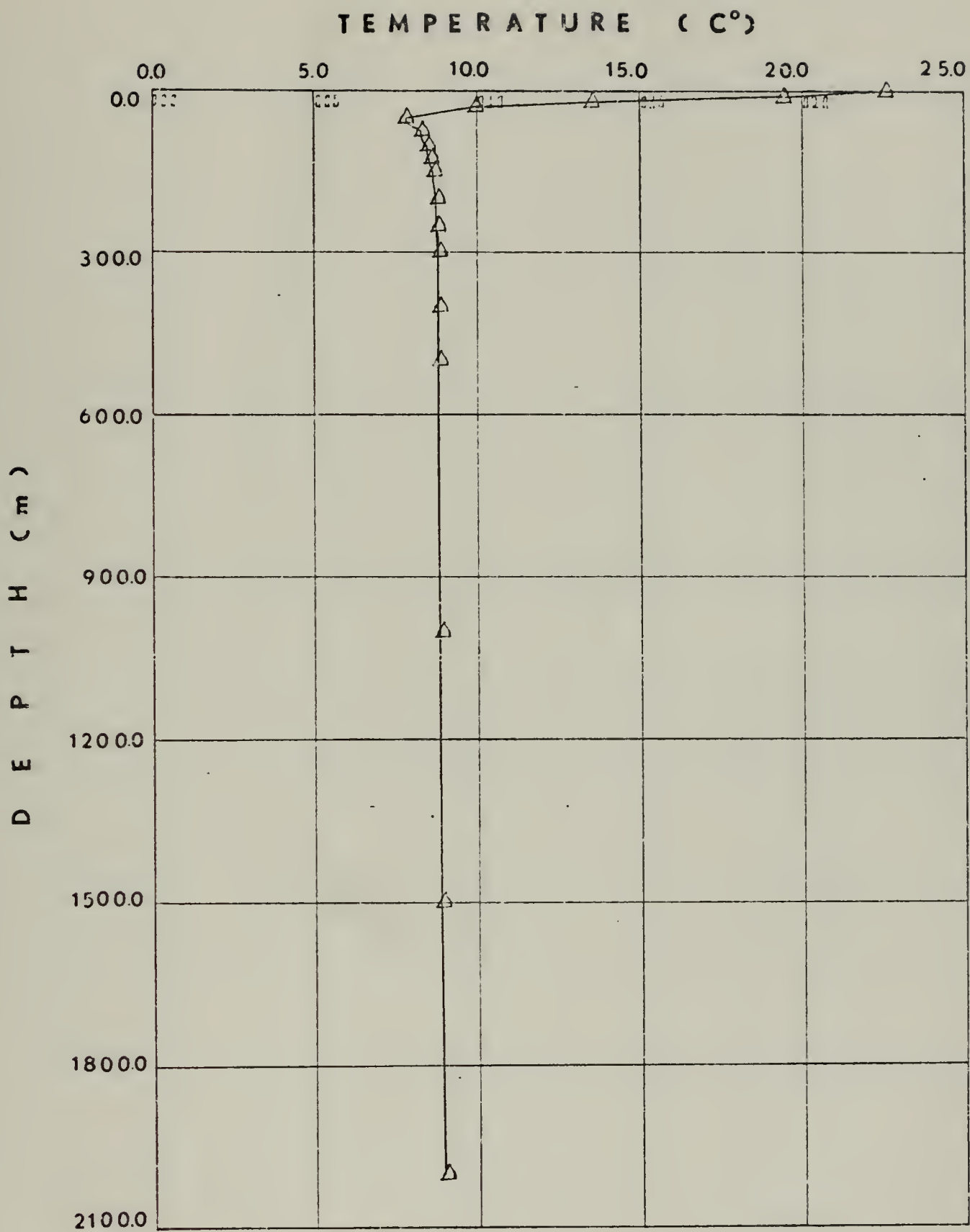


Figure 13. Average Temperature Profile for July.



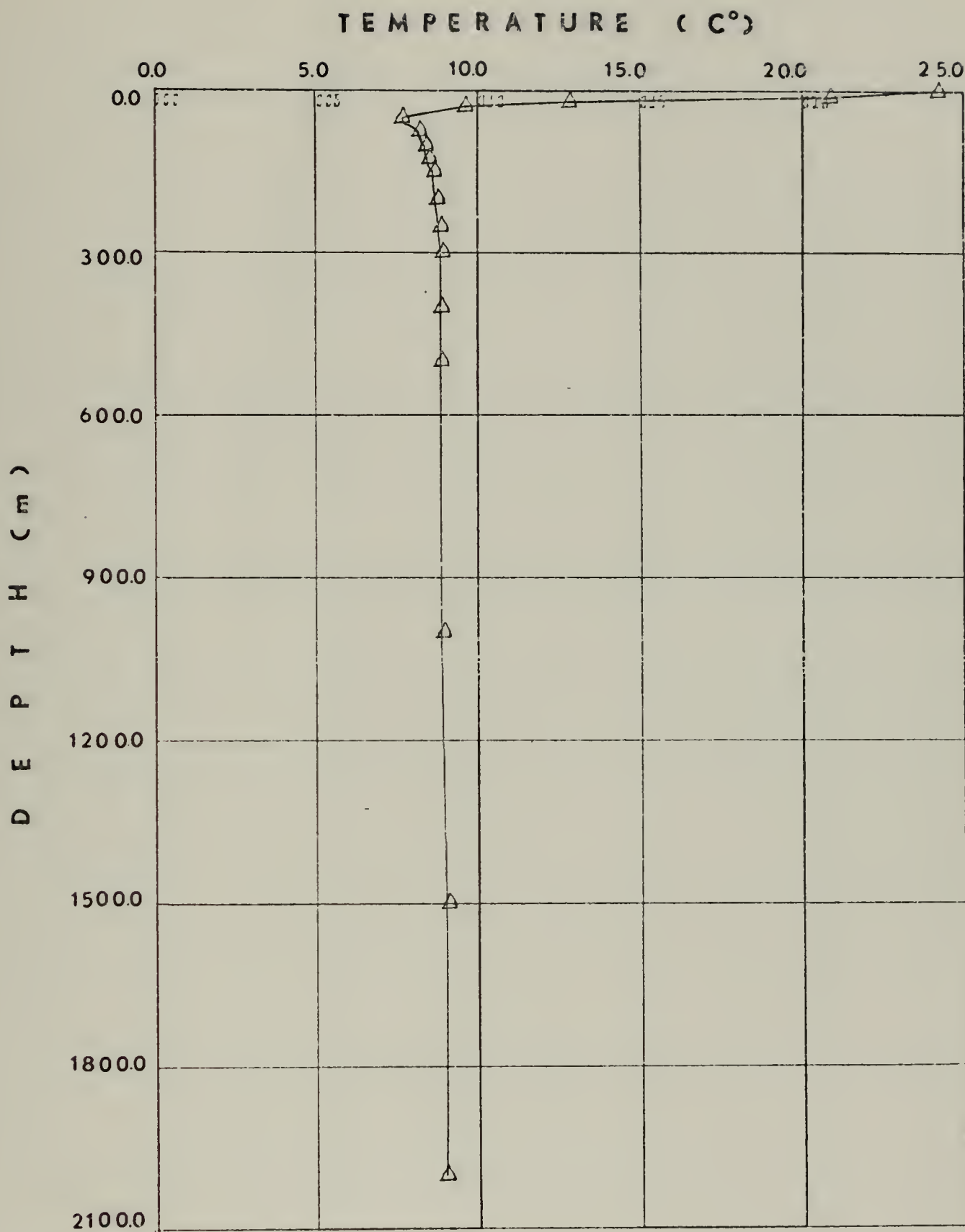


Figure 14. Average Temperature Profile for August.





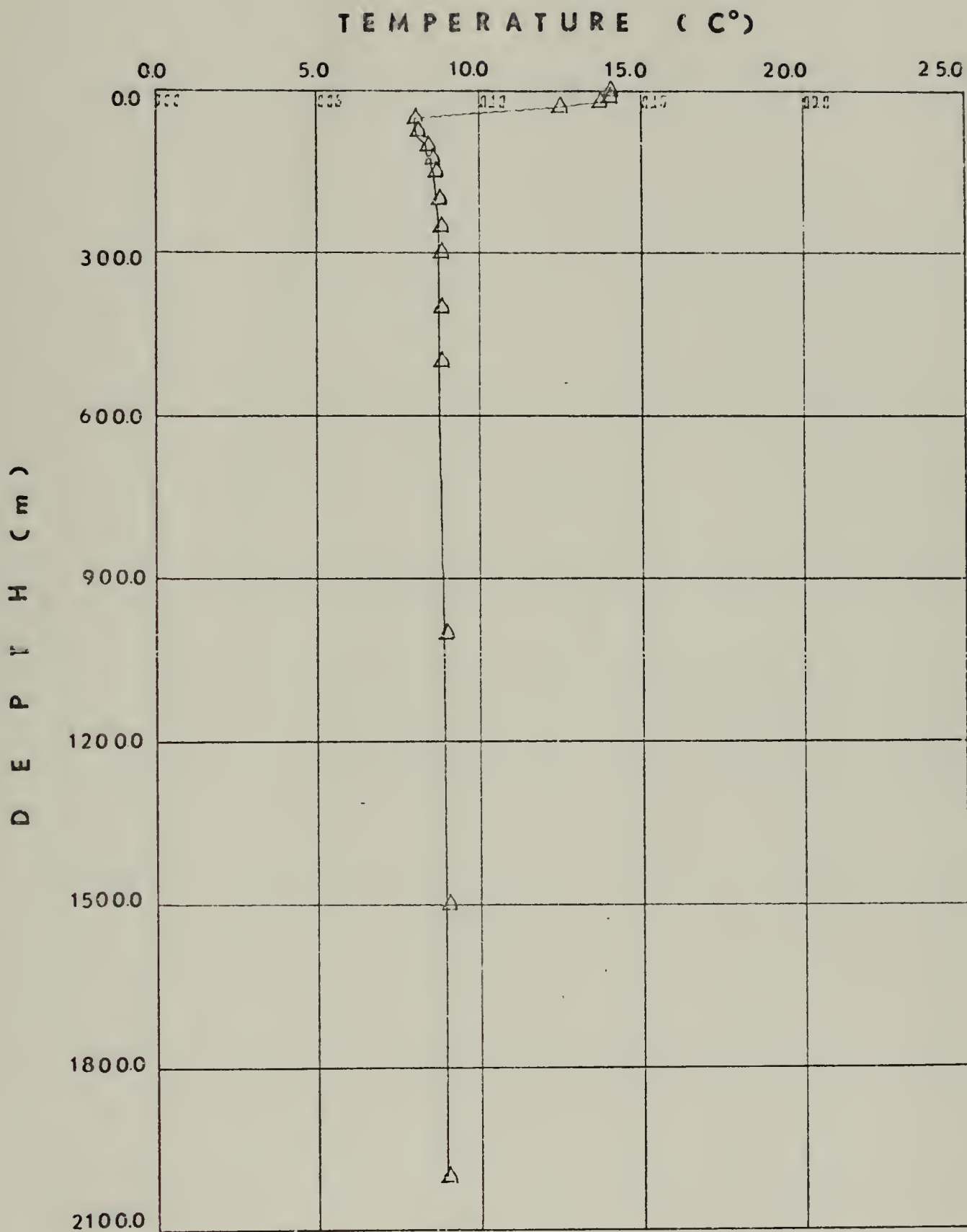


Figure 15. Average Temperature Profile for November.



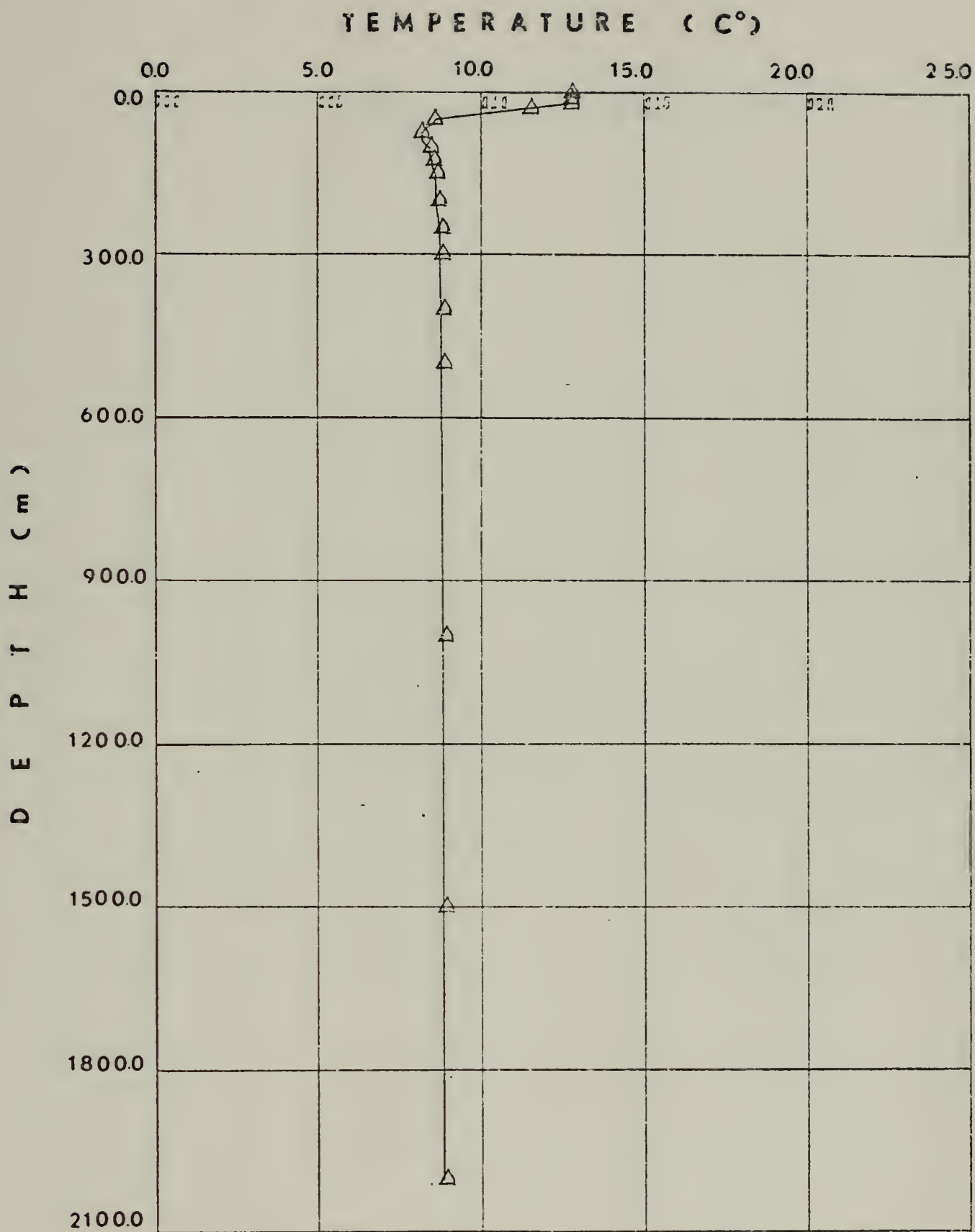


Figure 16. Average Temperature Profile for December.



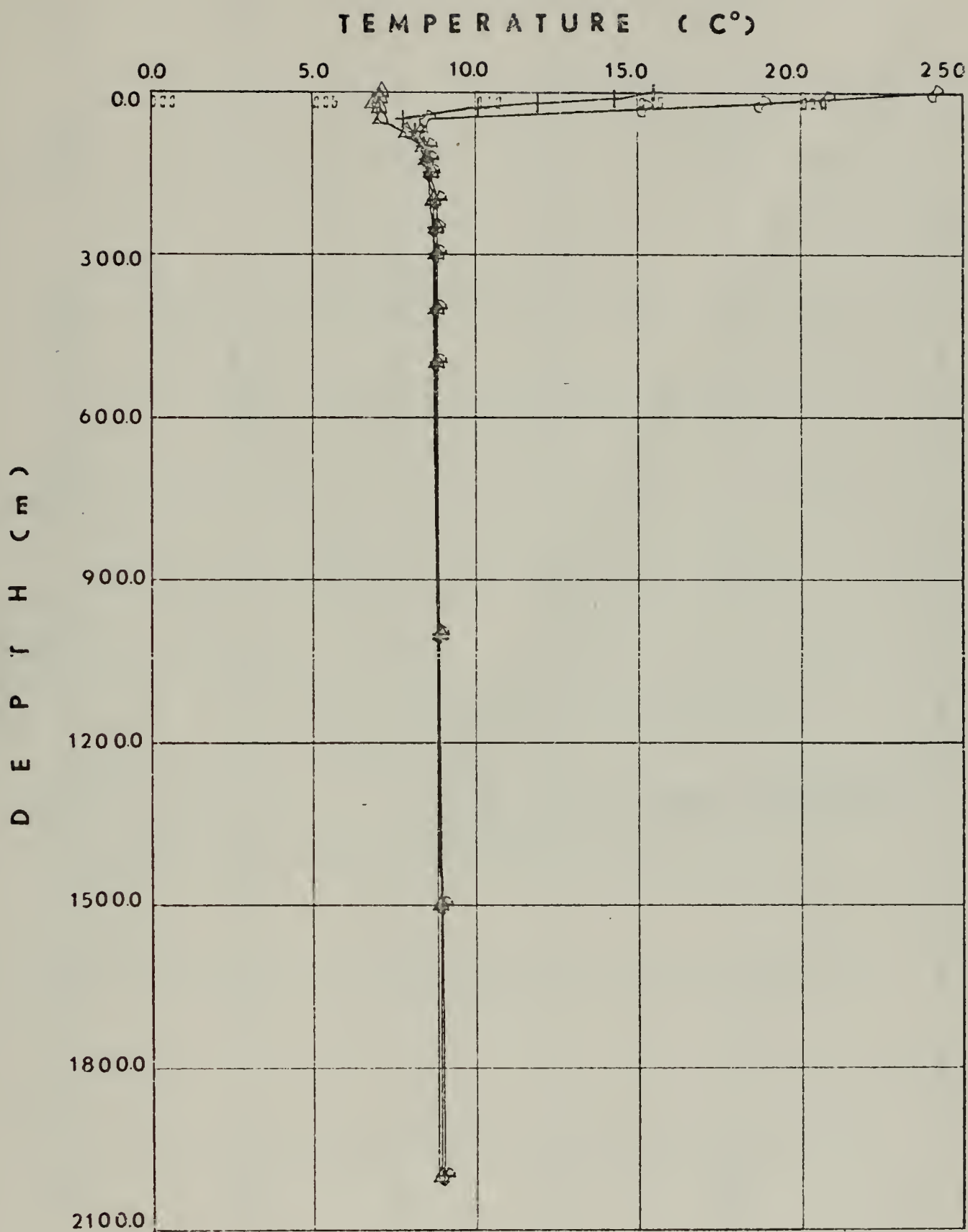


Figure 17. Annual Minimum, Maximum and Average Temperature Profiles.



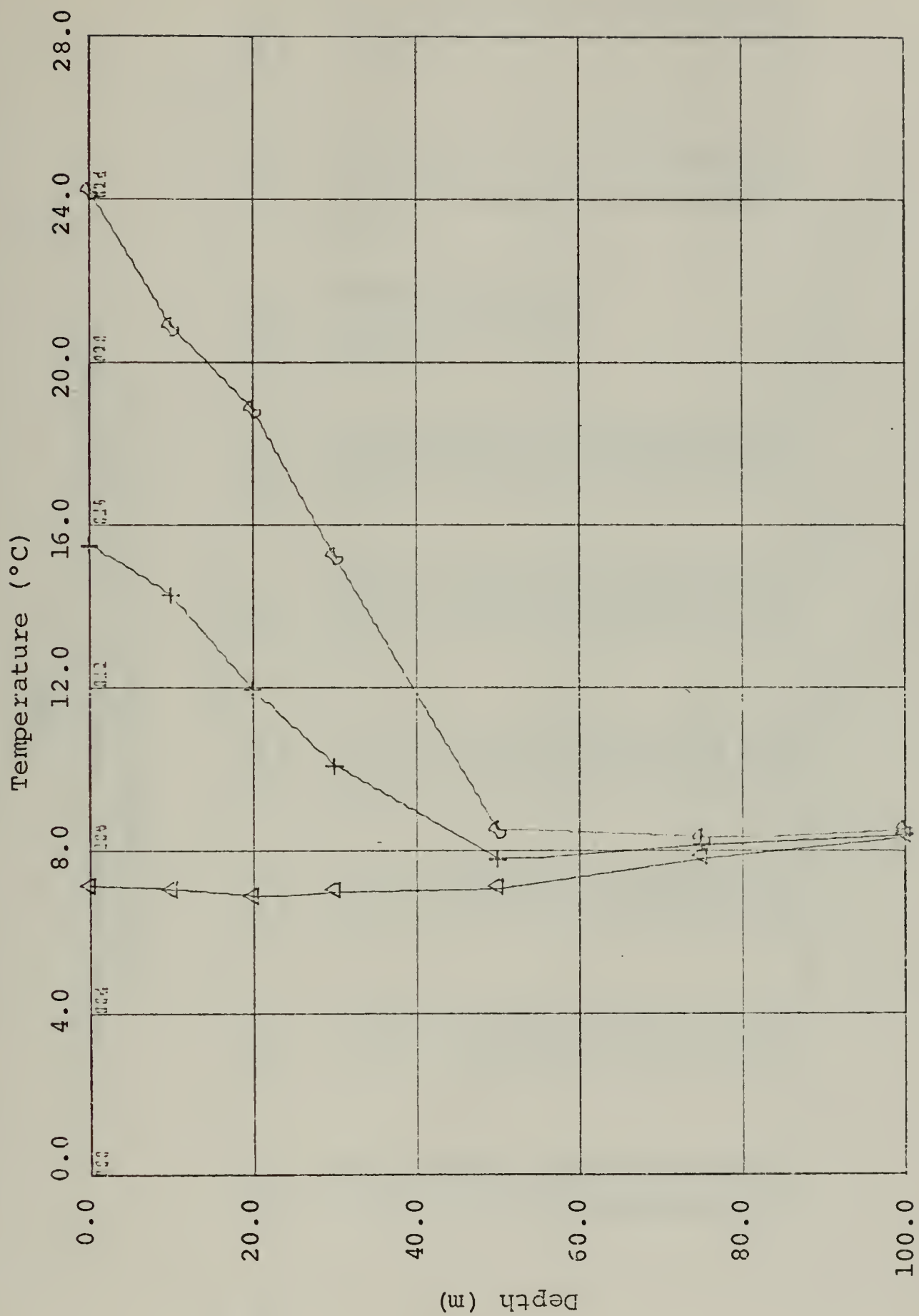


Figure 18. Minimum, Maximum and Average Temperature Profiles for Upper 100 m.





TABLE II  
AVERAGE MONTHLY TEMPERATURE (°C) DISTRIBUTION  
IN THE CENTRAL PART OF THE BLACK SEA

Depth (Meters)	M O N T H											
	Feb.	Mar.	May	June	July	Aug.	Oct.	Nov.	Dec.			
0	7.10	7.32	10.73	21.97	22.50	24.17	19.18	13.96	12.73			
10	7.04	7.03	10.72	17.44	19.36	20.85	19.16	13.97	12.72			
20	7.04	6.85	9.94	12.15	13.48	12.78	18.83	13.67	12.72			
30	7.05	7.04	8.53	9.38	9.91	9.56	15.21	12.42	11.46			
50	7.10	8.24	7.20	7.61	7.77	7.61	7.94	7.97	8.52			
75	7.88	8.46	8.18	8.24	8.29	8.16	8.29	8.07	8.12			
100	8.39	8.56	8.46	8.46	8.46	8.37	8.43	8.37	8.41			
125	8.53	8.63	8.59	8.57	8.58	8.47	8.53	8.53	8.52			
150	8.63	8.69	8.66	8.69	8.69	8.61	8.62	8.65	8.61			
200	8.69	8.73	8.76	8.78	8.75	8.73	8.88	8.72	8.70			
250	8.76	8.78	8.83	8.80	8.79	8.82		8.76	8.77			
300	8.80	8.81	8.87	8.81	8.81	8.86		8.78	8.80			
400	8.84	8.82	8.88	8.83	8.82	8.84		8.78	8.82			
500	8.85	8.83	8.88	8.85	8.83	8.83		8.80	8.85			
1000	8.93	8.89	8.95	8.90	8.88	8.87		8.92	8.86			
1500	9.03	8.92	9.05	8.93	8.90	9.00		8.98	8.87			
2000	9.09	8.94	8.96	8.95	8.98	8.91		8.95	8.87			



Table III  
ANNUAL MINIMUM, MAXIMUM AND AVERAGE  
TEMPERATURE (°C) DISTRIBUTION

<u>Depth (m)</u>	<u>Minimum</u>	<u>Maximum</u>	<u>Annual Average</u>
0.0	7.10	24.17	15.52
10.0	7.03	20.85	14.25
20.0	6.85	18.83	11.94
30.0	7.04	15.21	10.06
50.0	7.10	8.52	7.77
75.0	7.88	8.29	8.19
100.0	8.37	8.56	8.43
125.0	8.47	8.63	8.55
150.0	8.61	8.69	8.65
200.0	8.69	8.88	8.75
250.0	8.76	8.83	8.79
300.0	8.78	8.87	8.82
400.0	8.78	8.88	8.83
500.0	8.80	8.88	8.84
1000.0	8.86	8.95	8.90
1500.0	8.87	9.05	8.96
2000.0	8.87	9.09	8.96



### C. SALINITY DISTRIBUTION

The salinity distribution of the surface water for summer months (July, August and September) is presented in Figure 19 [7]. This Figure shows the salinity to be highest on the west coast of the Crimea and in the central parts of the eastern and western Black Sea basins. The highest salinity of these areas is greater than 18.2 parts per thousand. Neumann concluded that the high salinity that occurs northwest of the Crimea in summer is due to extensive evaporation. The lowest salinity values are observed near the coast, especially in the northwestern part, off the mouths of great rivers. This is also significant in the southeastern part of the Black Sea where numerous small rivers supply much fresh water, and, according to Neumann [7], the low salinity on the Anatolia Coast, east of Bosphorus, is the result of the fresh water discharge of the Sakarya River. Large seasonal salinity variations occur only near the coast [7]. The minimum salinity values in the vicinity of the northwest coast are observed during April and May, when the fresh water flow through the rivers is heaviest. The occurrence of minimum salinity is observed later with increasing distance from the coast. A salinity minimum occurs in the northern part of the Black Sea concurrently with the maximum river runoff during April and May. But, south of the Crimea ( $44^{\circ}\text{N}$ ,  $33^{\circ}\text{E}$ ), the minimum occurs about 3 to 4 months later [7].



The typical vertical salinity profiles in the central part of the Black Sea for several different months are shown in Figures 20 through 27. The monthly average salinity distribution for each depth is given in Table IV. Table V shows the minimum, maximum and average salinity values.

The average surface salinity ranges from 17.70 ‰ in early summer to 18.25 ‰ in the winter. The minimum salinities have been observed during summer months due to maximum runoff during April and May which spreads over the central regions 3 to 4 months later.

It can be seen, from vertical salinity profiles, that salinity increases gradually from the sea surface to the cold intermediate layer, where it reaches 18.70 to 19.62 ‰ at the depths of 50 to 75 m. The maximum seasonal range is found at a depth of 50 m, typically this range is approximately 1.60 ‰ (Figures 28 and 29). Below the cold intermediate layer, the steep positive halocline is observed to 300 m, and the salinity increases markedly with depth by as much as 2.9 ‰ in an interval of 200 m. After 300 m, the salinity increases slightly with depth. From a value of about 21.7 ‰ to 22.24 ‰ at a depth of 1000 m, and finally to 22.33 ‰ near the bottom.







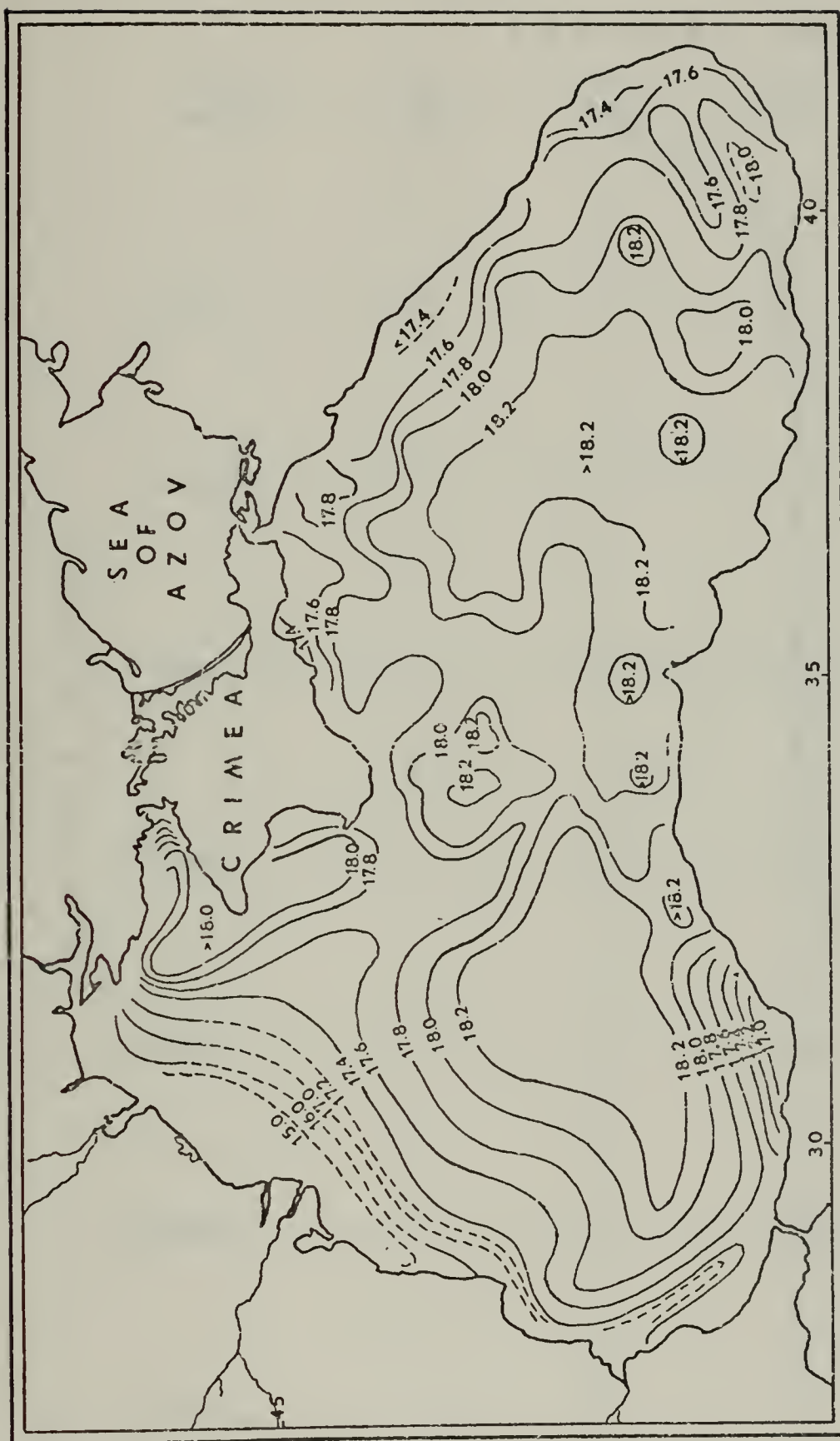


Figure 19. Salinity (‰) Distribution of the Sea Surface in Summer  
(July - August - September) [Neumann Ref. 7].



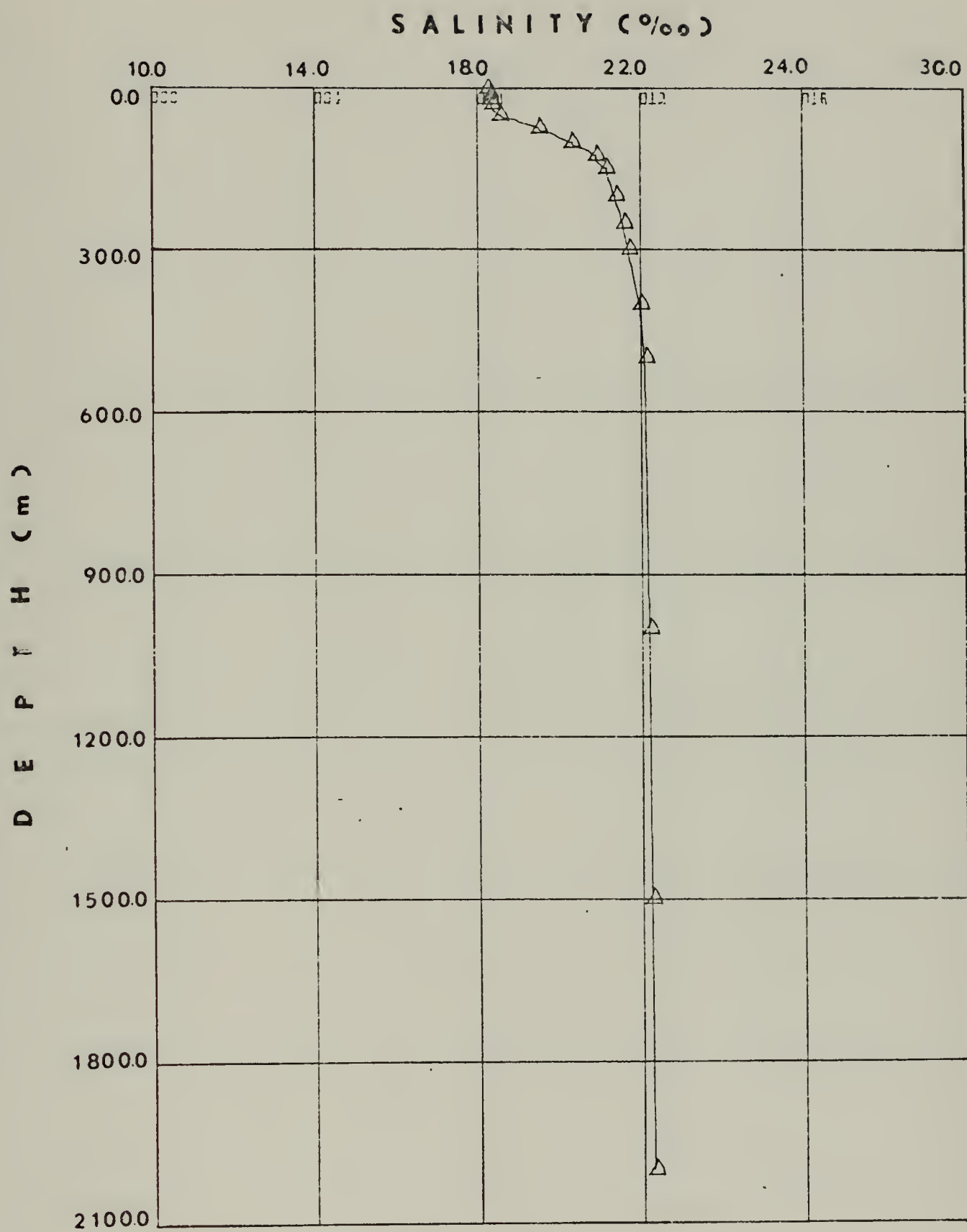


Figure 20. Average Salinity Profile for February.



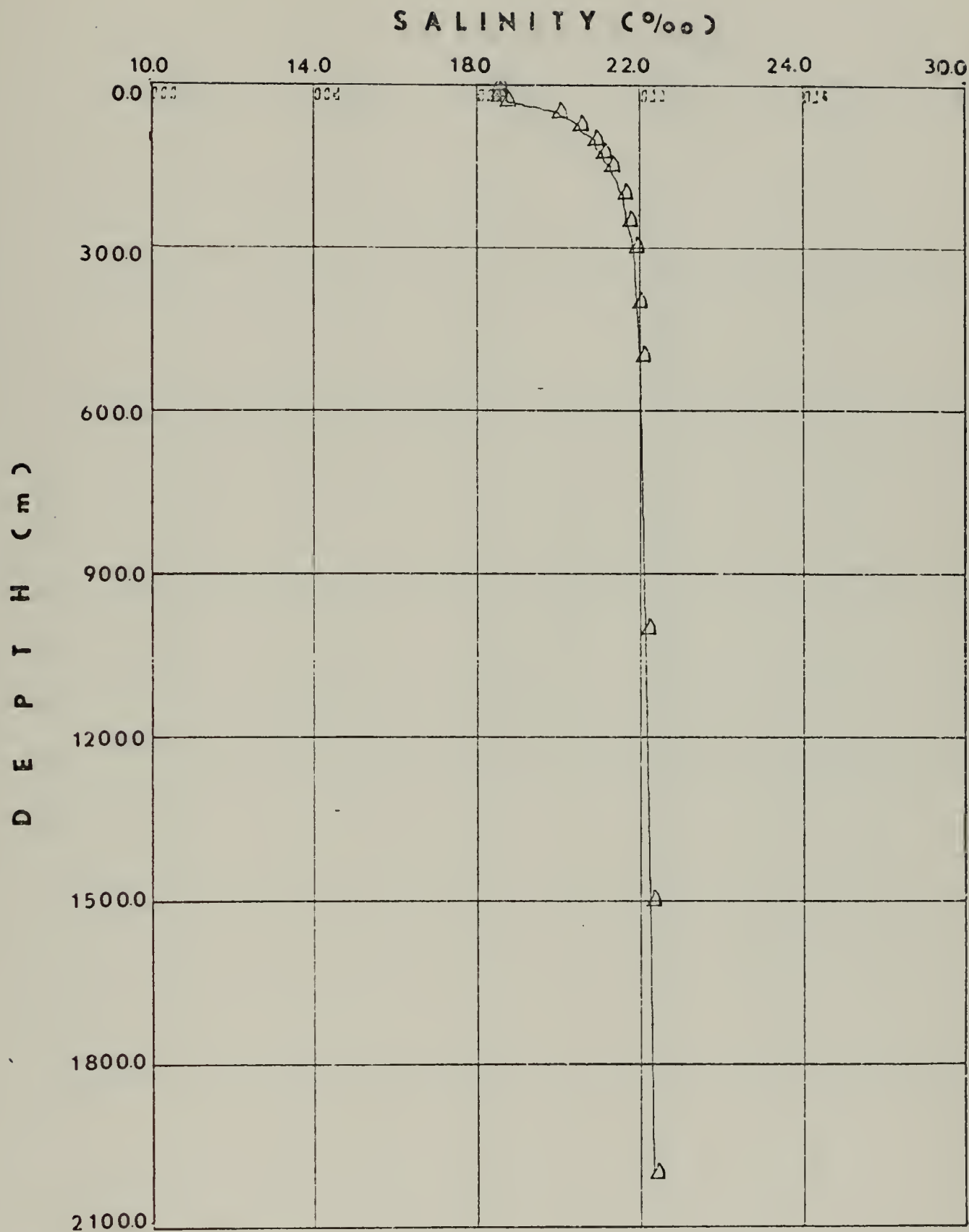


Figure 21. Average Salinity Profile for March.



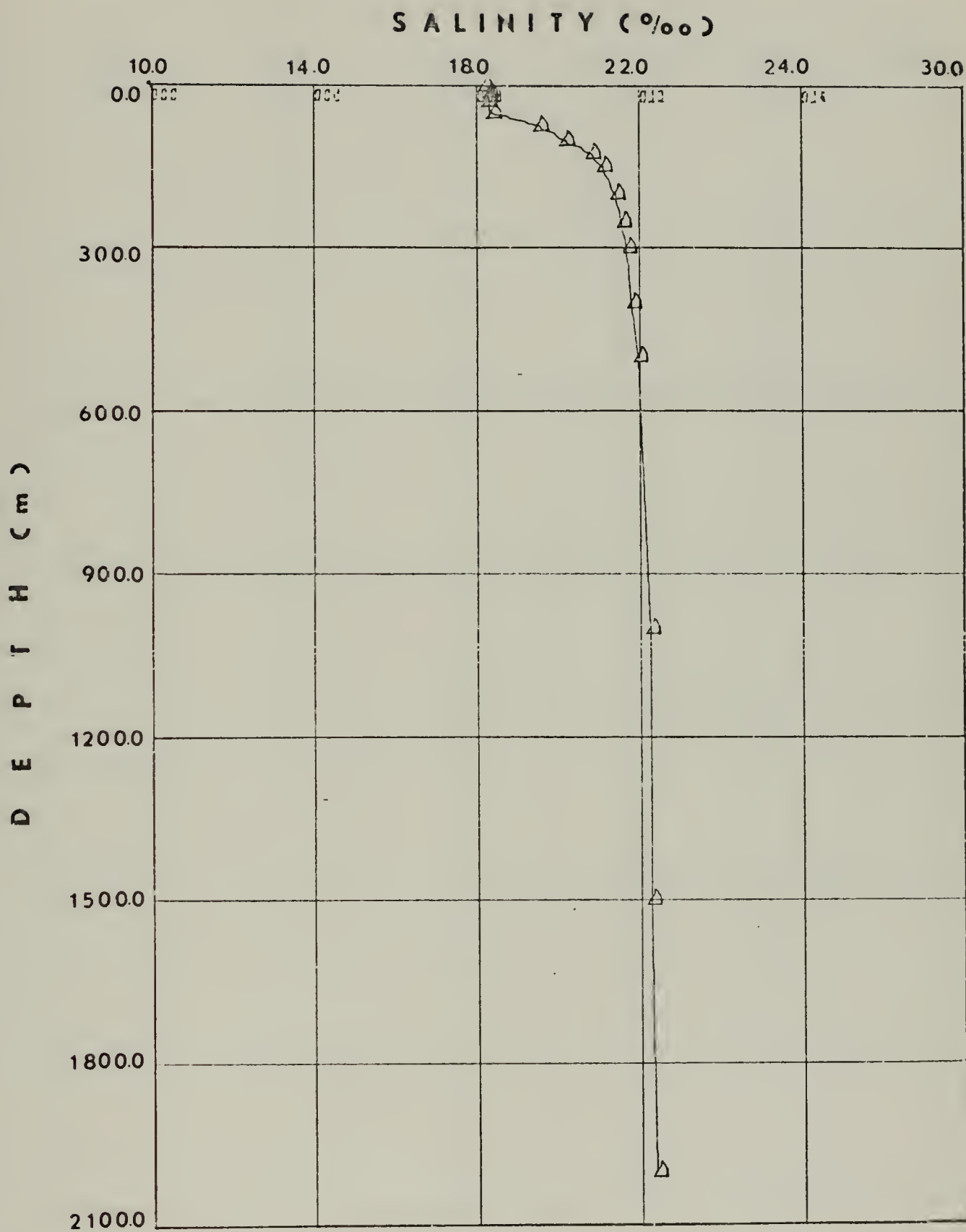


Figure 22. Average Salinity Profile for May.





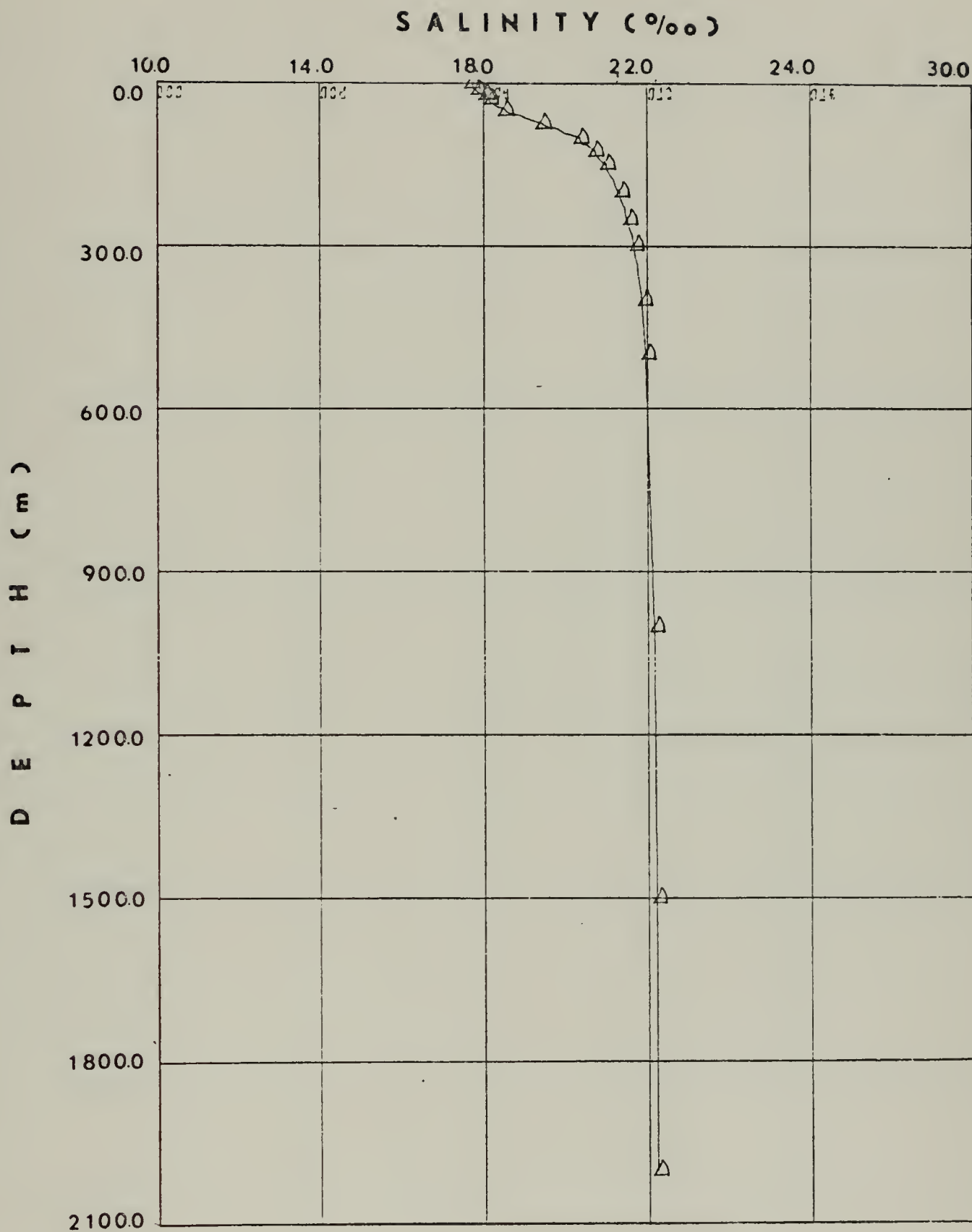


Figure 23. Average Salinity Profile for June.



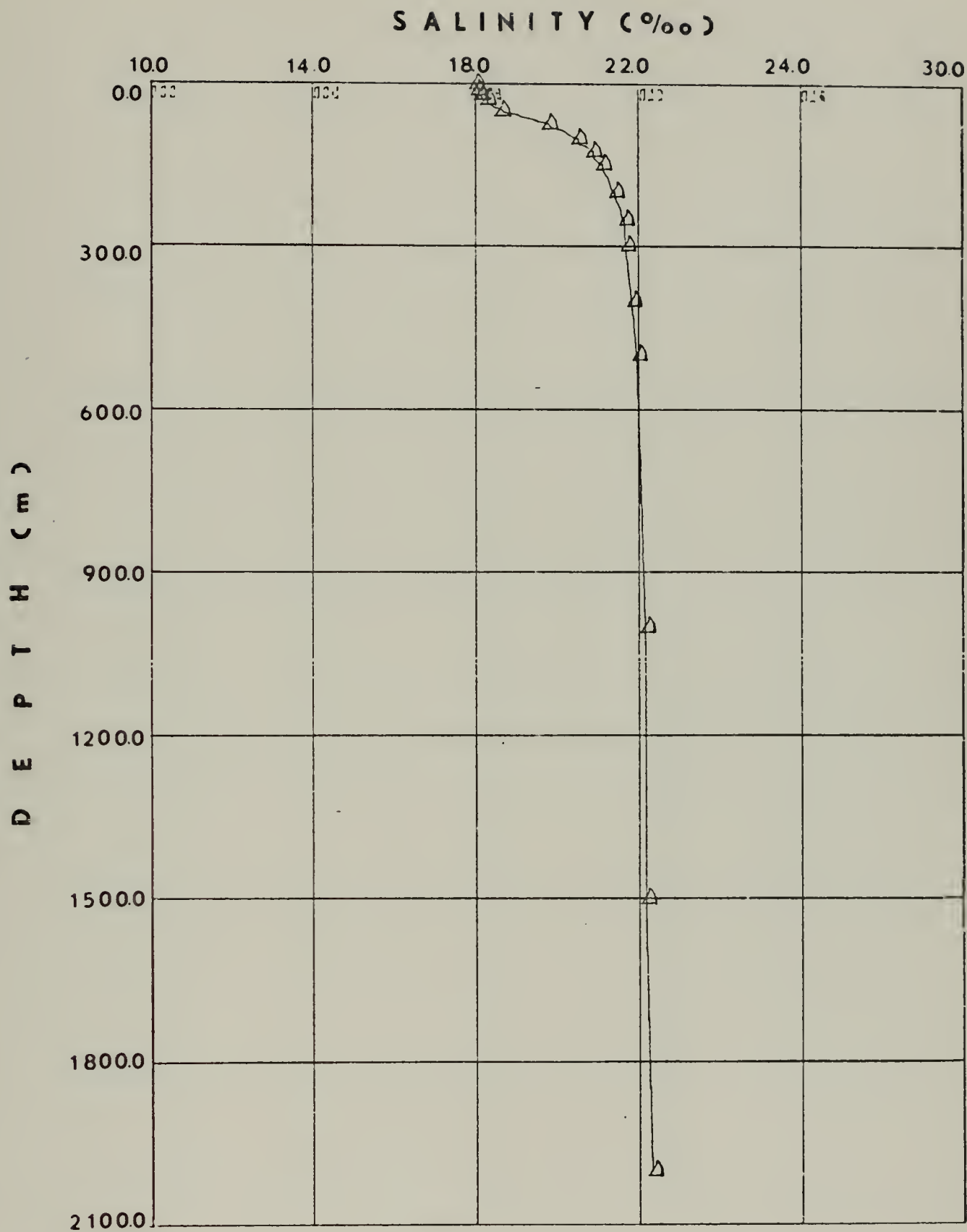


Figure 24. Average Salinity Profile for July.



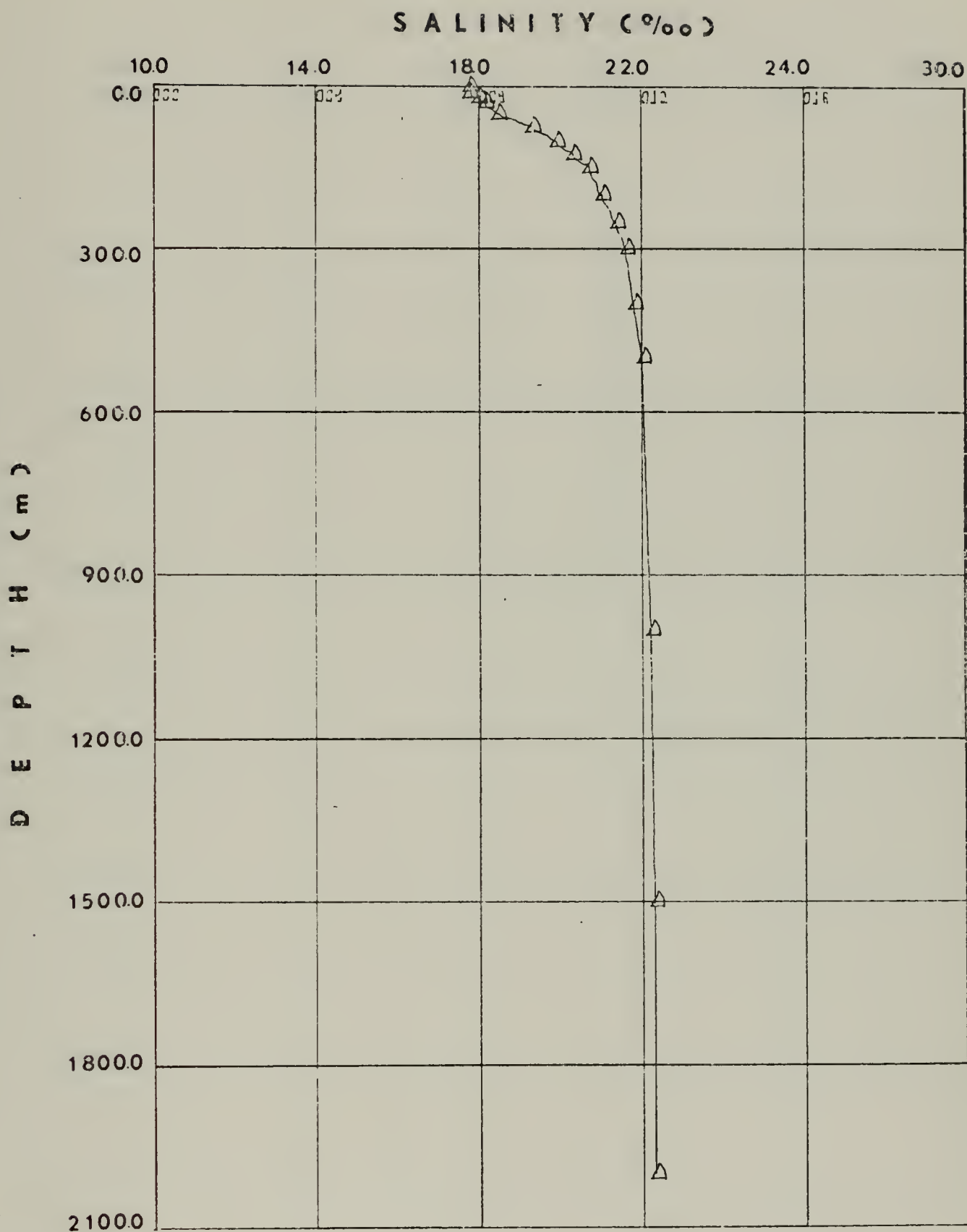


Figure 25. Average Salinity Profile for August.



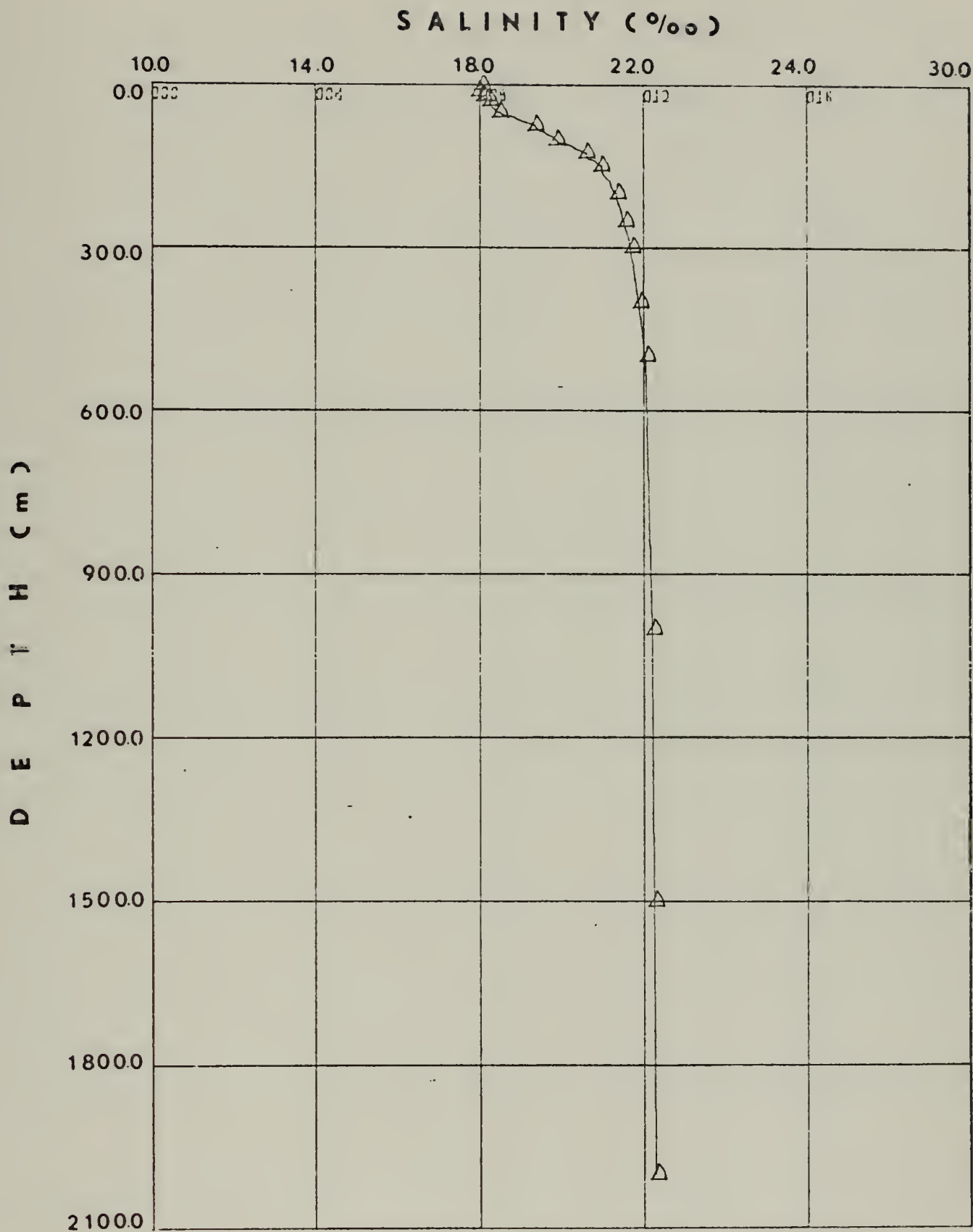


Figure 26. Average Salinity Profile for November.





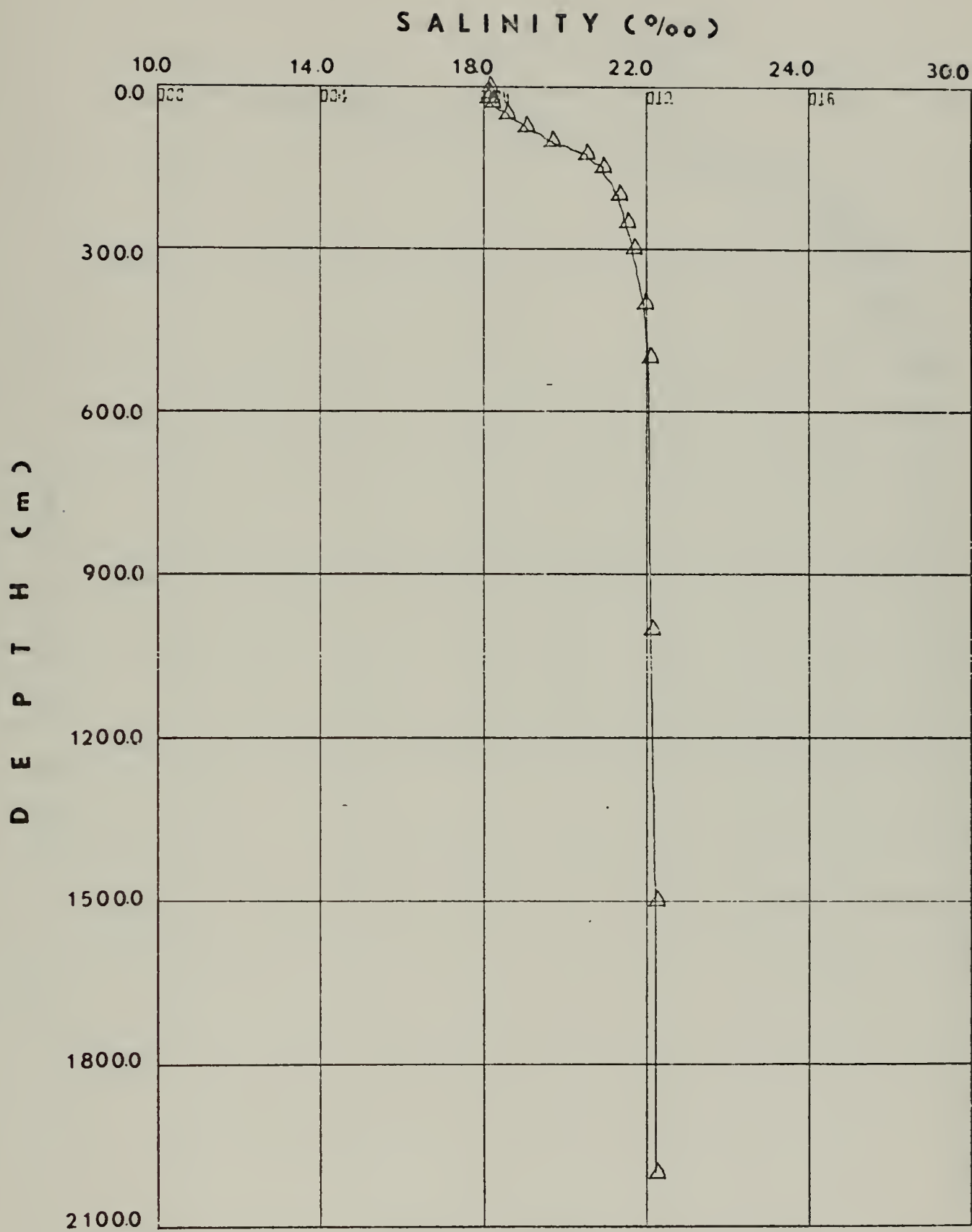


Figure 27. Average Salinity Profile for December.



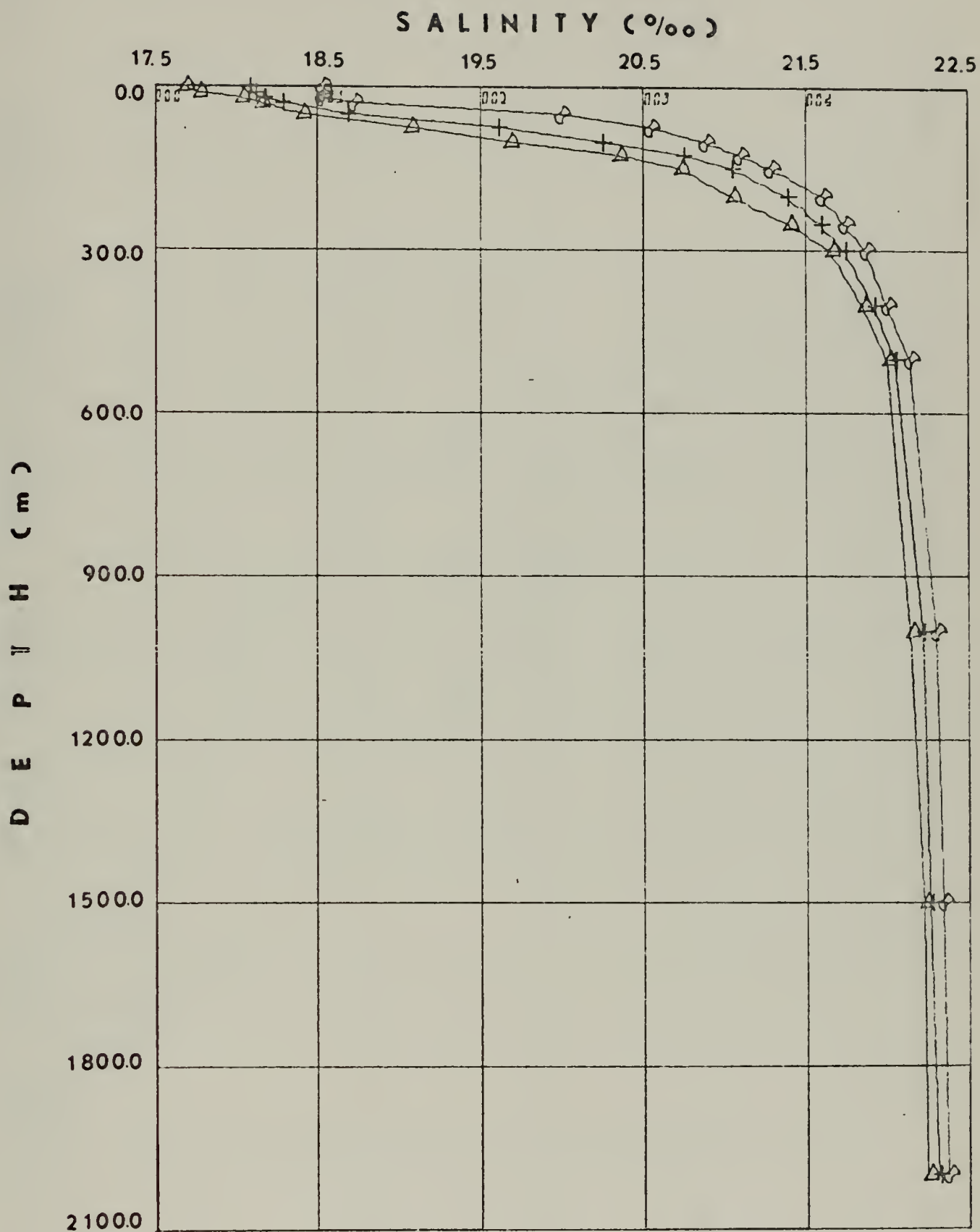


Figure 28. Annual Minimum, Maximum and Average Salinity Profiles.



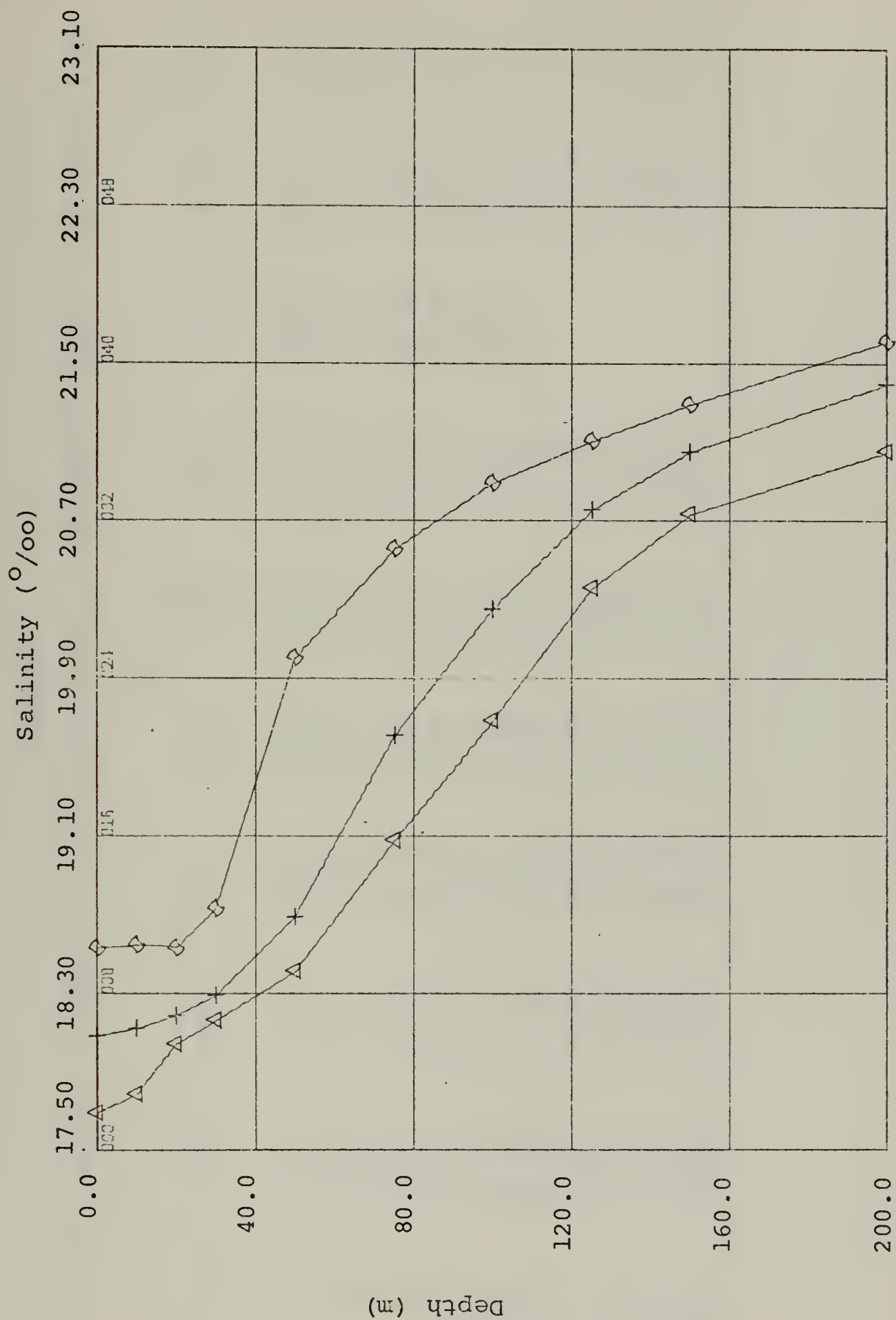


Figure 29. Annual Minimum, Maximum and Average Salinity Profiles for Upper 200 m.



TABLE IV

AVERAGE MONTHLY SALINITY (‰) DISTRIBUTION IN THE CENTRAL PART OF THE BLACK SEA

Depth (Meters)	M O N T H											
	Feb.	Mar.	May	June	July	Aug.	Oct.	Nov.	Dec.			
0	18.25	18.54	18.21	17.70	18.00	17.78	18.11	18.06	18.14			
10	18.33	18.55	18.36	17.85	18.06	17.79	18.11	17.98	18.13			
20	18.34	18.54	18.32	18.05	18.14	18.03	18.11	18.10	18.10			
30	18.37	18.74	18.32	18.17	18.29	18.18	18.17	18.25	18.23			
50	18.57	20.01	18.42	18.56	18.67	18.51	18.49	18.50	18.58			
75	19.54	20.56	19.60	19.48	19.83	19.36	19.78	19.39	19.08			
100	20.34	20.90	20.24	20.40	20.54	19.96	20.35	19.91	19.69			
125	20.94	21.11	20.87	20.76	20.92	20.36	20.73	20.62	20.55			
150	21.17	21.30	21.16	21.04	21.15	20.74	21.08	20.97	20.93			
200	21.44	21.62	21.47	21.38	21.48	21.06	21.42	21.38	21.34			
250	21.62	21.76	21.63	21.60	21.69	21.41		21.58	21.56			
300	21.75	21.89	21.73	21.76	21.75	21.67		21.74	21.70			
400	22.02	21.99	21.87	21.94	21.92	21.88		21.94	21.97			
500	22.16	22.07	22.03	22.02	22.04	22.05		22.10	22.11			
1000	22.23	22.20	22.32	22.24	22.22	22.25		22.26	22.16			
1500	22.28	22.30	22.30	22.25	22.24	22.36		22.29	22.25			
2000	22.30	22.39	22.41	22.25	22.37	22.34		22.33	22.27			





TABLE V  
ANNUAL MINIMUM, MAXIMUM AND AVERAGE  
SALINITY (°/oo) DISTRIBUTION

<u>Depth</u>	<u>Minimum</u>	<u>Maximum</u>	<u>Average</u>
0.0	17.70	18.54	18.09
10.0	17.79	18.55	18.13
20.0	18.05	18.54	18.19
30.0	18.17	18.74	18.30
50.0	18.42	20.01	18.70
75.0	19.08	20.56	19.62
100.0	19.69	20.90	20.26
125.0	20.36	21.11	20.76
150.0	20.74	21.30	21.06
200.0	21.06	21.62	21.40
250.0	21.41	21.76	21.51
300.0	21.67	21.89	21.75
400.0	21.87	22.02	21.94
500.0	22.02	22.16	22.07
1000.0	22.16	22.32	22.24
1500.0	22.24	22.36	22.28
2000.0	22.25	22.39	22.33



#### IV. BOTTOM SEDIMENTS

Figure 30 is a bathymetric chart of bottom sediments prepared by Arkhangel'skiy using older bottom sediment information to supplement his data. According to Arkhangel'skiy and Strakhov, the sediments of the Black Sea are classified into three groups [17]:

##### A. COASTAL SEDIMENTS

The coastal sediments are represented by pebble, boulder, gravel and sand zones [18].

###### 1. Pebble Zone

The pebbles are adjacent to the shore in depths of 1 - 2 m in a belt not exceeding the width of 5 - 10 m. The pebble belt is frequently interrupted by boulders and gravel with a mixture of sand shingles. The petrographic composition of the pebbles is identical to the composition of the adjoining coastline and the alluvium supplied by the rivers.

###### 2. Boulder Zone

The boulder accumulations are most commonly found in bays and along the coasts and are of igneous composition. The zone varies in width to 150 m and is found in depths 10 to 40 m. In the estuarian areas, the zone is probably covered fragmented material transported by the rivers.

Usually the boulders have rounded elipsoidal form. Their size varies from 0.5 to 1.2 m in diameter.



### 3. Gravel Zone

There are several gravel belts. The assortment of gravel size is more or less uniform. The sizes range from 2 to 5 mm. The aleurite and pelite fractions make up approximately 3 percent of the well sorted gravel. Along the massifs of effusive rocks and fine grain limestone, the gravel is represented by somewhat coarser fractions, including a large quantity of pebbles. In estuarian areas, the gravel belt begins at the shoreline and reaches a depth of 1.5 to 30 m, forming a belt 5 - 60 m wide. In rare cases, the gravel is found at the depths of 10 - 40 m as a continuous independent zone, 40 to 800 m wide.

### 4. Sand Zone

Sand is widely distributed in areas of detritus from river alluvium, shore erosion and land slides. Water depths over sand sediment vary depending on the steepness of the shelf and the quantity and size of the deposited detritus. Along deep shores, the sand usually extends to a depth of 25 - 30 m and along shoaling shores it reaches depths of 15 - 20 m.

In estuarian areas, the depth of sand deposits varies and the width of the belt is irregular. In areas near large rivers, the sand belt begins adjacent to the coast and is composed mainly of medium and fine grain materials.

The distribution of sand is affected by the coastal configuration and the slope of the shelf. When the shelf is steep, the sand is found at maximum depths (to 50 m), but the width of the belt is insignificant. In cape shoreline areas,



sand grain size varies and is poorly sorted from gravel to fine aleurite and pelite particles, and contains a large quantity of organic shell materials.

#### B. SHALLOW WATER SEDIMENTS

The shallow water sediments are divided into the *Mytilus* mud (*Mytilus galloprovincialis*), lying to a depth of 60 m and the *Phaseolina* mud (*Modiola phaseolina*), found on the outer edge of the coastal platform [17]. Both of the sediments represent darkish-gray plastic mass containing fragments and pieces of shells. Sometimes these sediments contain whole shell interlayers.

The *Mytilus* mud with respect to petrographic composition and shape, differs little from *Phaseolina* mud. The former is characterized by a rather higher content of organic matter and a coarser mechanical composition than the *Phaseolina* mud. The mineral material of this mud consists of particles ranging from 0.05 to 0.01 mm and less than 0.01 mm in diameter. Along the minerals, the angular grains of quartz prevail. In addition to quartz, muscovite, glauconite occasionally biotite, magnetite, anatite, hornblende and sillimanite are found [17].

#### C. DEEP WATER SEDIMENTS

Deep water sediments are found below the depth of 170 m. Deep water sediments are sharply different from coastal and shallow water sediments. These sediments show a complete absence of the remains of benthic organisms. The sediments consist of three types [17]:



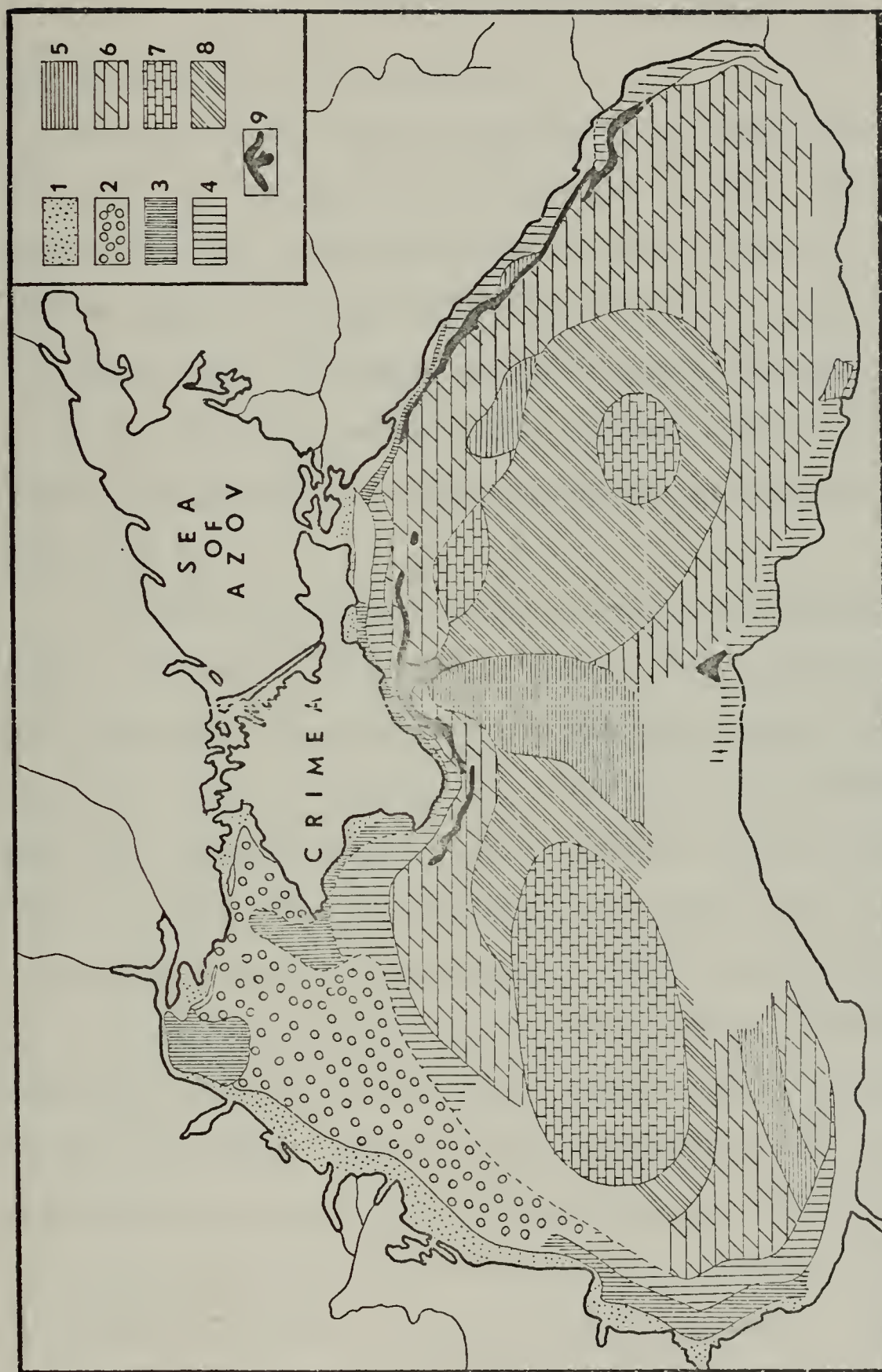




1. Gray deep water clay
2. Clayey calcareous (Transitional) mud
3. Calcareous mud

The clay material consists of terrigenous particles (73 percent on the average), whose diameters are smaller than 0.01 mm, pulverized calcite (approximately 15 percent) and organic matter (3 - 4 percent). The transitional clayey calcareous mud represents an elastic greenish-gray sediment with a marked stratification. In the bottom areas lying far off the coast, the transitional mud replaced by calcareous mud. This is a dirty white slightly plastic mass which brightens when drying and becomes fragile, breaking into irregular lumps.





1. Sand
2. Shells
3. Mytilus mud
4. Phaseolina mud
5. A series of clay with calcareous clay interlayers.
6. Transitional mud with gray clay interlayers.
7. Calcareous mud
8. Calcareous mud with gray clay interlayers.
9. Areas devoid of recent sediments.

Figure 30. Bottom Sediment Distribution in the Black Sea [Arkhangel'skiy 17].



## V. ACOUSTICAL CHARACTERISTICS

### A. SOUND VELOCITY STRUCTURE

The sound velocity structure is the most important factor for the propagation of sound in the sea. The typical sound velocity profiles in the central part of the Black Sea can be seen in Figure 31 through 38. The sound velocity profiles were calculated using Wilson's equation. Temperature and salinity values were obtained from Tables II and IV. Detail information of sound velocity calculation is given in Appendix A.

The monthly average sound velocity distribution for each depth is given in Table VI. Table VII is obtained from Table VI, and shows the minimum, maximum and average sound velocity values. Figure 39 gives the profiles of the minimum, maximum and average sound velocity values that are drawn from the data in Table VII. The profiles for upper 200 m are represented in Figure 40 in expanded scale for resolution.

In the central part of the Black Sea, surface sound velocity changes within a year from 1457.8 m/sec to 1513.9 m/sec in summer. The minimum and maximum sound velocities always occurring in February and August respectively; February through August, the surface sound velocity increasing monotonically due to surface heating, however, the summer freshening of the central Black Sea compensates for some of the increase expected from warming. After August, surface sound velocity decreases until February.





During the winter, in the surface isothermal layer, the sound velocity increases approximately linearly to a depth of 50 m. From 50 m to 200 m, sound velocity increases more rapidly than in the surface layer due to sharp increases in salinity and temperature. Below 200 m, the temperature and salinity continue to increase gradually with depth, and the sound velocity increases with increasing depth and it reaches 1503.9 m/sec at a depth of 2000 m in February.

During the spring, the surface temperature increases creating a shallow thermocline in the surface layer and for this reason, sound velocity increases at the surface (Figure 33). The sound velocity decreases monotonically from the lower limit of isothermal layer to the cold intermediate layer (50-75 m). Between 50 to 75 m, sound velocity reaches its minimum value. So, the sound channel develops at depths below the shallow thermocline. The sound channel axis is seen at the bottom of the thermocline where the sound velocity is at a minimum of 1459.3 m/sec at a depth of 50 - 75 m in May.

During the summer, when the near-surface waters are warm, a well defined thermocline develops in the central part of the Black Sea. So, that near the surface the sound velocity decreases rapidly with depth, and at the bottom of thermocline, it reaches its minimum value. Within this negative sound velocity gradient, the sound velocity decreases by as much as 52 m/sec an interval of 50 m (Figure 36). And, the sound channel axis occurs at a depth of 50 m in August. Below the sound channel axis, the sound velocity begins to increase with depth until the bottom is reached.





During the fall, the thermocline is not strong. Near the surface layer, a shallow isothermal layer develops with wind and convective mixing. Sound velocity increases with depth in the isothermal layer and then begins to decrease with temperature effect in the thermocline. Below the thermocline, it increases again to the bottom of the sea (Figure 37).

Large seasonal sound velocity variations occur only in the upper layer of the Black Sea. Maximum variation is seen at the surface and it decreases with depth. Below 125 m, maximum variation is not more than 1 m/sec at the same depths for each month (Table VII), so, it can be concluded, below 125 m in the Black Sea, sound velocity profiles do not show significant seasonal changes.



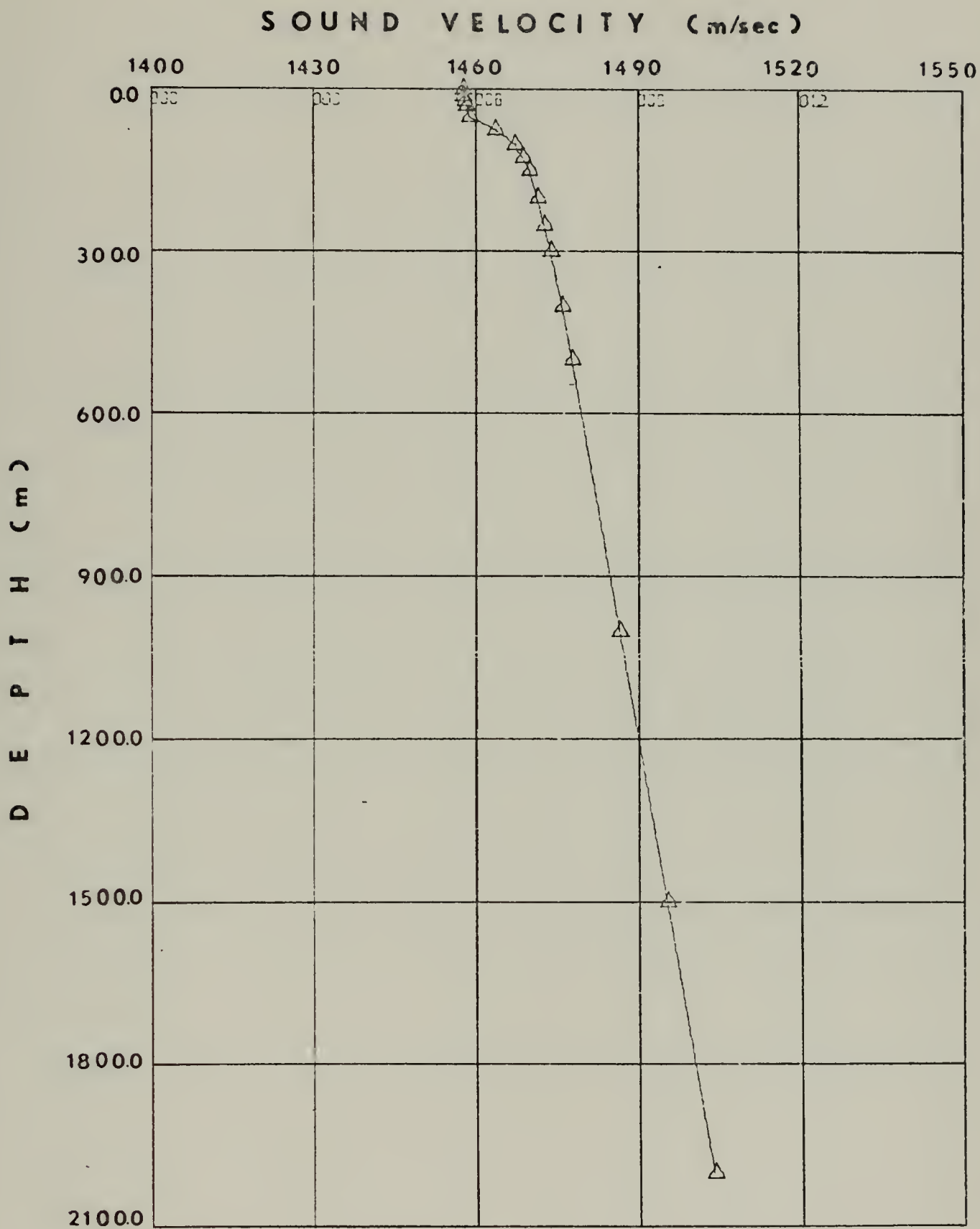


Figure 31. Average Sound Velocity Profile for February.



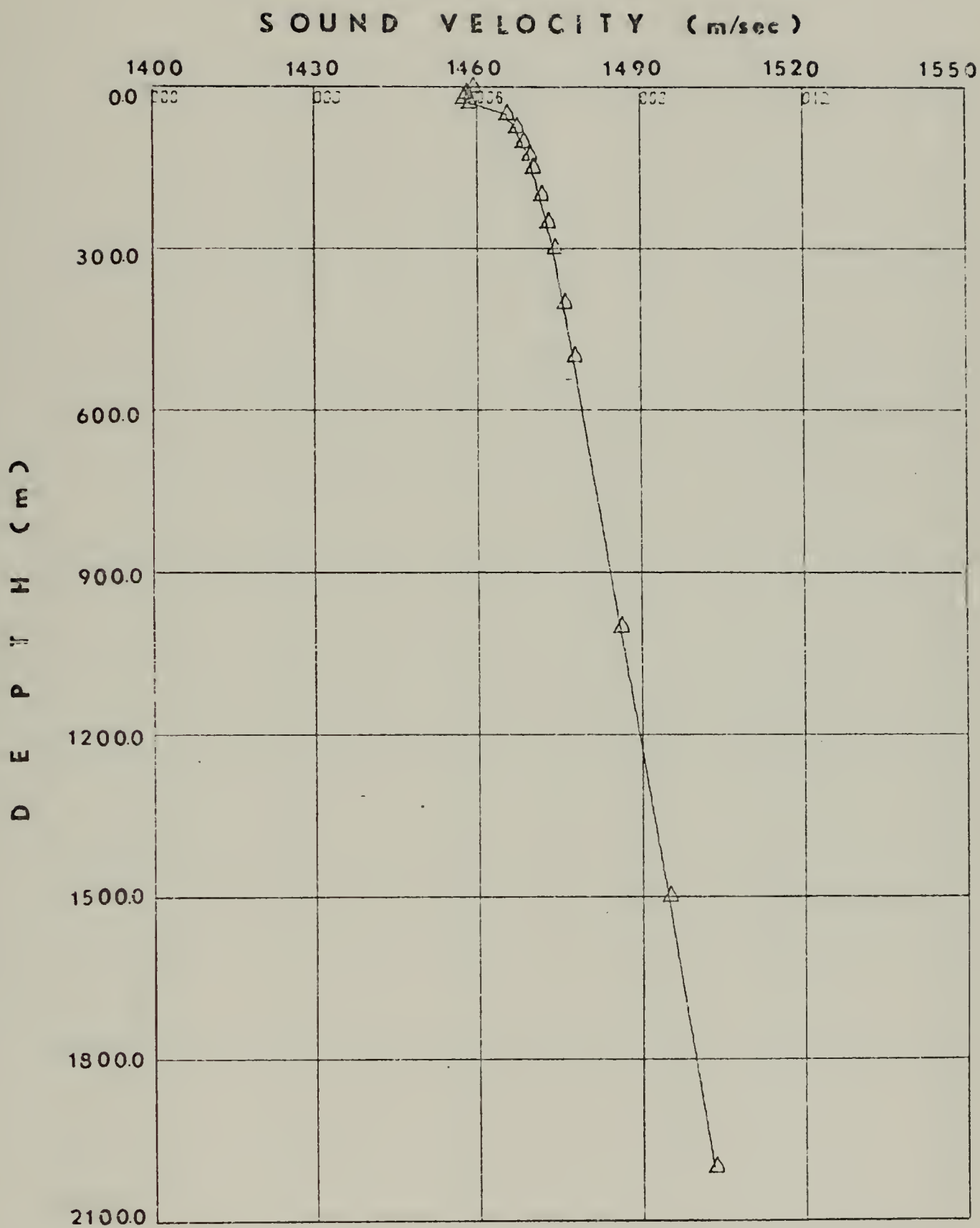


Figure 32. Average Sound Velocity Profile for March.



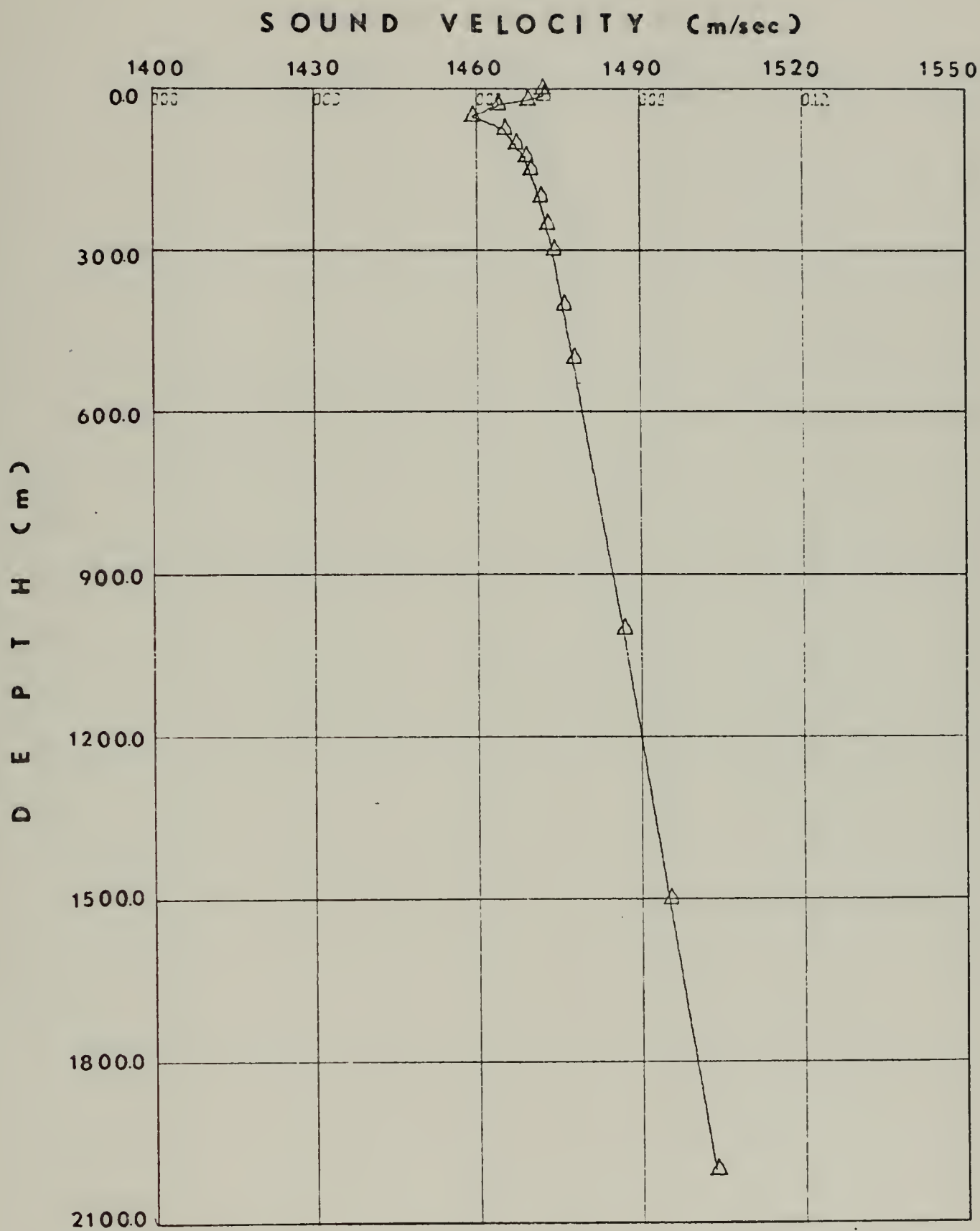


Figure 33. Average Sound Velocity Profile for May.





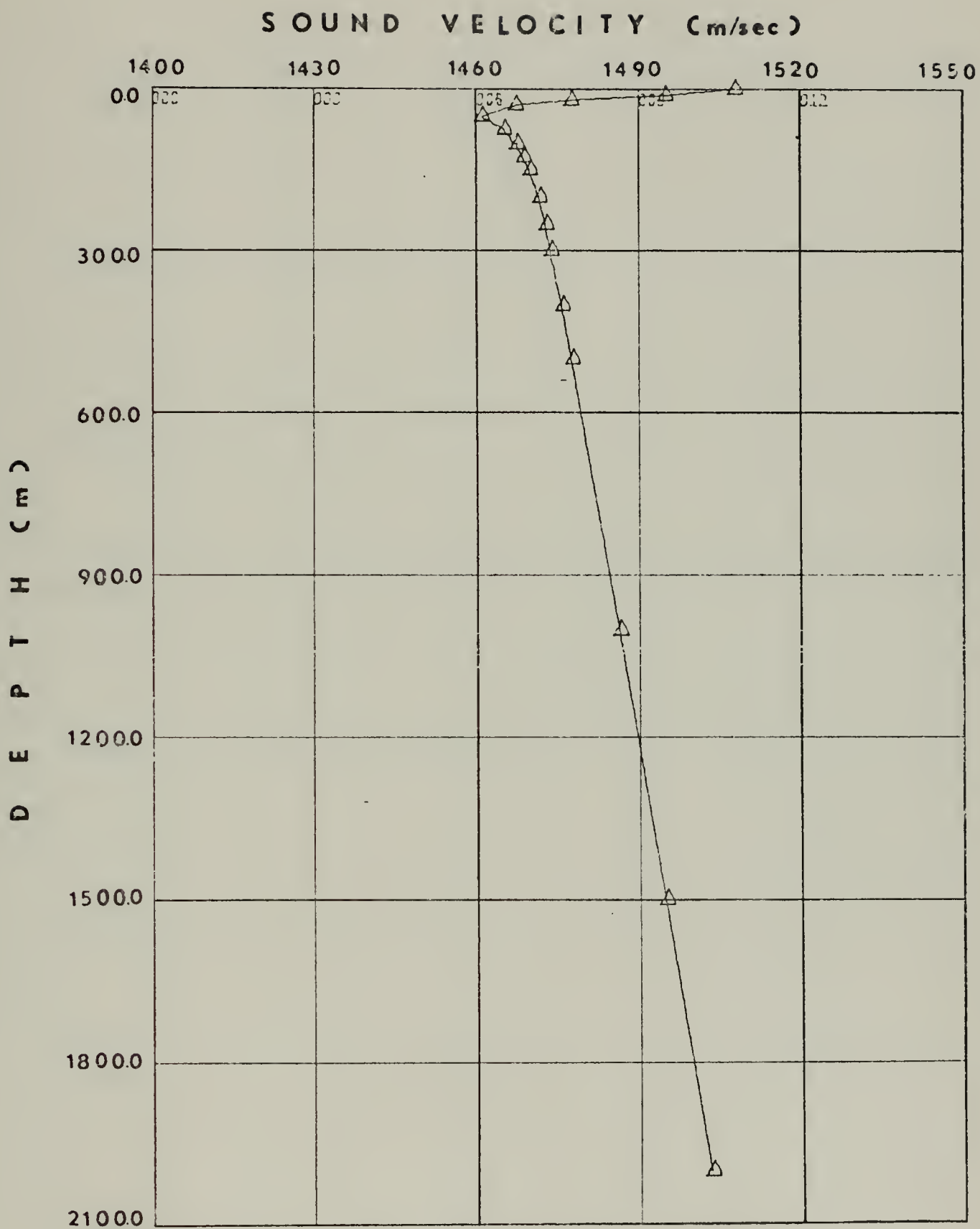


Figure 34. Average Sound Velocity Profile for June.



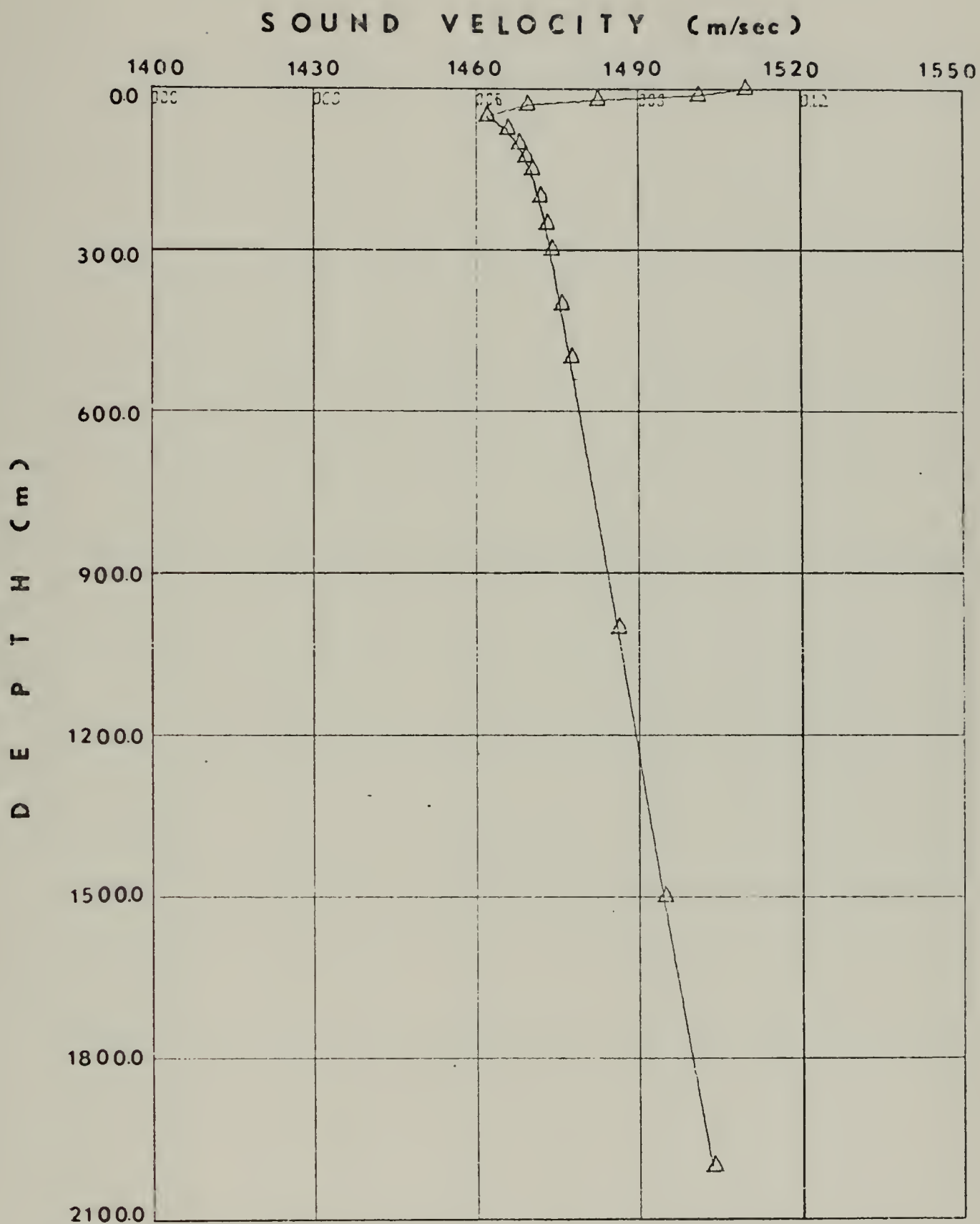


Figure 35. Average Sound Velocity Profile for July.



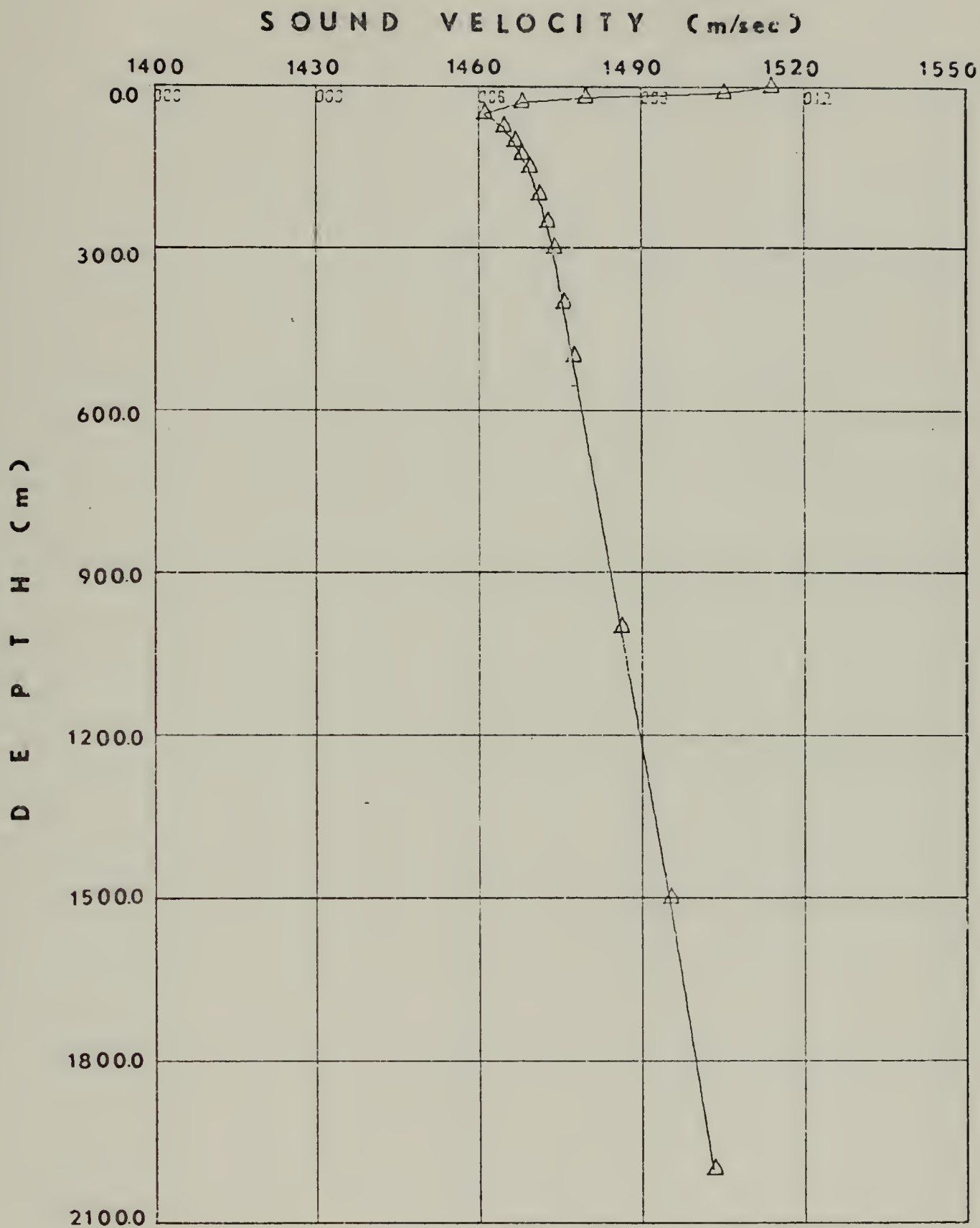


Figure 36. Average Sound Velocity Profile for August.



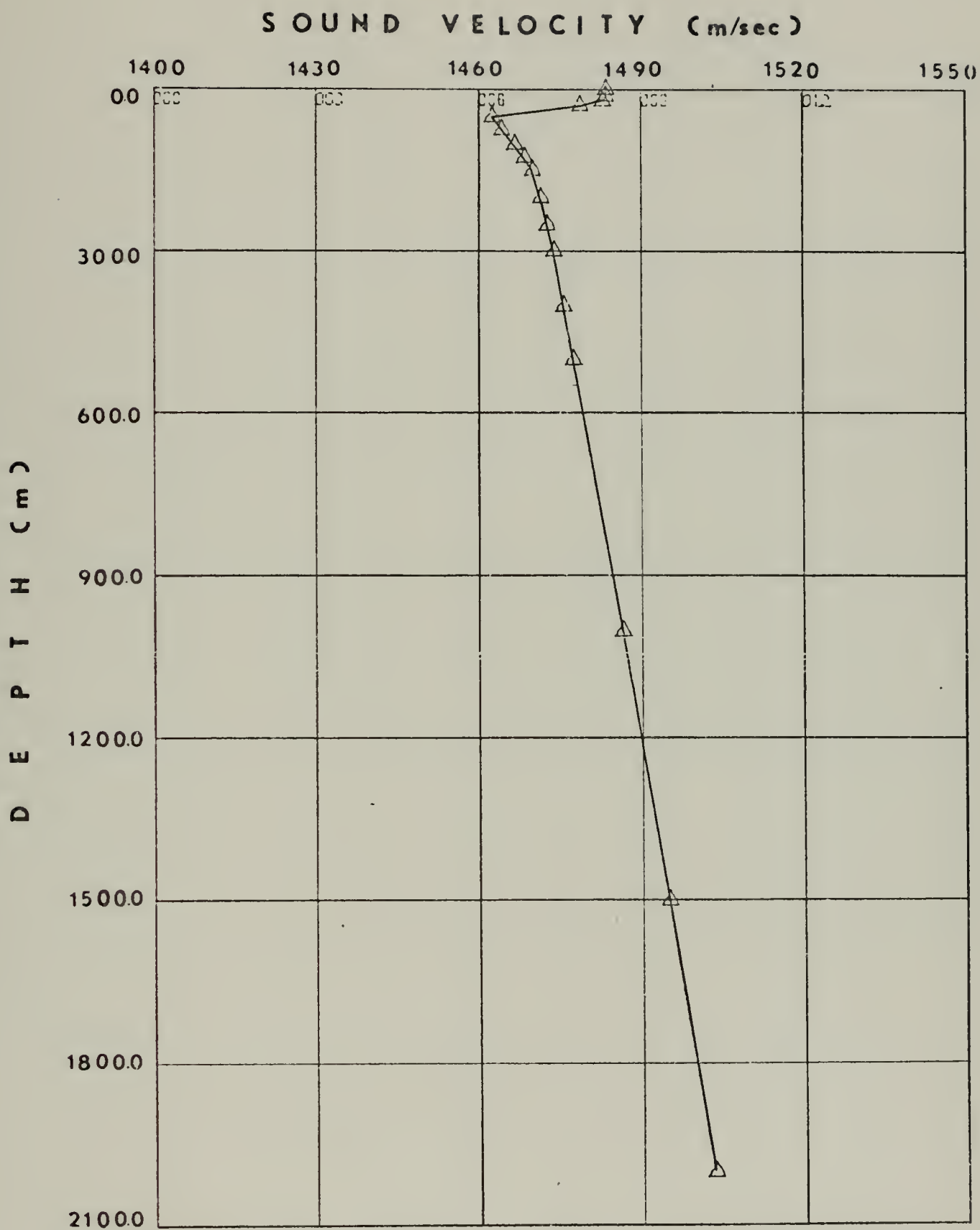


Figure 37. Average Sound Velocity Profile for November.





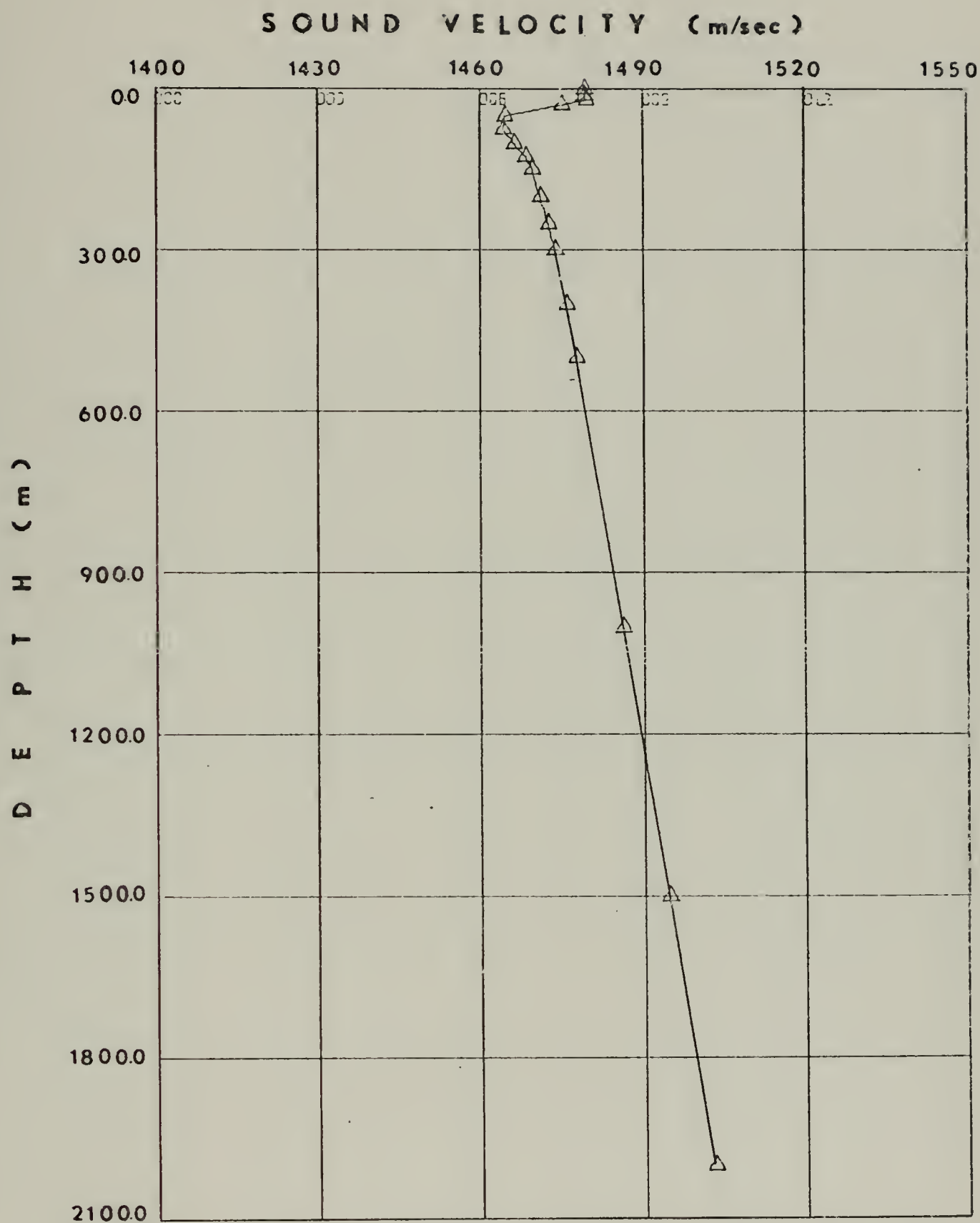


Figure 38. Average Sound Velocity Profile for December.



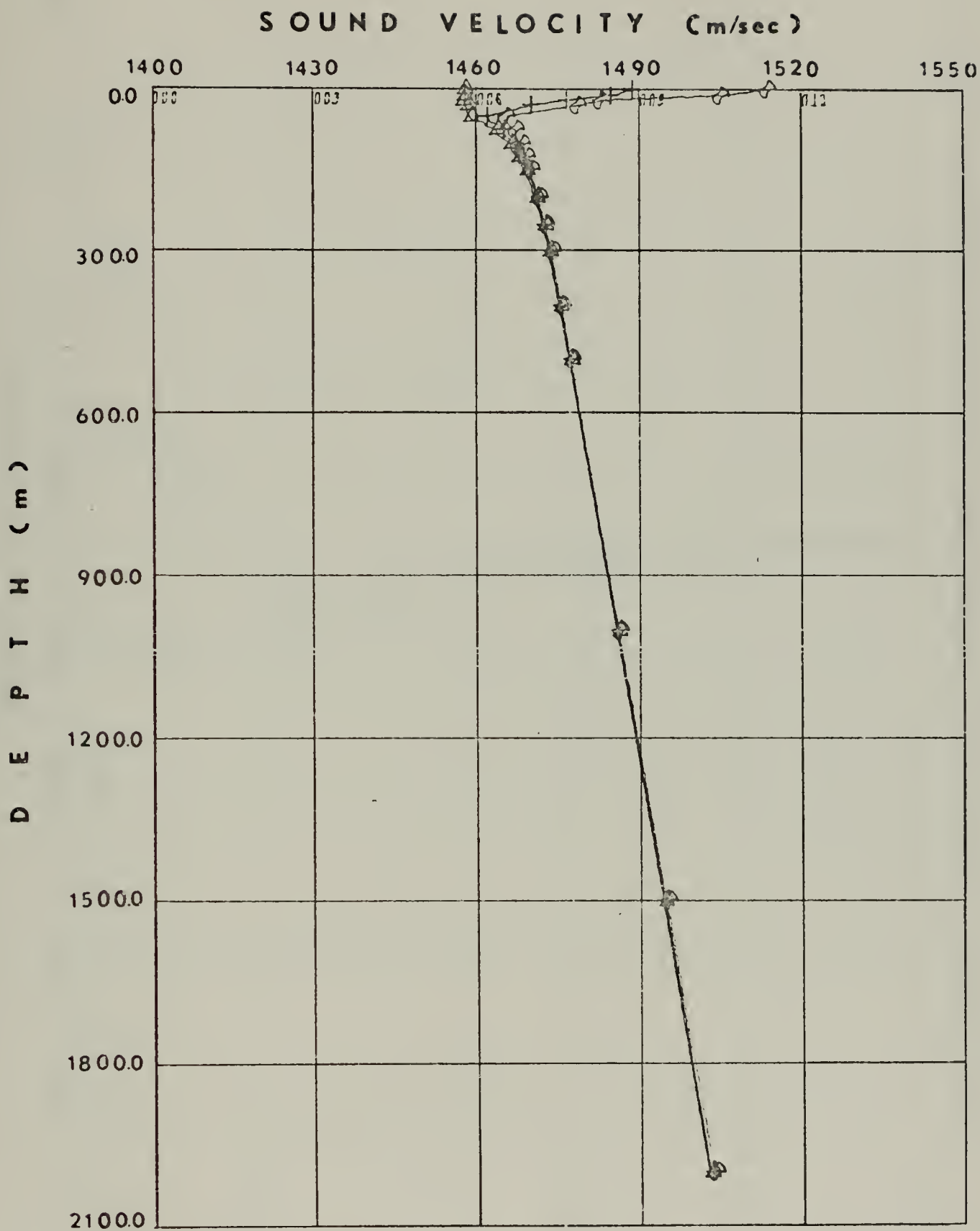


Figure 39. Annual Minimum, Maximum and Average Sound Velocity Profiles.



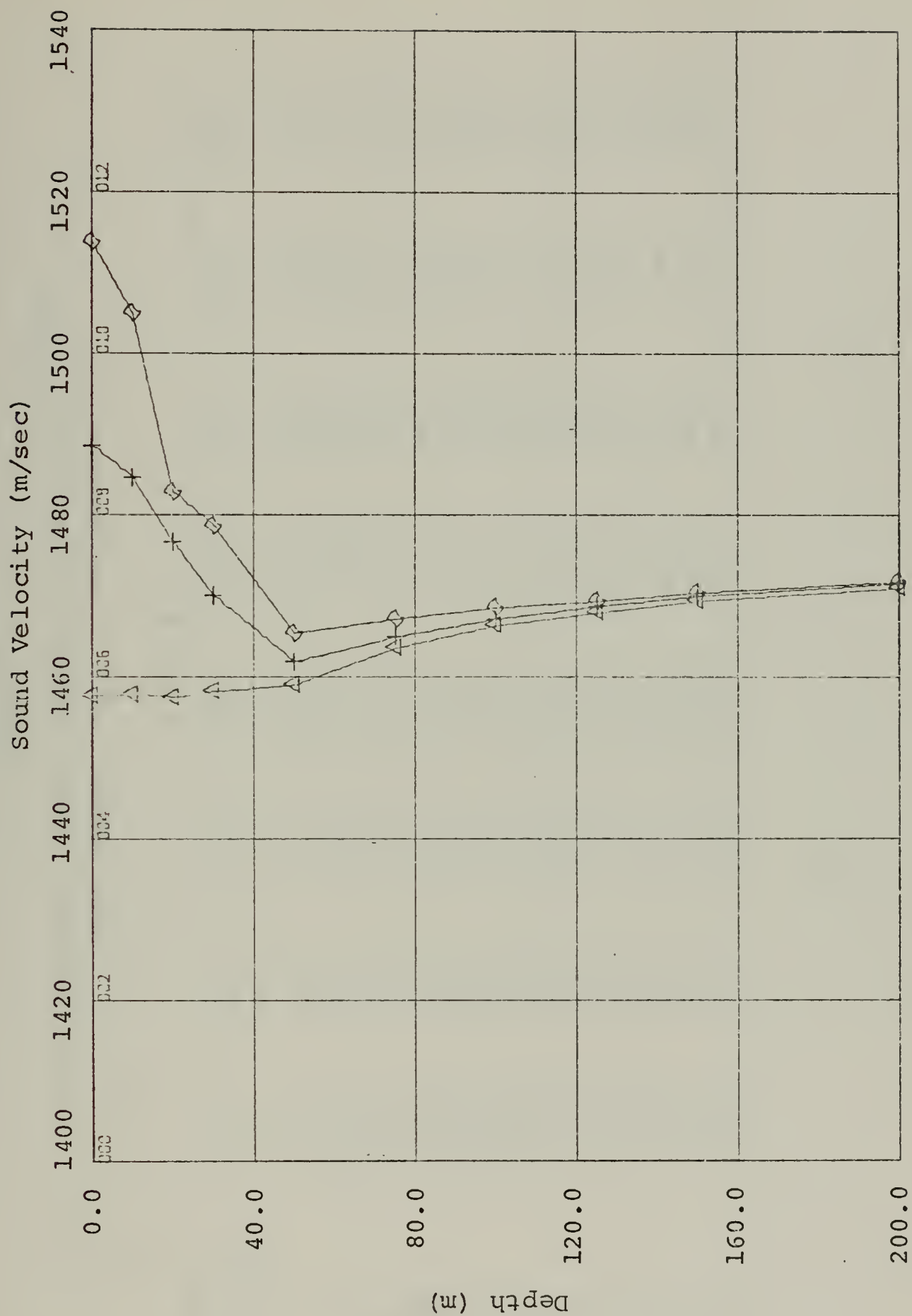


Figure 40. Annual Minimum, Maximum and Average Sound Velocity Profiles for Upper 200 m.



TABLE VI

AVERAGE MONTHLY SOUND VELOCITY (m/sec) DISTRIBUTION  
IN THE CENTRAL PART OF THE BLACK SEA

Depth (Meters)	M O N T H											
	Feb.	Mar.	May	June	July	Aug.	Nov.	Dec.				
0	1457.8	1459.1	1472.0	1507.9	1509.7	1513.9	1483.5	1479.3				
10	1457.9	1458.1	1472.4	1494.9	1501.0	1505.1	1483.6	1479.4				
20	1458.0	1457.5	1469.5	1477.4	1482.3	1479.7	1482.9	1479.5				
30	1458.3	1458.7	1464.2	1467.3	1469.5	1468.0	1478.8	1475.3				
50	1459.1	1465.5	1459.3	1461.1	1461.9	1461.1	1462.5	1464.8				
75	1463.8	1467.4	1465.1	1465.2	1465.8	1464.7	1464.4	1464.2				
100	1467.3	1468.7	1467.4	1467.6	1467.8	1466.7	1466.7	1466.6				
125	1469.0	1469.6	1469.1	1468.9	1469.2	1468.0	1468.6	1468.5				
150	1470.1	1470.5	1470.2	1470.2	1470.3	1469.5	1469.9	1469.7				
200	1471.5	1471.9	1471.8	1471.8	1471.8	1471.2	1471.5	1471.4				
250	1472.8	1473.0	1473.1	1472.9	1473.0	1472.8	1472.7	1472.8				
300	1473.9	1474.1	1474.2	1474.0	1474.0	1474.1	1473.8	1473.9				
400	1476.0	1475.9	1476.0	1475.9	1475.8	1475.9	1475.7	1475.9				
500	1477.9	1477.7	1477.9	1477.7	1477.7	1477.7	1477.6	1477.8				
1000	1486.5	1486.3	1486.7	1486.4	1486.3	1486.3	1486.5	1486.2				
1500	1495.3	1494.9	1495.4	1494.8	1494.7	1495.2	1495.1	1494.6				
2000	1503.9	1503.4	1503.5	1503.3	1503.6	1503.2	1503.4	1503.0				





TABLE VII

ANNUAL MINIMUM, MAXIMUM AND AVERAGE  
SOUND VELOCITY (m/sec) DISTRIBUTION

<u>Depth</u>	<u>Minimum</u>	<u>Maximum</u>	<u>Average</u>
0.0	1457.8	1513.9	1488.8
10.0	1457.9	1505.1	1484.7
20.0	1457.5	1482.9	1476.8
30.0	1458.3	1478.8	1470.1
50.0	1459.1	1465.5	1461.9
75.0	1463.8	1467.4	1465.2
100.0	1466.6	1468.7	1467.3
125.0	1468.0	1469.6	1468.9
150.0	1469.5	1470.5	1470.0
200.0	1471.2	1471.9	1471.7
250.0	1472.7	1473.1	1472.9
300.0	1473.8	1474.2	1474.0
400.0	1475.7	1476.0	1475.9
500.0	1477.6	1477.9	1477.7
1000.0	1486.2	1486.7	1486.4
1500.0	1494.6	1495.4	1495.0
2000.0	1503.0	1503.9	1503.4



## B. BOTTOM REFLECTION

The sea bottom plays an important role in the propagation of sound acting as an acoustical reflector. A sound ray striking the bottom will be partly reflected and partly transmitted depending on the acoustic impedance contrast. The character of the bottom topography and the bottom sediments are the most important considerations. A flat bottom of nearly uniform composition of clastic sediment provides very good bottom reflective conditions. For example, sand, would be expected to absorb a small fraction of the incident sound and consequently reflect very well. But, irregular bottom topography and poorly sorted or soft sediments tend to worsen bottom reflective conditions. Mud might be expected to absorb a large fraction of incident sound.

According to Liebermann [9], the reflection properties of bottom sediments are classified such as:

"Mud is the poorest reflector, mud-sand nearly as poor, sand-mud appreciably better, and sand the best reflector of all; stony bottoms are better reflectors than mud but worse, in general, than sand."<sup>2</sup>

The bottom reflection coefficients in the central part of the Black Sea are calculated with several assumptions, because the bathymetry and the distribution of bottom sediments are not well known, and in addition the physical properties of

---

<sup>2</sup> Liebermann, L. N., "Reflection of Sound from Coastal Sea Bottom," The Journal of the Acoustical Society of America, V. 20, No. 3, p. 305-309, May 1948.



these sediments have not been determined. Therefore, the following assumptions are necessary:

1. The bottom of the sea is smooth and uniform.
2. The bottom is covered by clay. And the physical properties of this clay are taken to be the same as gray clay, which was described by Nafe and Drake [10].

The physical properties of sea water and bottom sediments in the selected stations are represented in Table VIII.

The critical angle is the most important feature in bottom reflection. Because, as the sound hits the bottom with an angle less than critical angle, a part of the energy is transmitted to the bottom and the ray rapidly becomes weaker. But, if the sound ray hits the bottom with an angle equal to or greater than the critical angle, little acoustic energy is transmitted into the bottom.

The bottom critical angles in the Black Sea were calculated by Snell's law where the critical angle is defined by the relation [11]:

$$\sin \theta_c = \frac{C_1}{C_2}$$

where,

$\theta_c$  = Critical angle (Degrees)

$C_1$  = Sound velocity in the sea water (m/sec)

$C_2$  = Sound velocity in the bottom sediment (m/sec)

Computed critical angles in selected stations for several months are given in Table IX. It can be seen from the table, that the critical angles in the central part of the Black Sea



change from 69° 40' to 73° 19'. Therefore, any sound ray that hits the bottom with an angle greater than 73° 19' will be mostly reflected.

The bottom reflection coefficients are obtained from Rayleigh's formula. According to this formula, bottom amplitude reflection coefficients are defined by the relation [12]:

$$R = \frac{\rho_2 C_2 \cos \theta_i - \rho_1 C_1 \cos \theta_t}{\rho_2 C_2 \cos \theta_i + \rho_1 C_1 \cos \theta_t}$$

where,

R = Reflection coefficient

$\rho_1$  = Density of the sea water (g/cm<sup>3</sup>)

$C_1$  = Sound velocity in the sea water (m/sec)

$\rho_2$  = Density of the bottom sediment (g/cm<sup>3</sup>)

$C_2$  = Sound velocity in the bottom sediment (m/sec)

$\theta_i$  = Incident angle (Degrees)

$\theta_t$  = Transmitted angle (Degrees)

Reflection coefficients for each incident angle are given in Table IX. From this table, it can be observed that the reflection coefficients change very slightly with incident angle and they reach unity at the critical angle. Figure 41, 42 and 43 represent reflectivity versus incident angle diagrams for February, May and October. The data for these diagrams is obtained from Table IX.







TABLE VIII

PHYSICAL PROPERTIES OF SEA WATER  
and  
BOTTOM SEDIMENTS IN THE BLACK SEA

	February	March	May	July	August	October	November	December
Position	43°26'N 33°30'E	43°26'N 33°44'E	43°28'N 33°48'E	43°33'N 33°39'E	43°12'N 33°41'E	43°53'N 33°22'E	43°00'N 33°00'E	43°00'N 33°47'E
Sound Velocity in the Sea Water (m/sec)	1503.9	1503.4	1487.0	1503.4	1503.2	1472.2	1486.7	1473.7
Density of Sea Water (gr/cm <sup>3</sup> )	1.02871	1.02875	1.02375	1.02870	1.02871	1.01880	1.02362	1.01948
Density of Bottom Sediment (gr/cm <sup>3</sup> )	1.62000	1.62000	1.62000	1.62000	1.62000	1.62000	1.62000	1.62000
Sound Velocity in the Bottom Sed. (m/sec)	1570.0	1570.0	1570.0	1570.0	1570.0	1570.0	1570.0	1570.0



TABLE IX

MONTHLY REFLECTION COEFFICIENTS DISTRIBUTION  
in  
THE CENTRAL PART OF THE BLACK SEA

Reflection Coefficients

Incident Angle	February	March	May	July	August	October	November	December
0°	0.2435	0.2437	0.2511	0.2437	0.2437	0.2580	0.2513	0.2573
5°	0.2437	0.2438	0.2513	0.2438	0.2439	0.2583	0.2515	0.2575
10°	0.2442	0.2443	0.2519	0.2443	0.2444	0.2590	0.2521	0.2582
15°	0.2450	0.2452	0.2530	0.2452	0.2453	0.2603	0.2532	0.2595
20°	0.2463	0.2465	0.2547	0.2465	0.2466	0.2623	0.2548	0.2615
25°	0.2482	0.2483	0.2570	0.2484	0.2484	0.2651	0.2572	0.2642
30°	0.2507	0.2509	0.2602	0.2509	0.2510	0.2689	0.2604	0.2680
35°	0.2541	0.2543	0.2646	0.2543	0.2544	0.2742	0.2648	0.2732
40°	0.2588	0.2591	0.2707	0.2591	0.2592	0.2816	0.2709	0.2804
45°	0.2655	0.2658	0.2794	0.2659	0.2660	0.2921	0.2797	0.2907
50°	0.2753	0.2757	0.2922	0.2758	0.2759	0.3079	0.2926	0.3062
55°	0.2905	0.2910	0.3124	0.2910	0.2913	0.3329	0.3128	0.3307
60°	0.3158	0.3166	0.3469	0.3166	0.3169	0.3770	0.3475	0.3737
65°	0.3641	0.3654	0.4168	0.3654	0.3660	0.4722	0.4178	0.4661
70°	0.4862	0.4896	0.6393	0.4896	0.4910	1.0000	0.6431	1.0000
71°	0.5382	0.5428	0.8020	0.5429	0.5447	1.0000	0.8124	1.0000
72°	0.6181	0.6254	1.0000	0.6254	0.6283	1.0000	1.0000	1.0000
73°	0.7815	0.8013	1.0000	0.8014	0.8101	1.0000	1.0000	1.0000
74-90°	1.0000	1.0000	1.0000	1.0000	1.0000	1.0000	1.0000	1.0000
Critical Angle	73°19'	73°15'	71°17'	73°15'	73°14'	69°40'	71°15'	69°50'



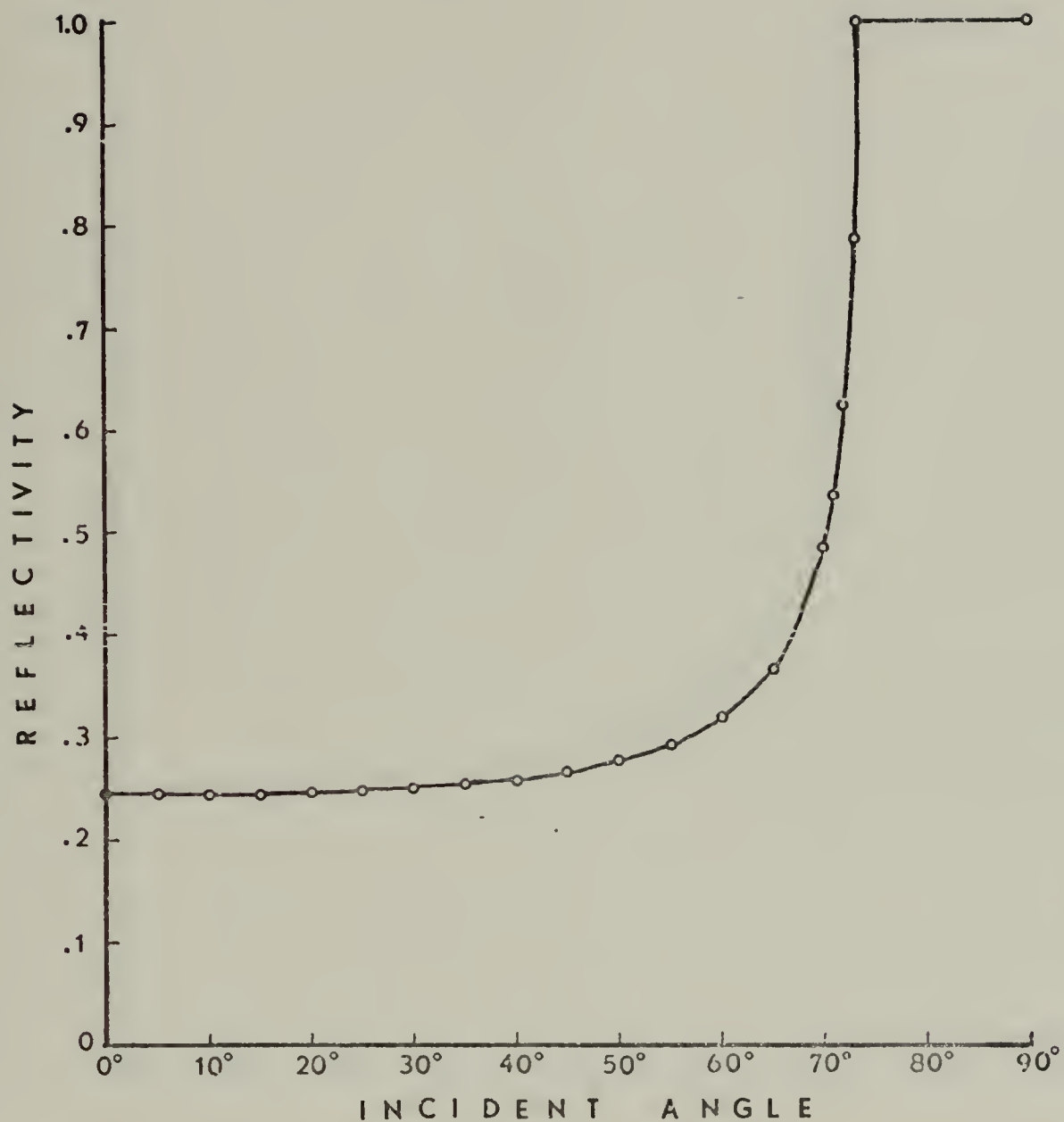


Figure 41. Reflectivity Versus Incident Angle Diagram for February.



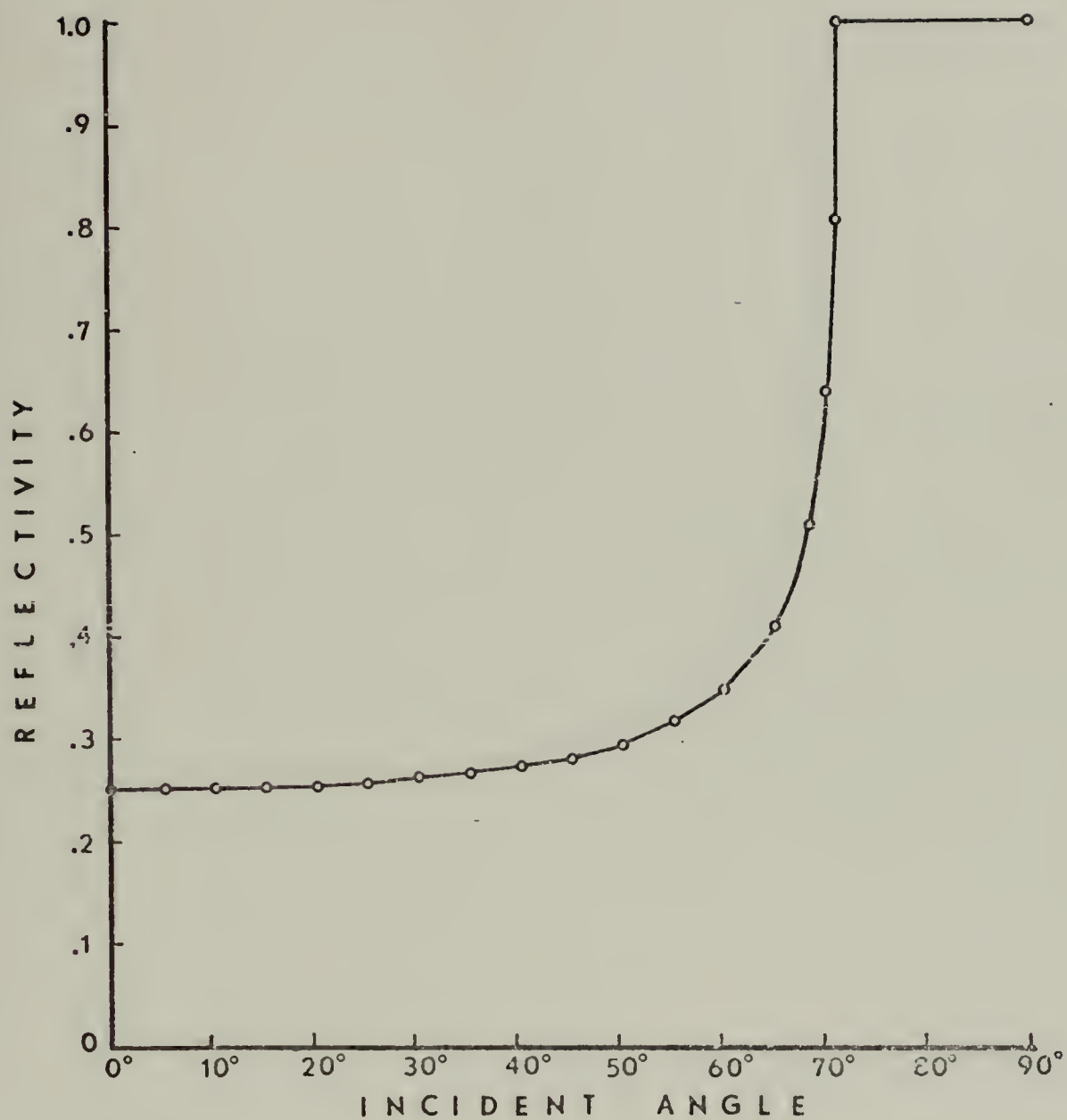


Figure 42. Reflectivity Versus Incident Angle Diagram for May.





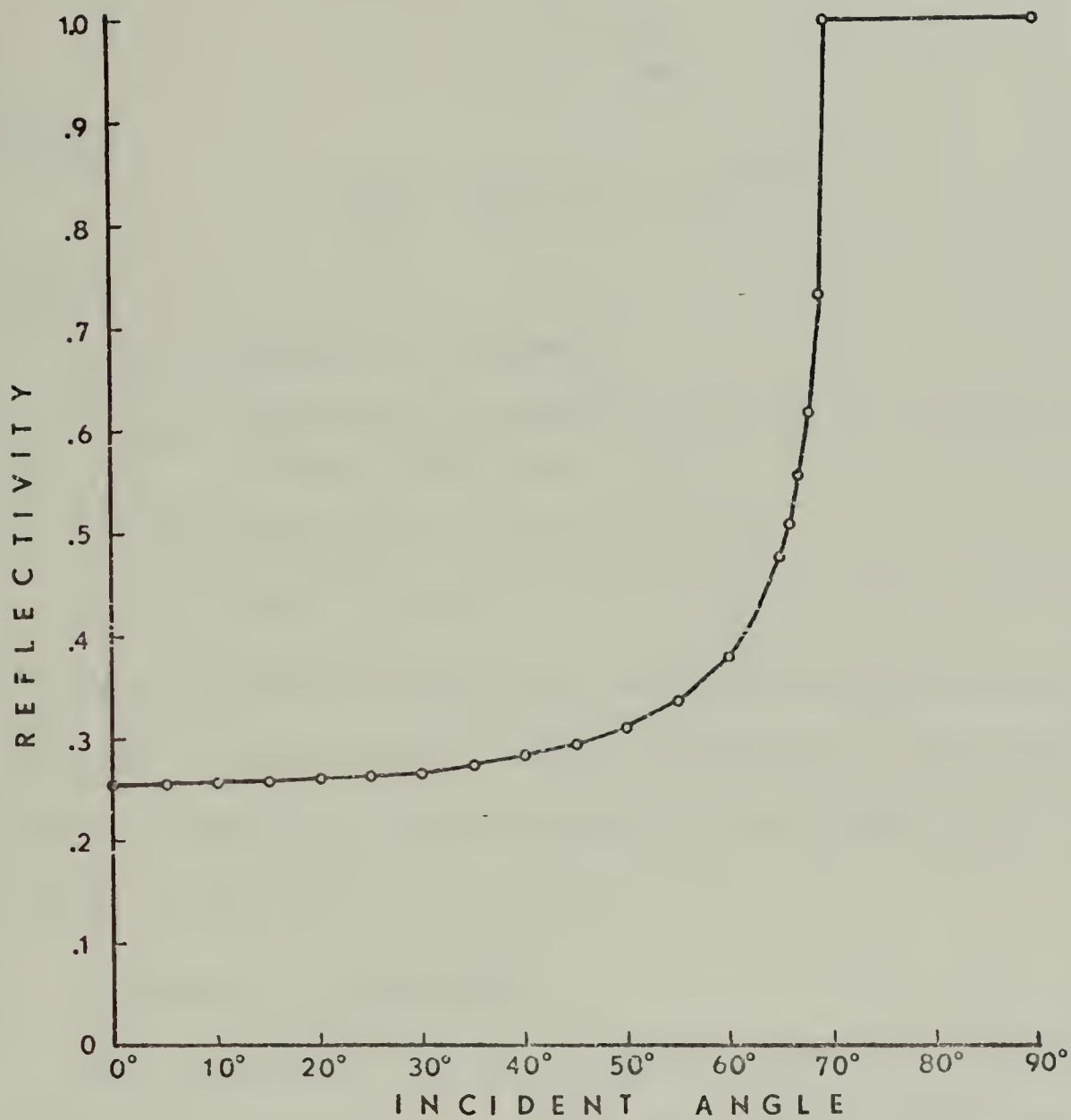


Figure 43. Reflectivity Versus Incident Angle Diagram for October.



### C. DUCT PROPAGATION

Duct propagation in the Black Sea is limited as the mixed layer is very shallow if present. The maximum wavelength that can be contained in a duct is given by:

$$f_c = \frac{C}{\lambda_{\max}}$$

where,

$$\lambda_{\max} = 4.7 \times 10^{-3} H^{3/2}$$

and,

$f_c$  = Cutoff low frequency

$\lambda_{\max}$  = Maximum wavelength that can be trapped in a  
mixed layer duct (ft)

H = Mixed layer duct thick (ft)

C = Sound velocity in the mixed layer duct (ft/sec)

For frequencies below the cutoff frequency attenuation increases rapidly during duct propagation. Low cutoff frequency values for several months in the Black Sea are represented in Table X.

### D. SURFACE BACKSCATTERING

The surface of the sea plays an important part in the propagation of acoustic energy by confining and dispersing sound that impinges upon it. If, the surface of the sea was an ideal plane surface, it should act like a mirror, merely reflecting any incident sound energy into the reflected angle and producing no distribution of energy other than this single change of direction. But the sea surface is generally



rough, when a pulse of underwater sound strikes the surface, a portion of its energy is returned or reradiates back to the source. This reradiation of sound is called sea surface backscattering [13].

The degree of scattering of the sea surface has been found to change with grazing angle, frequency and the roughness of the surface.

The sea surface backscattering strength in the central part of the Black Sea for several months was calculated using the formula of Schulkin and Shaffer's [14]. According to this formula, backscattering strength is given by the relation:

$$S_s = 10 \text{ Log } (fh \sin\theta)^{0.99} - 45.3$$

where,

$S_s$  = Sea surface backscattering strength

$h$  = The mean peak-trough sea surface roughness (ft)

$f$  = Frequency (kHz)

$\theta$  = Grazing angle (Degrees)

To obtain backscattering strength, a relationship was used between sea surface roughness and wind speed which was also given by Schulkin and Shaffer as:

$$h = 0.026 v^{5/2}$$

where,

$V$  = Wind speed (knt)

$h$  = Sea surface roughness (ft)



Monthly wind speed values in the central part of the Black Sea were obtained from surface wind charts [16].

Table XI gives backscattering strength as found from the above formula. The frequency used to calculate backscattering strength was the lowest frequency that could be contained in the surface duct. Frequencies lower than this would be strongly attenuated by leakage from the duct. Figures 44 through 50 are obtained from Table XI, and show backscattering versus grazing angle diagrams for several months. Tables XII, XIII, and XIV give backscattering strength values calculated for 10, 15 and 20 kHz.

Given the backscattering strength ( $S_s$ ) as a function of grazing angle ( $\theta$ ) the reverberation level  $RL_s$  can be calculated by the following relationship [20]:

$$RL_s = SL - 40 \log r + S_s + 10 \log A$$

where,

$$SL = \text{Source level}$$

$$r = \text{Range}$$

$$A = \frac{C\gamma}{2} \phi_r$$

and

$$C = \text{Speed of sound}$$

$$\gamma = \text{Ping length}$$

$$\phi_r = \text{The equivalent ideal width}$$

The reverberation level expected for a given range can be determined if the ray path from the source is known. The ray diagram provides this information





TABLE X  
MONTHLY SURFACE BACKSCATTERING PARAMETERS  
in  
THE CENTRAL PART OF THE BLACK SEA

Month	Wind Velocity (Knt.)	Sea Surface Roughness (Ft.)	Cutoff Frequency (Hz.)	Duct Thickness (Ff.)
May	16.71	2.985	1915.14	66.0
June	19.43	4.343	5523.68	33.0
July	5.83	0.214	5558.92	33.0
August	10.49	0.935	3079.46	49.0
October	23.51	7.020	1411.60	82.0
November	6.99	0.338	1054.70	99.0
December	6.99	0.338	1395.01	82.0



TABLE XI  
MONTHLY SURFACE BACKSCATTERING STRENGTH (db)  
in  
THE CENTRAL PART OF THE BLACK SEA FOR CUTOFF FREQUENCIES

Grazing Angle (Degrees)	Surface Backscattering Strength					
	May	June	July	August	October	November
1	-55.2	-49.0	-61.9	-58.2	-52.8	-67.1
5	-48.3	-42.1	-55.0	-51.2	-45.9	-60.2
10	-45.3	-39.2	-52.1	-48.3	-42.9	-57.3
15	-43.6	-37.5	-50.4	-46.6	-41.3	-55.5
20	-42.4	-36.3	-49.2	-45.4	-40.0	-54.3
25	-41.5	-35.3	-48.3	-44.5	-39.0	-53.1
30	-40.8	-34.6	-47.5	-43.7	-38.4	-52.2
35	-40.2	-34.0	-46.9	-43.1	-37.8	-51.5
40	-39.7	-33.5	-46.4	-42.7	-37.3	-50.9
45	-39.3	-33.1	-46.0	-42.2	-36.9	-50.4
50	-38.9	-32.8	-45.7	-41.9	-36.6	-50.0
55	-38.6	-32.5	-45.4	-41.6	-36.3	-49.7
60	-38.4	-32.3	-45.2	-41.4	-36.1	-49.4
65	-38.2	-32.0	-44.9	-41.2	-35.9	-49.1
70	-38.0	-31.9	-44.8	-41.0	-35.7	-49.0
75	-37.9	-31.8	-44.7	-40.9	-35.6	-48.8
80	-37.9	-31.7	-44.6	-40.8	-35.5	-48.7
85	-37.8	-31.7	-44.6	-40.8	-35.5	-48.6
90	-37.8	-31.6	-44.5	-40.7	-35.4	-48.5



TABLE XII

MONTHLY SURFACE BACKSCATTERING STRENGTH (db)  
in  
THE CENTRAL PART OF THE BLACK SEA FOR 10 kHz

Grazing Angle (Degrees)	Surface Backscattering Strength											
	February	March	May	June	July	August	October	November	December			
1	-46.5	-52.0	-48.1	-46.5	-59.4	-53.1	-44.5	-57.5	-57.5			
5	-39.6	-45.1	-41.2	-39.6	-52.5	-46.2	-37.5	-50.6	-50.6			
10	-36.6	-42.1	-38.3	-36.6	-49.6	-43.3	-34.6	-47.6	-47.6			
15	-34.9	-40.4	-36.5	-34.9	-47.9	-41.5	-32.9	-45.9	-45.9			
20	-33.7	-39.2	-35.3	-33.7	-46.7	-40.3	-31.7	-44.7	-44.7			
25	-32.8	-38.3	-34.4	-32.8	-45.7	-39.4	-30.8	-43.8	-43.8			
30	-32.1	-37.6	-33.7	-32.1	-45.0	-38.7	-30.0	-43.1	-43.1			
35	-31.5	-37.0	-33.1	-31.5	-44.4	-38.1	-29.4	-42.5	-42.5			
40	-31.0	-36.5	-32.6	-31.0	-44.0	-37.6	-29.0	-42.0	-42.0			
45	-30.6	-36.1	-32.2	-30.6	-43.5	-37.2	-28.5	-41.6	-41.6			
50	-30.2	-35.7	-31.9	-30.2	-43.2	-36.8	-28.2	-41.2	-41.2			
55	-29.9	-35.4	-31.6	-29.9	-42.9	-36.6	-28.0	-41.0	-41.0			
60	-29.7	-35.2	-31.3	-29.7	-42.7	-36.3	-27.7	-40.7	-40.7			
65	-29.5	-35.0	-31.1	-29.5	-42.5	-36.2	-27.5	-40.5	-40.5			
70	-29.4	-34.9	-31.0	-29.4	-42.3	-36.0	-27.3	-40.4	-40.4			
75	-29.3	-34.7	-30.9	-29.3	-42.2	-35.9	-27.2	-40.3	-40.3			
80	-29.2	-34.6	-30.8	-29.2	-42.1	-35.8	-27.1	-40.2	-40.2			
85	-29.1	-34.6	-30.7	-29.1	-42.0	-35.7	-27.0	-40.1	-40.1			
90	-29.1	-34.6	-30.7	-29.1	-42.0	-35.7	-27.0	-40.1	-40.1			



TABLE XIII  
MONTHLY SURFACE BACKSCATTERING STRENGTH (db)  
IN THE CENTRAL PART OF THE BLACK SEA FOR 15 KHz

Grazing Angle (Degrees)	Surface Backscattering Strength											
	February	March	May	June	July	August	October	November	December			
1	-44.8	-50.3	-46.4	-44.8	-57.7	-51.4	-42.7	-55.8	-55.8			
5	-37.9	-43.3	-39.5	-37.9	-50.8	-44.5	-35.8	-48.8	-48.8			
10	-34.9	-40.4	-36.5	-34.9	-47.8	-41.5	-32.8	-45.9	-45.9			
15	-33.2	-38.7	-34.8	-33.2	-46.1	-39.8	-31.1	-44.2	-44.2			
20	-32.0	-37.5	-33.6	-32.0	-44.9	-38.6	-29.9	-43.0	-43.0			
25	-31.1	-36.6	-32.7	-31.1	-44.0	-37.7	-29.0	-42.1	-42.1			
30	-30.3	-35.8	-32.0	-30.3	-43.3	-37.0	-28.3	-41.3	-41.3			
35	-29.7	-35.2	-31.4	-29.7	-42.7	-36.4	-27.7	-40.7	-40.7			
40	-29.3	-34.7	-30.9	-29.3	-42.2	-35.9	-27.2	-40.2	-40.2			
45	-28.9	-34.3	-30.5	-28.9	-41.8	-35.5	-26.8	-39.8	-39.8			
50	-28.5	-34.0	-30.1	-28.5	-41.4	-35.1	-26.5	-39.5	-39.5			
55	-28.2	-33.7	-29.8	-28.2	-41.2	-34.8	-26.2	-39.2	-39.2			
60	-28.0	-33.5	-29.6	-28.0	-41.0	-34.6	-26.0	-39.0	-39.0			
65	-27.8	-33.3	-29.4	-27.8	-40.7	-34.4	-25.7	-38.8	-38.8			
70	-27.6	-33.1	-29.2	-27.6	-40.6	-34.3	-25.6	-38.6	-38.6			
75	-27.5	-33.0	-29.1	-27.5	-40.5	-34.2	-25.5	-38.5	-38.5			
80	-27.4	-32.9	-29.0	-27.4	-40.4	-34.1	-25.4	-38.4	-38.4			
85	-27.3	-32.8	-29.9	-27.3	-40.3	-34.0	-25.3	-38.3	-38.3			
90	-27.3	-32.8	-29.9	-27.3	-40.3	-34.0	-25.3	-38.3	-38.3			





TABLE XIV

MONTHLY SURFACE BACKSCATTERING STRENGTH (db)  
IN THE CENTRAL PART OF THE BLACK SEA FOR 20 kHz

Grazing Angle (Degrees)	Surface Backscattering Strength										
	February	March	May	June	July	August	October	November	December		
1	-43.5	-49.0	-45.1	-43.5	-56.5	-50.2	-41.5	-54.5	-54.2		
5	-35.8	-42.1	-38.2	-35.8	-49.5	-43.2	-34.6	-47.6	-47.6		
10	-33.7	-39.1	-35.3	-33.7	-45.6	-40.3	-31.6	-44.6	-44.6		
15	-31.9	-37.4	-33.6	-31.9	-44.9	-38.6	-29.8	-42.9	-42.9		
20	-30.7	-36.2	-32.4	-30.7	-43.7	-37.4	-28.9	-41.7	-41.7		
25	-29.8	-35.3	-31.4	-29.8	-42.8	-36.4	-27.8	-40.8	-40.8		
30	-29.1	-34.6	-30.7	-29.1	-42.0	-35.7	-27.1	-40.1	-40.1		
35	-28.5	-34.0	-30.1	-28.5	-41.5	-35.1	-26.5	-39.5	-39.5		
40	-28.0	-33.5	-29.6	-28.0	-41.0	-34.6	-26.0	-39.0	-39.0		
45	-27.6	-33.1	-29.2	-27.6	-40.5	-34.2	-25.6	-38.6	-38.6		
50	-27.3	-32.8	-28.9	-27.3	-40.2	-33.9	-25.2	-38.3	-38.3		
55	-27.0	-32.5	-28.6	-27.0	-40.0	-33.6	-24.9	-38.0	-38.0		
60	-26.7	-32.2	-28.4	-26.7	-39.7	-33.4	-24.7	-37.7	-37.7		
65	-26.5	-32.0	-28.2	-26.5	-39.5	-33.2	-24.5	-37.5	-37.5		
70	-26.4	-31.9	-28.0	-26.4	-39.3	-33.0	-24.3	-37.4	-37.4		
75	-26.3	-31.8	-27.9	-26.3	-39.2	-32.9	-24.2	-37.3	-37.3		
80	-26.2	-31.7	-27.8	-26.2	-39.1	-32.8	-24.2	-37.2	-37.2		
85	-26.1	-31.6	-27.7	-26.1	-39.0	-32.7	-24.1	-37.1	-37.1		
90	-26.1	-31.6	-27.7	-26.1	-39.0	-32.7	-24.1	-37.1	-37.1		



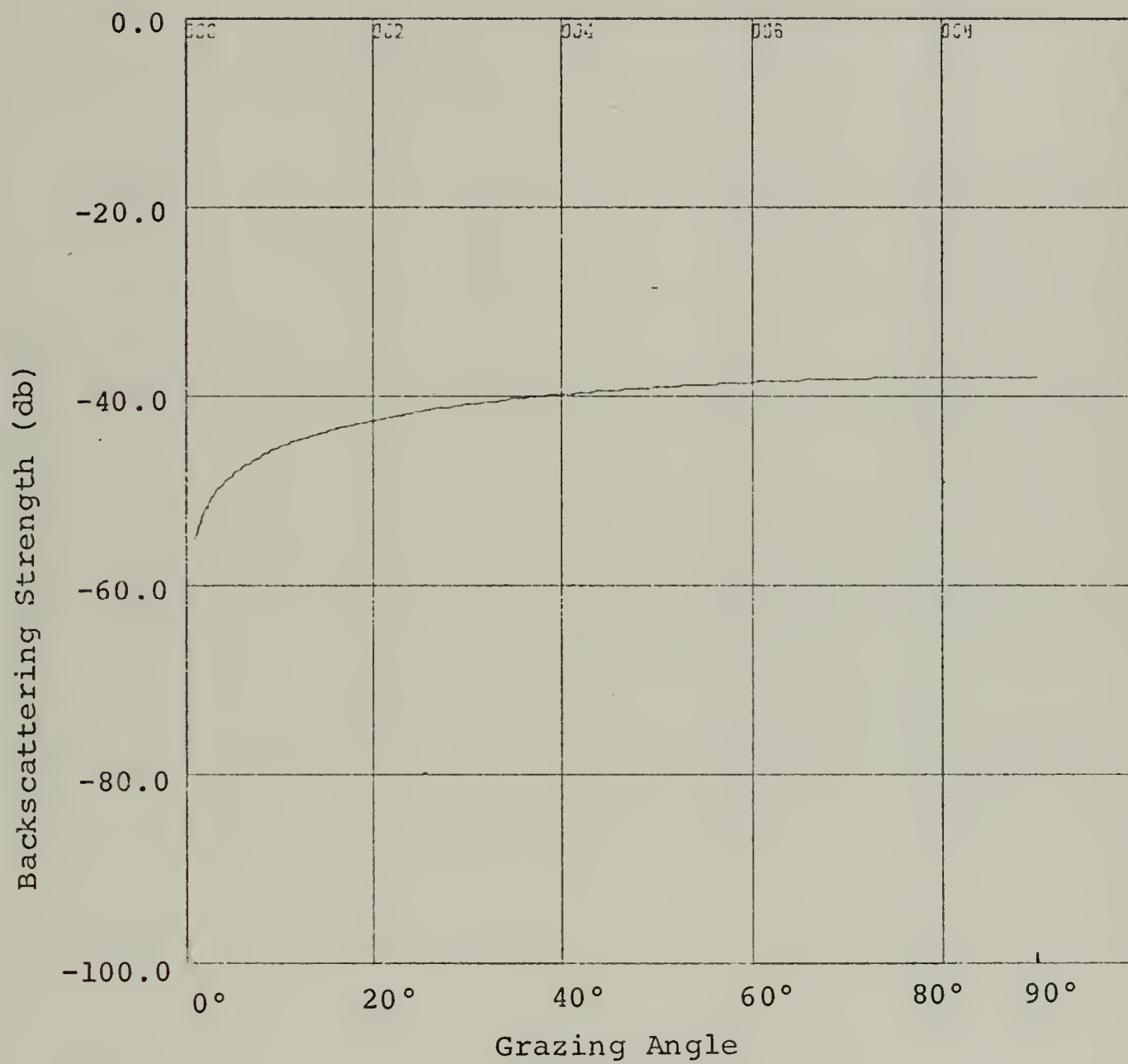


Figure 44. Surface Backscattering Strength Versus Grazing Angle Diagram for May.



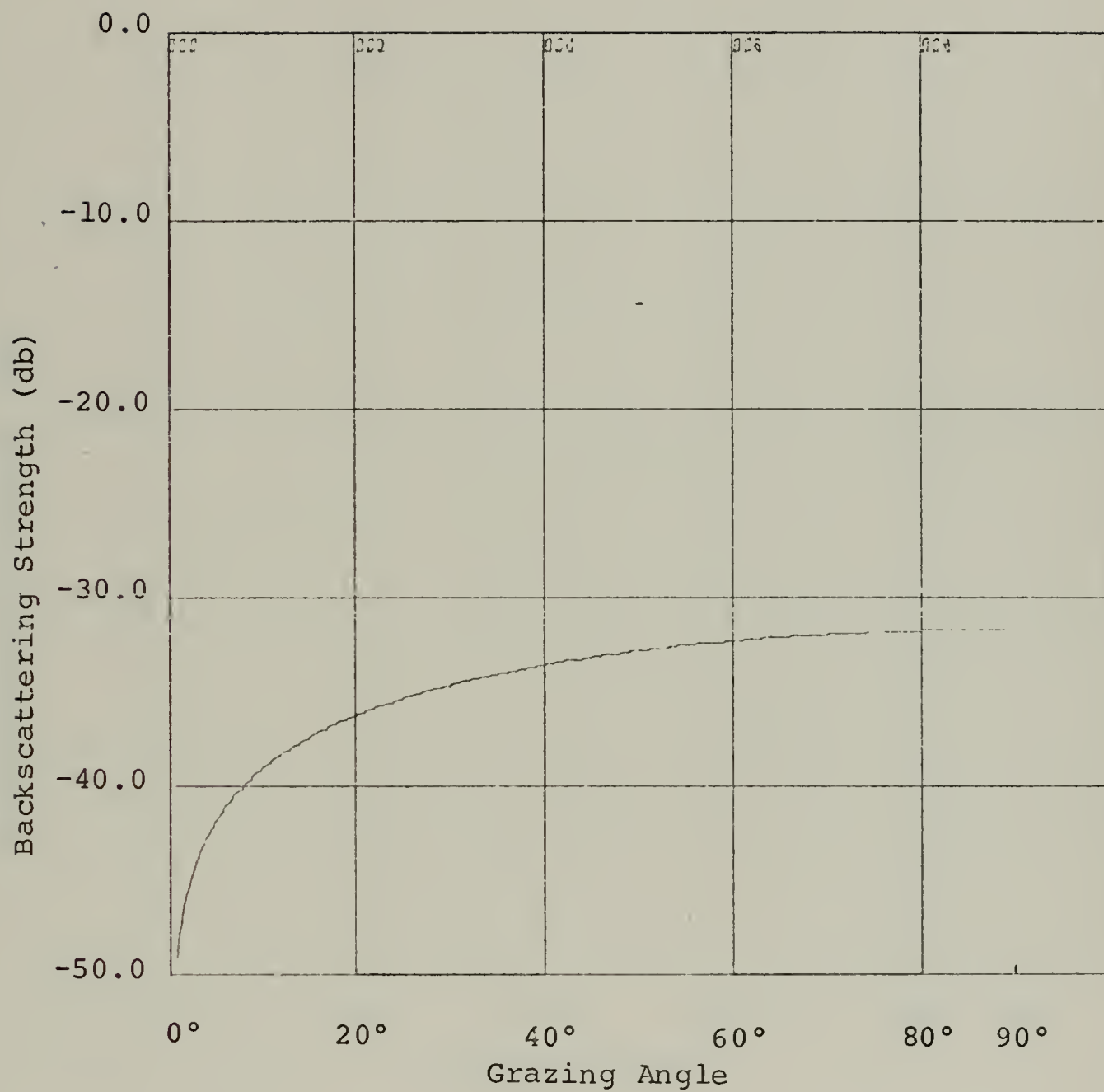


Figure 45. Surface Backscattering Strength Versus Grazing Angle Diagram for June.



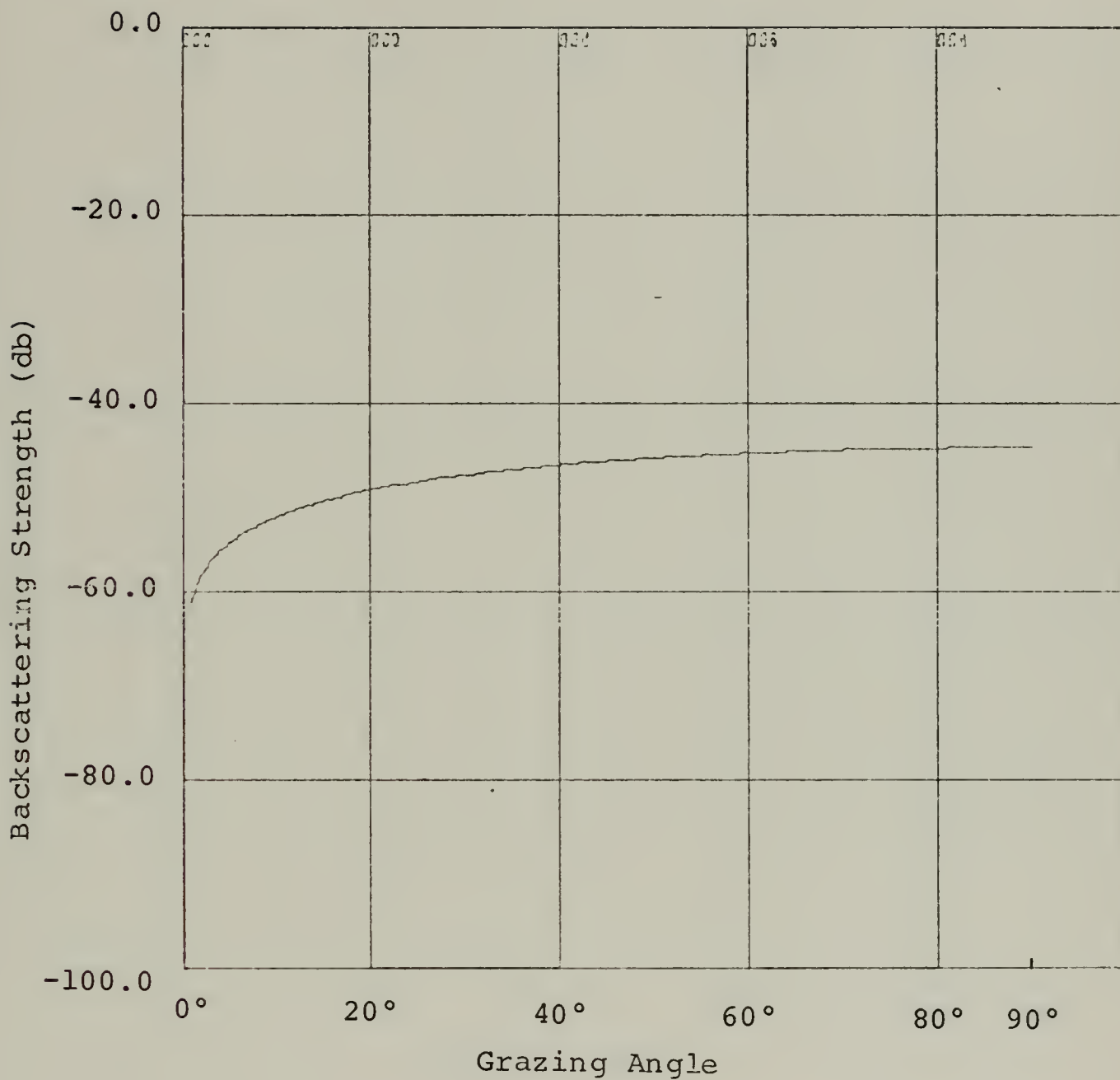


Figure 46. Surface Backscattering Strength Versus Grazing Angle Diagram for July.





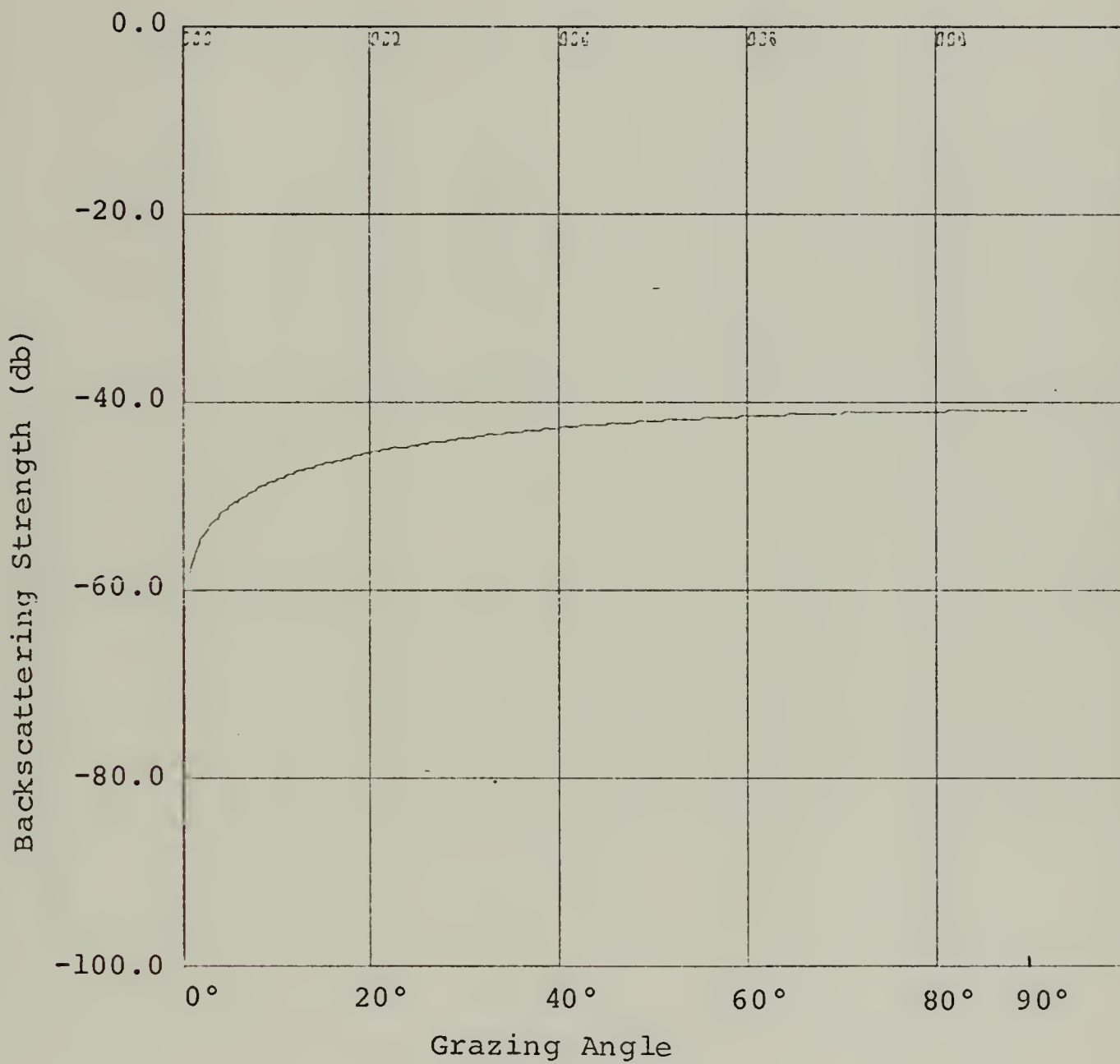


Figure 47. Surface Backscattering Strength Versus Grazing Angle Diagram for August.



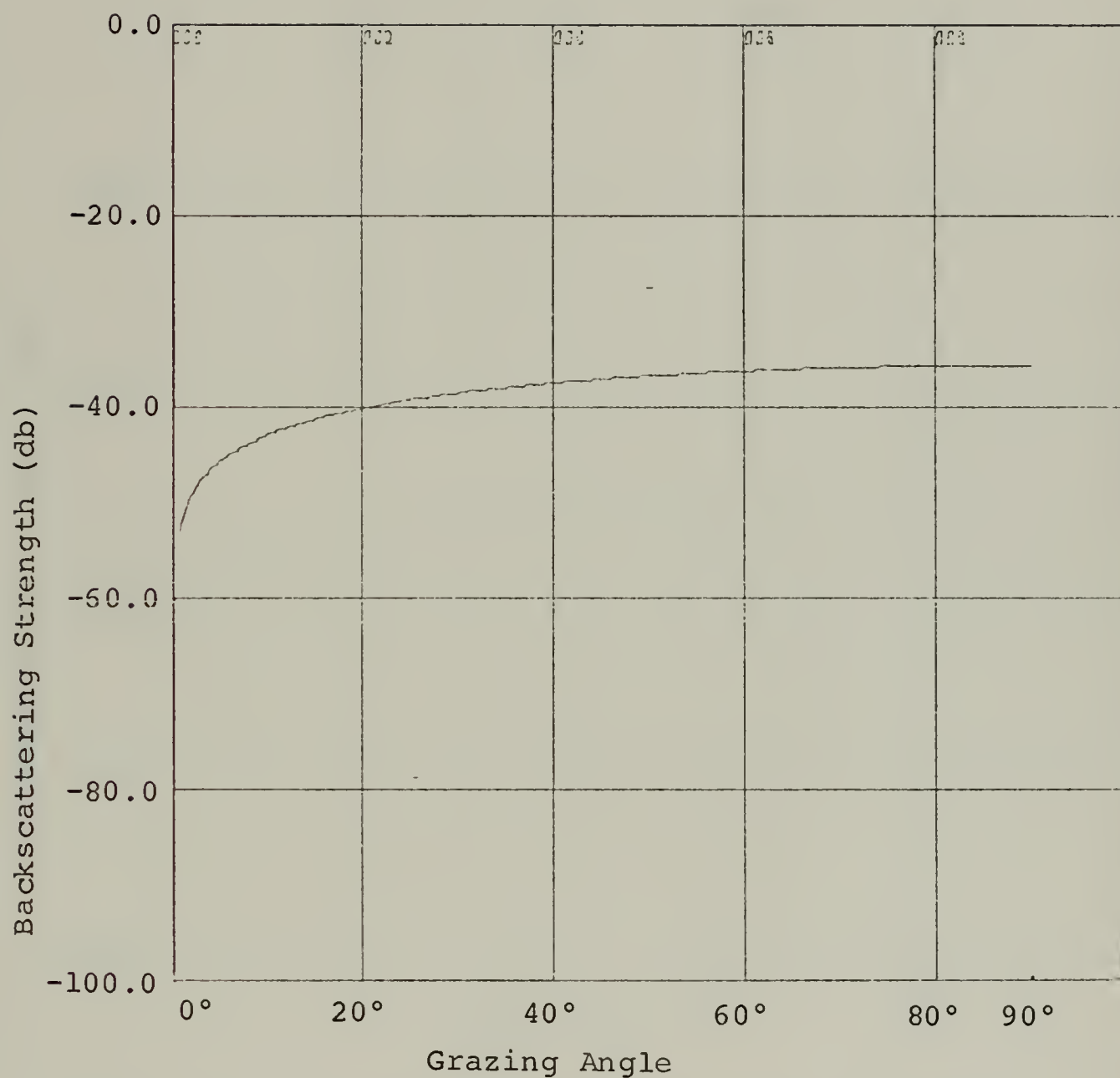


Figure 48. Surface Backscattering Strength Versus Grazing Angle Diagram for October.



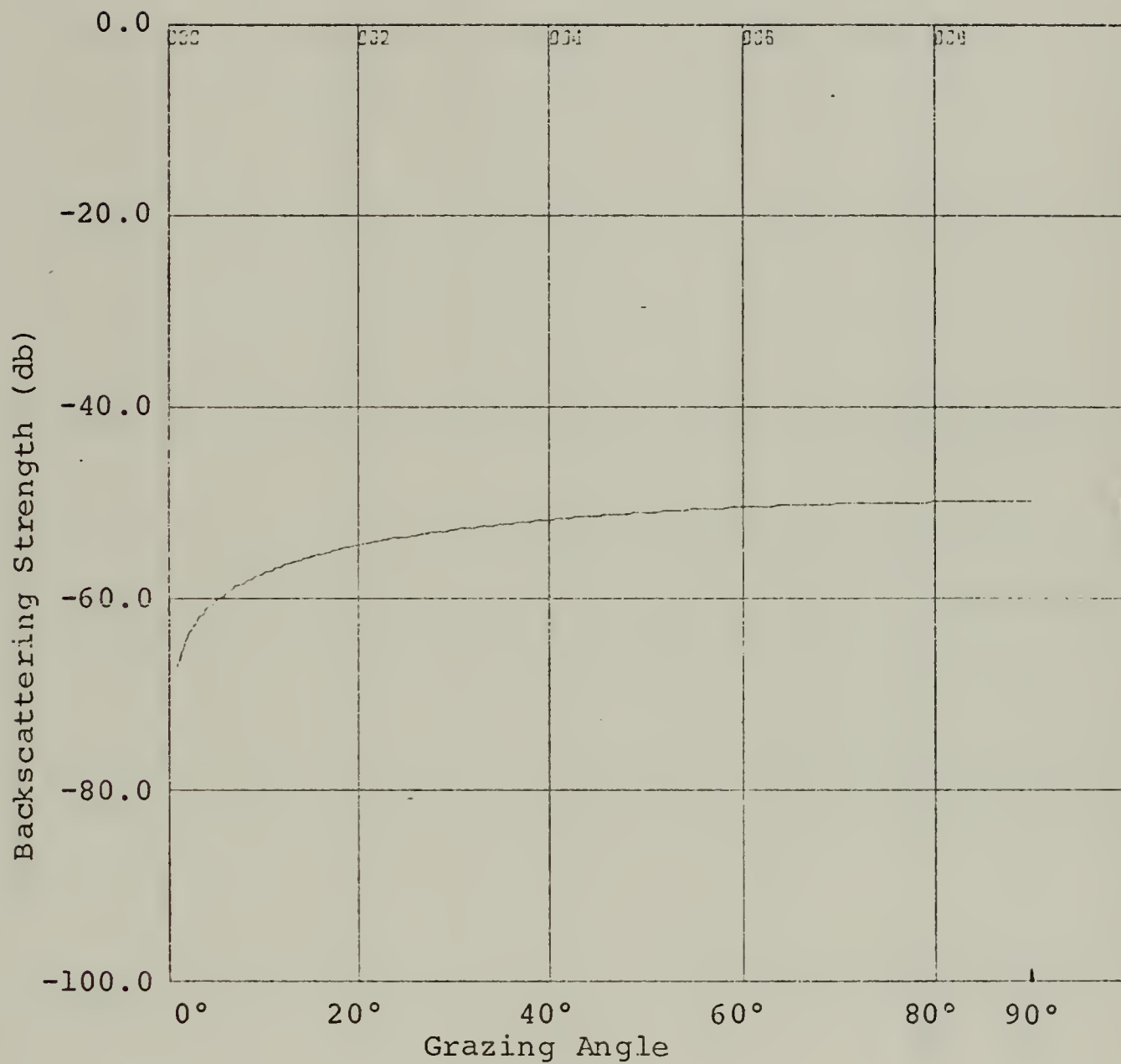


Figure 49. Surface Backscattering Strength Versus Grazing Angle Diagram for November.



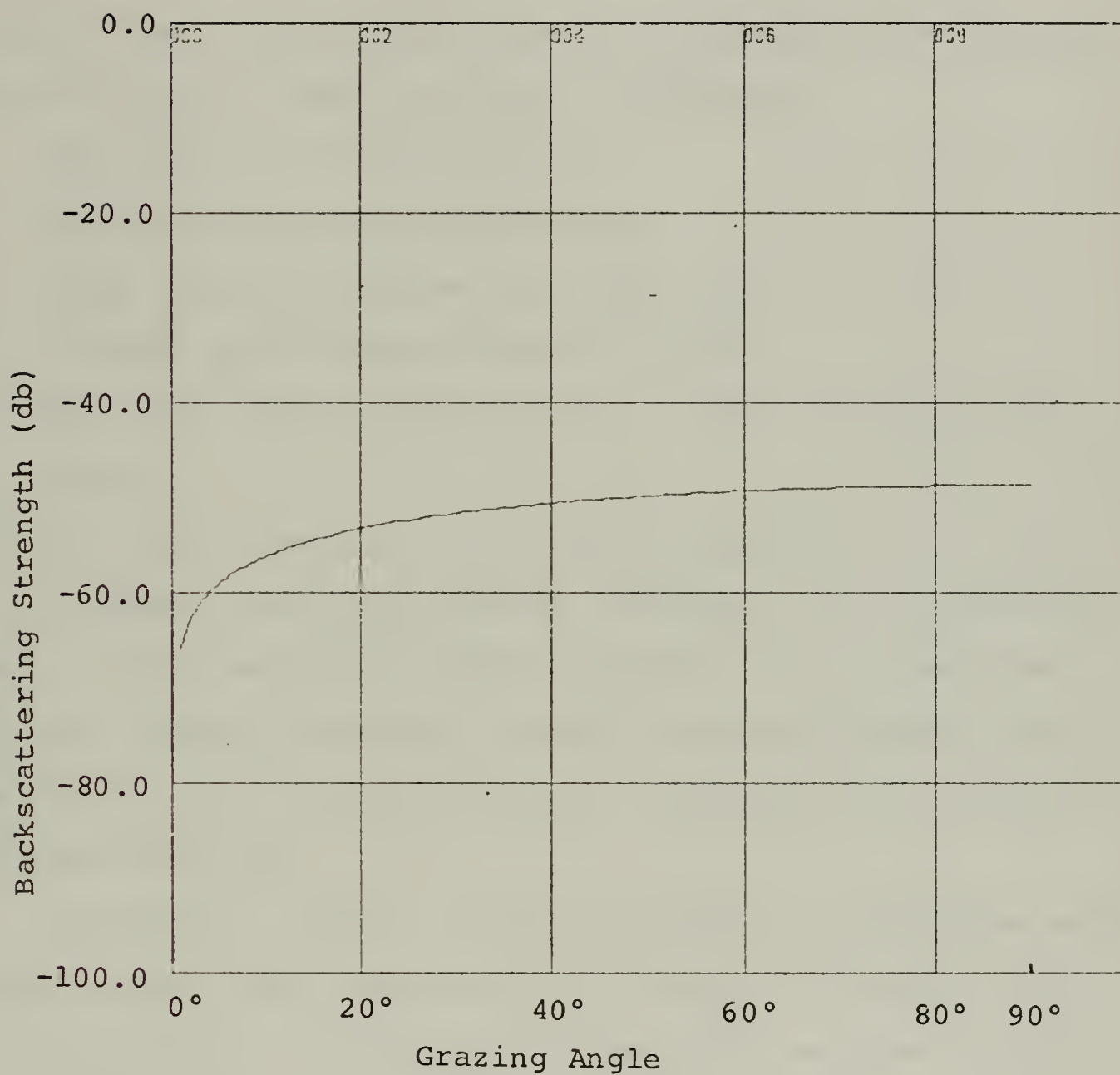


Figure 50. Surface Backscattering Strength Versus Grazing Angle Diagram for December.





## E. RAY DIAGRAMS

The ray diagrams for several months in the central part of the Black Sea are presented in Figures 51, 52, 53, 54, 55, 56, 57, and 58. The ray diagrams were obtained using a sophisticated digital ray trace program from Fleet Numerical Weather Central (FNWC), Monterey, California.

Data inputs to the program are:

1. Acoustic source depth is 20 feet.
2. Sound velocity profiles from Table VI.
3. A smooth flat bottom of depth 2,000 m.
4. Rays with source angles between  $-2$  and  $+20$  degrees are traced.
5. Rays were traced out to a maximum range of 34 N. Miles.

A typical winter ray diagram (February) for the central part of the Black Sea is shown in Figure 51. As mentioned earlier, during the winter, a positive sound velocity gradient exists from surface to bottom. Therefore, all rays are refracted upwards.

In February, between  $-2$  and  $+16$  degrees transmission angle, sound reaches long ranges only by repeated reflections from the sea surface, to which it is repeatedly returned by upward refraction (Refracted Surface - Reflected) path. The refraction is strong in the upper layers and 290 feet is the maximum depth to penetration for rays having an angle of depression less than  $6^\circ$  resulting in duct like propagation in the upper layers. This surface duct would be uniformly in sonified for frequencies above 207.34 Hz, the cutoff frequency.



Beyond a +16 degrees angle, bottom incident sound rays are reflected. The transmission angles between +16 and +20 degrees reach the bottom with incident angles of 76 - 83°. Therefore, almost 100 percent of the initial transmitted energy would be available in the upper layers. (According to Table IX). However, beyond the 21°55' degrees transmission angle, the rays would be strongly absorbed in the sea bottom.

Horizontal range from the source to the first surface reflection is 39,020 yd for the +14 degrees transmission angle in February.

Similar sound ray propagation is seen during March. The bottom reflectivity is unity beyond the critical angle (73° 15'). And, at angles greater than 21°51' sound energy will be strongly absorbed by the sea bottom.

Convergence zone formation exists only during early winter (December), because at a well defined sound channel at depths of 50 - 75 m (Figure 58). Therefore, the ray that leaves the source between +2 and +10 degrees will be refracted downward at steep angles until it crosses the axis of the sound channel, after which it will be refracted upward until it is horizontal, finally turning upward and crossing the axis, arriving at the surface once again horizontally. The convergence zone is composed of these rays which penetrate below the sound channel axis.

Convergence zone width with +2 to +10 degrees transmission angles in December is 17,204 yd and horizontal range from



the source to the first surface reflection is 39,020 yd for +10 degrees transmission angle.

The transmission angles between +12 and +20 degrees reach the bottom with  $84^{\circ}02'$  -  $72^{\circ}29'$  degrees incident angles. Therefore, bottom reflectivity is almost unity due to Table IX. The critical angle for December has been previously calculated as  $69^{\circ}50'$ , and after  $23^{\circ}00'$  degrees transmission angle, sound rays will be strongly absorbed in the sea bottom.

In May, the convergence zone propagation is available with transmission angles between +2 and +10 degrees (Figure 53). The convergence zone width in May, between +2 and +10 degrees transmission angles is 22,564 yd and horizontal range from the source to the first surface reflection is 34,361 yd for the +10 degrees ray.

The typical value of critical angle in May is  $71^{\circ}17'$  and beyond  $21^{\circ}58'$  degrees transmission angle, bottom absorption will be important.

In summer (July-August), a very unique sound propagation occurs in the central part of the Black Sea. No refracted sound propagation is seen, and all rays that leave the source at any angle are reflected from the bottom of the sea. The reason is a strong surface negative velocity gradient. So the sound level near the surface decreases rapidly in a horizontal direction away from the source. Thus resulting in shadow zone formation (Figures 55 and 56).

The critical angles for July and August have been previously calculated  $73^{\circ}15'$  and  $73^{\circ}14'$  (Table IX). Therefore,



all the rays leaving the source beyond  $17^{\circ}17'$  and  $16^{\circ}38'$  transmission angles would be strongly absorbed. Therefore, little bottom reflected energy would be available in the upper layers.

During the fall, in November, sound propagation paths are the same as in December. A well defined convergence zone occurs within 20 miles of the source, and its width is 10,148 yd with +2 to +8 degrees transmission angle.

In November, the bottom reflected sound propagation commence with transmission angle between +8 and +10 degrees. Beyond this transmission angle, all sound rays reflect from the bottom. A sound ray leaving the source at less than  $21^{\circ}03'$  transmission angle will mostly reflect. The critical angle in November is  $71^{\circ}15'$ .







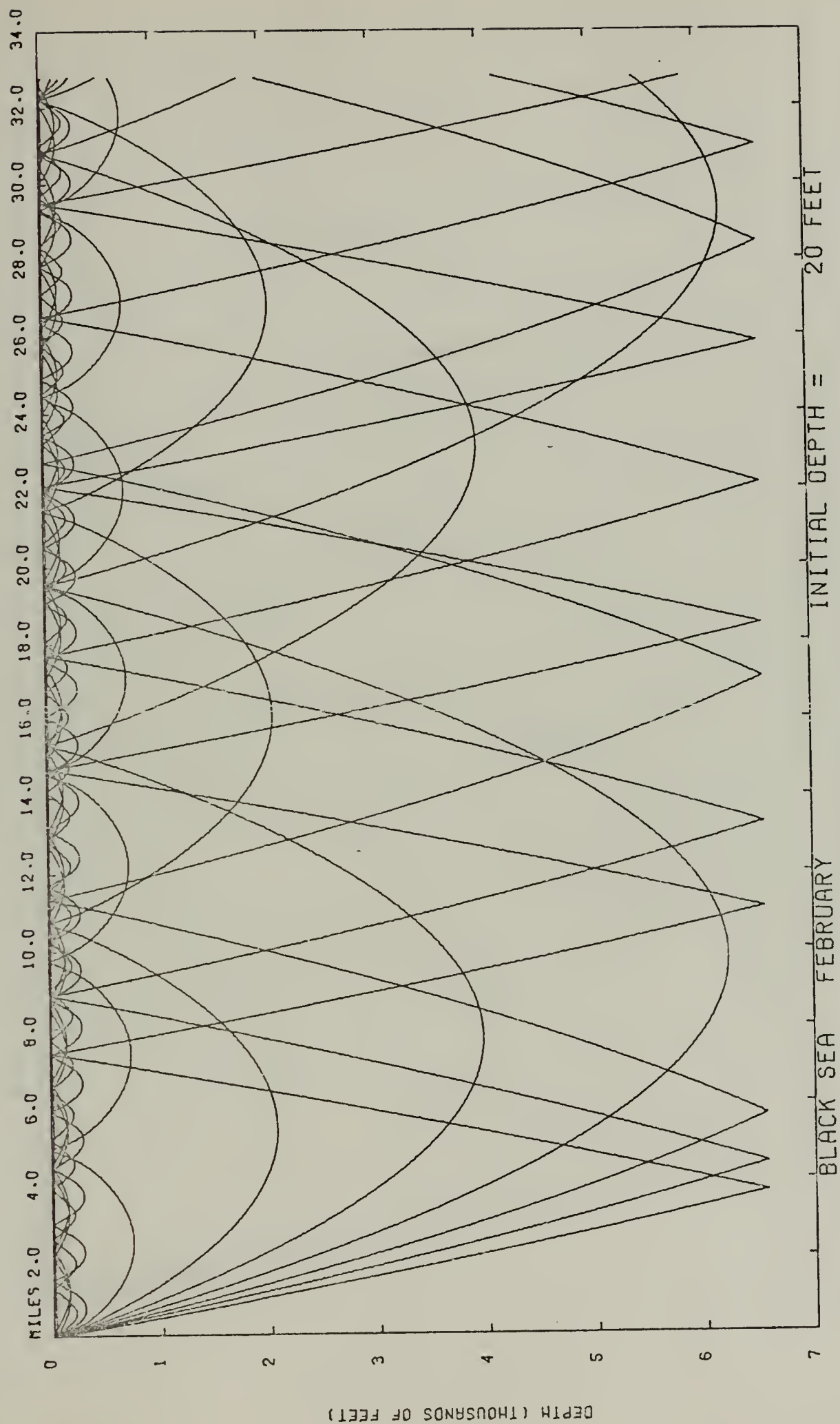


Figure 51. Ray Diagram in the Central Part of the Black Sea for February.



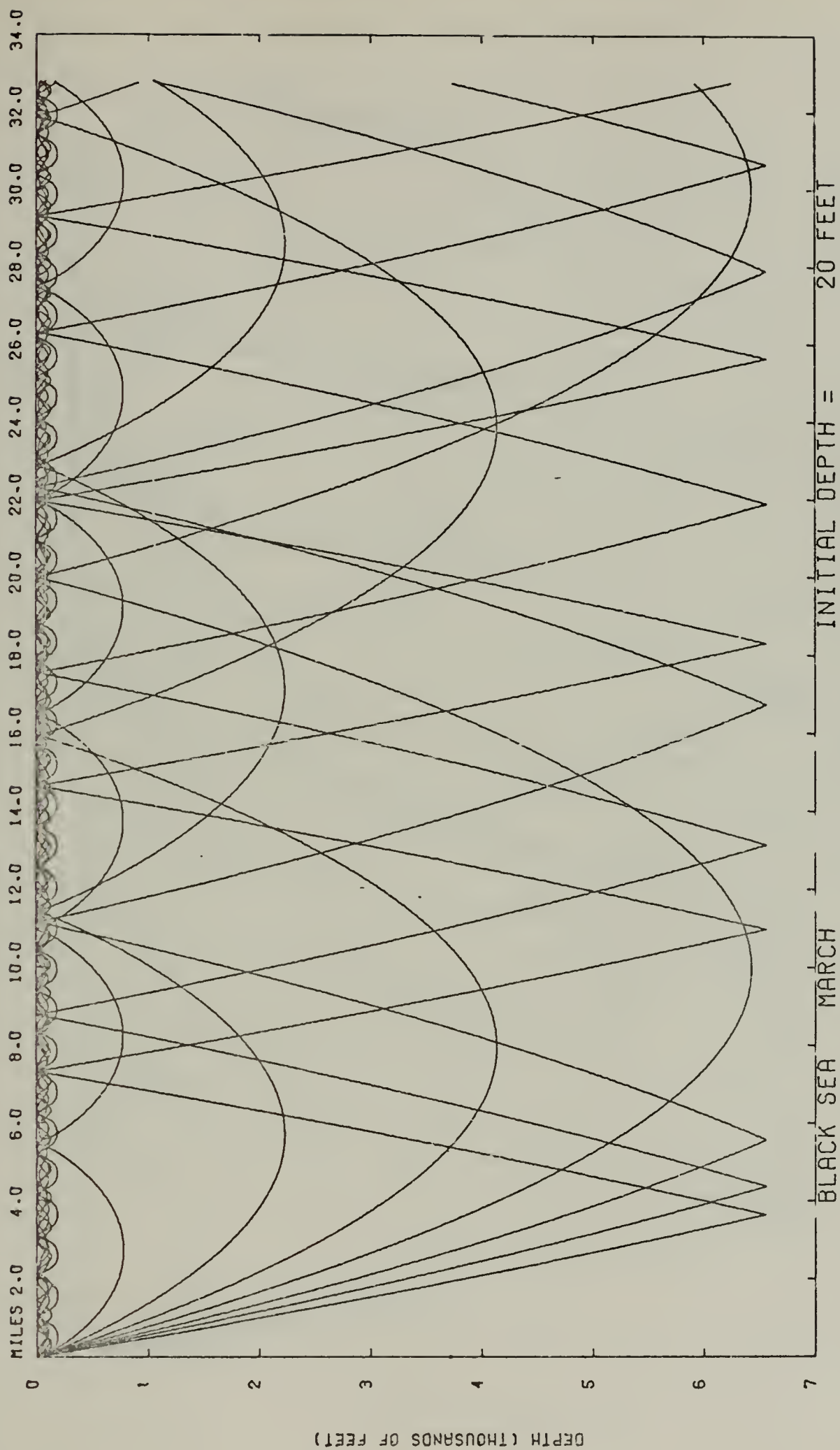


Figure 52. Ray Diagram in the Central Part of the Black Sea for March.



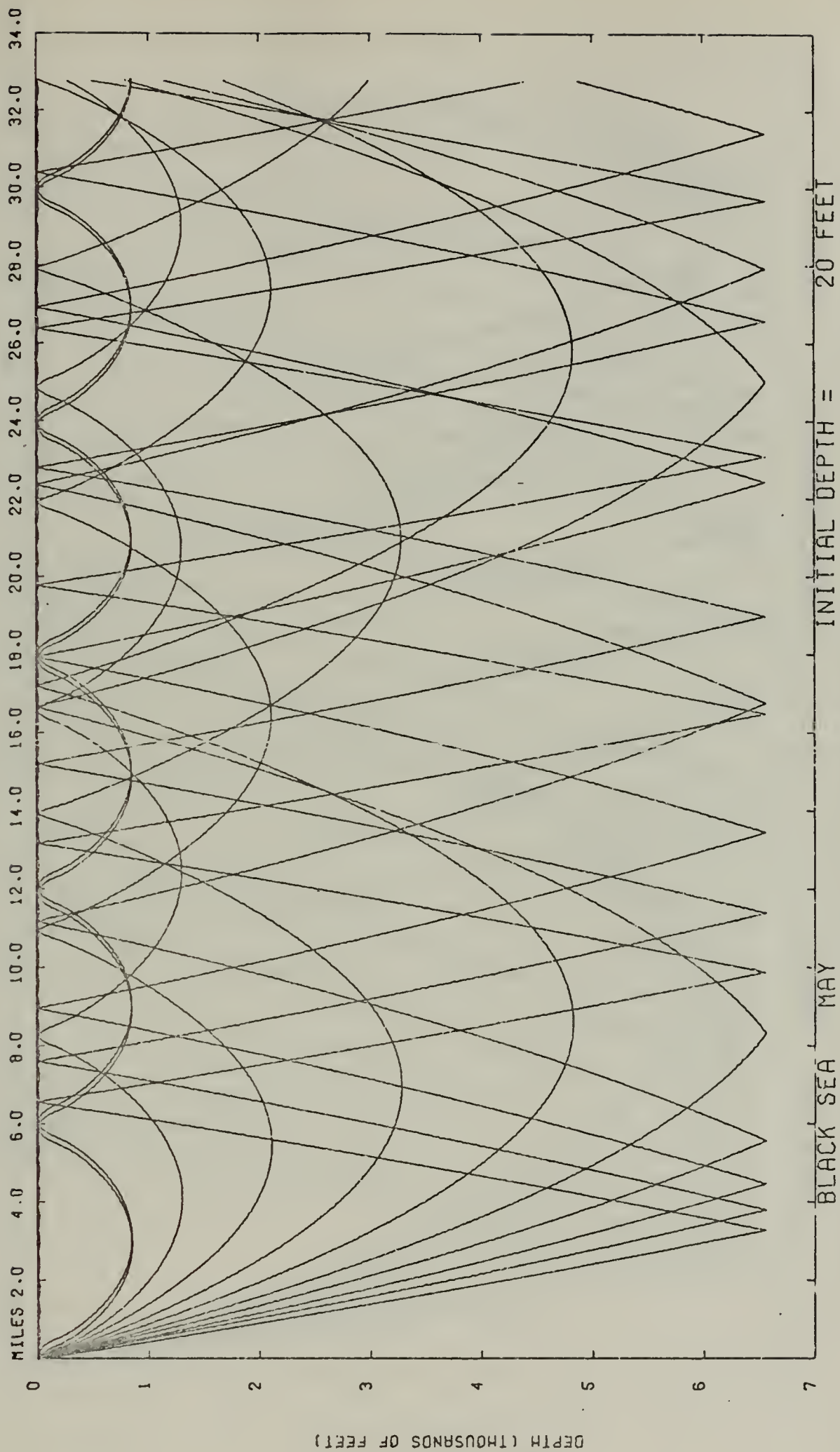


Figure 53. Ray Diagram in the Central Part of the Black Sea for May.





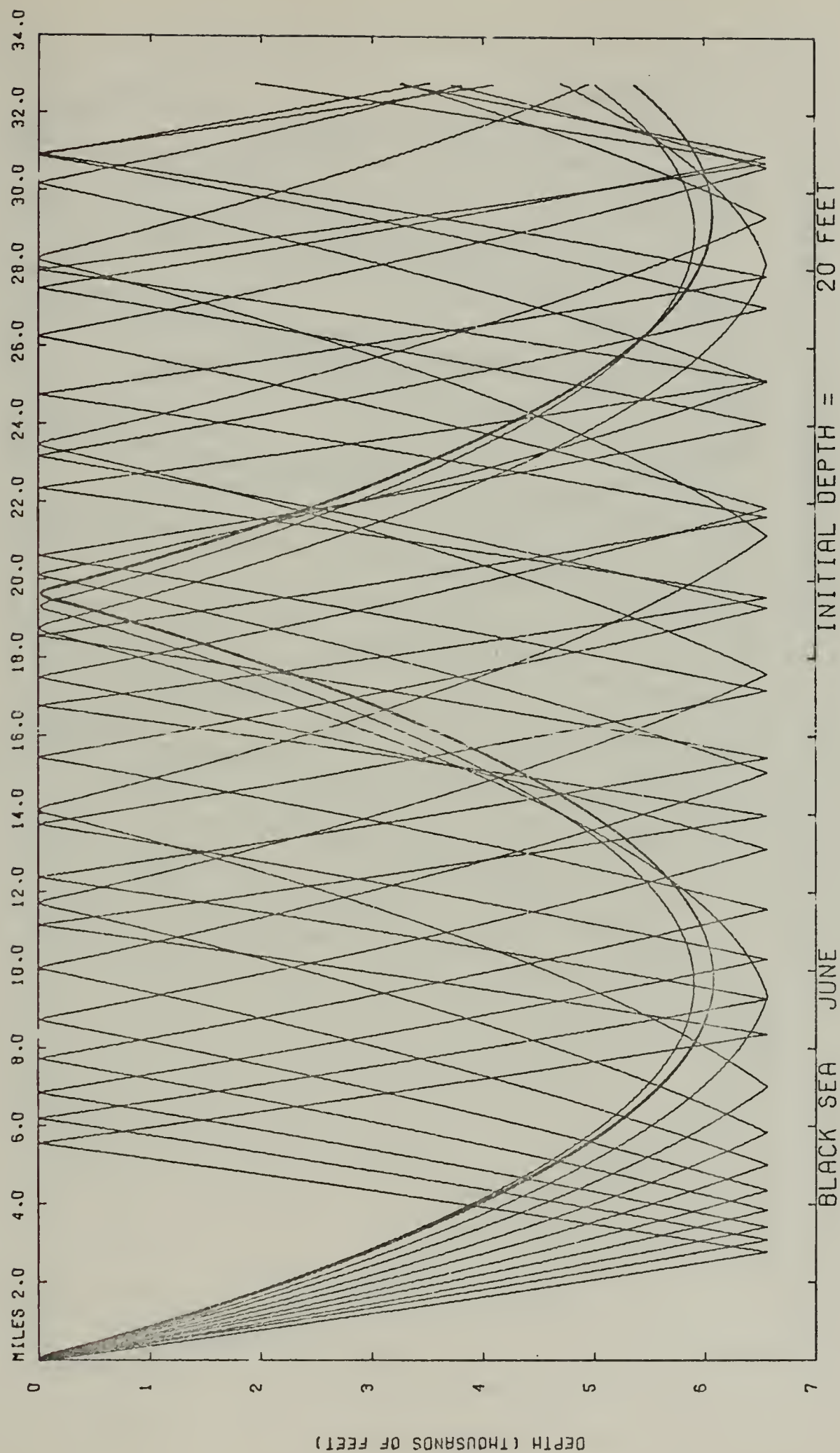


Figure 54. Ray Diagram in the Central Part of the Black Sea for June.





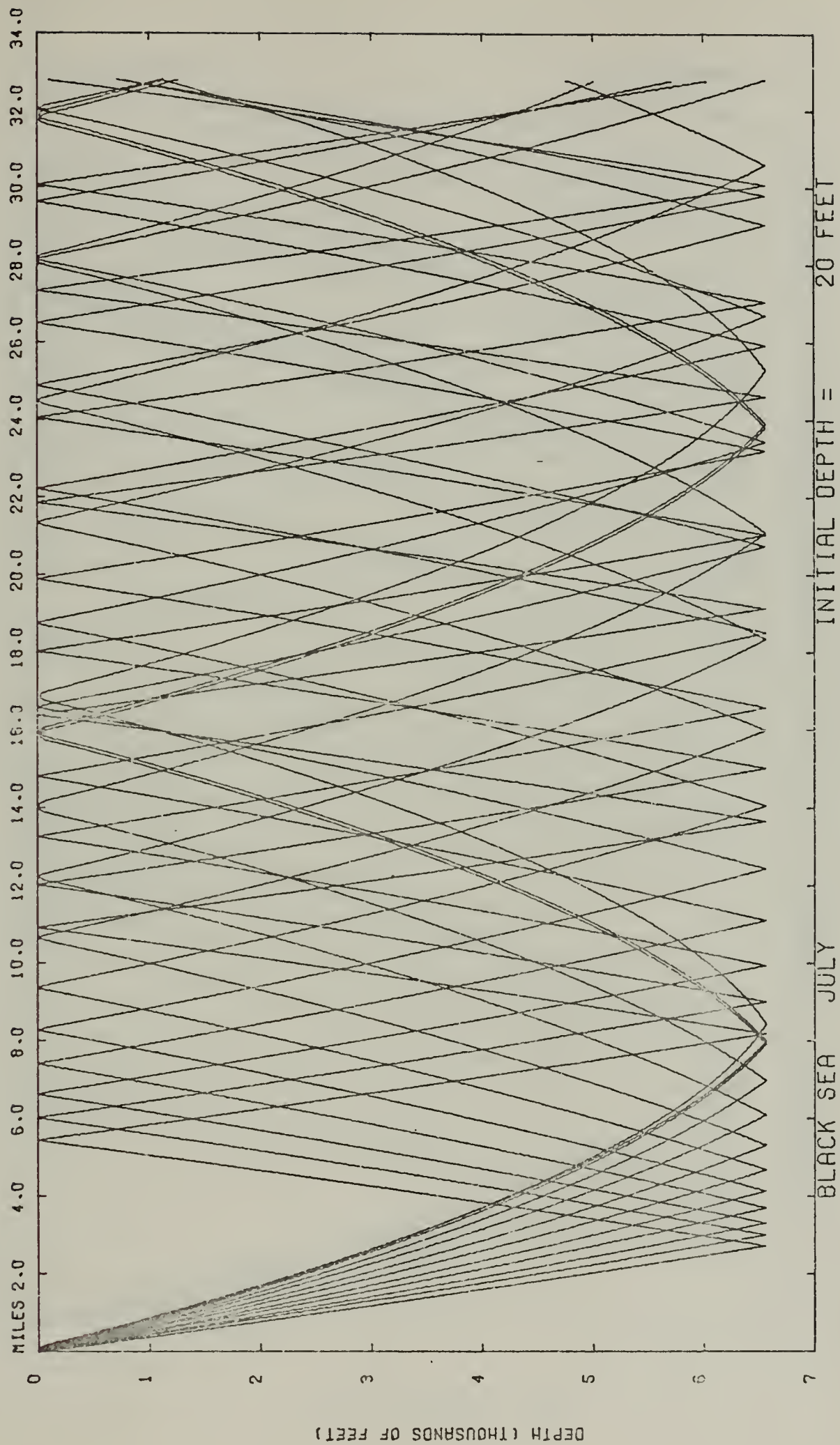


Figure 55. Ray Diagram in the Central Part of the Black Sea for July.



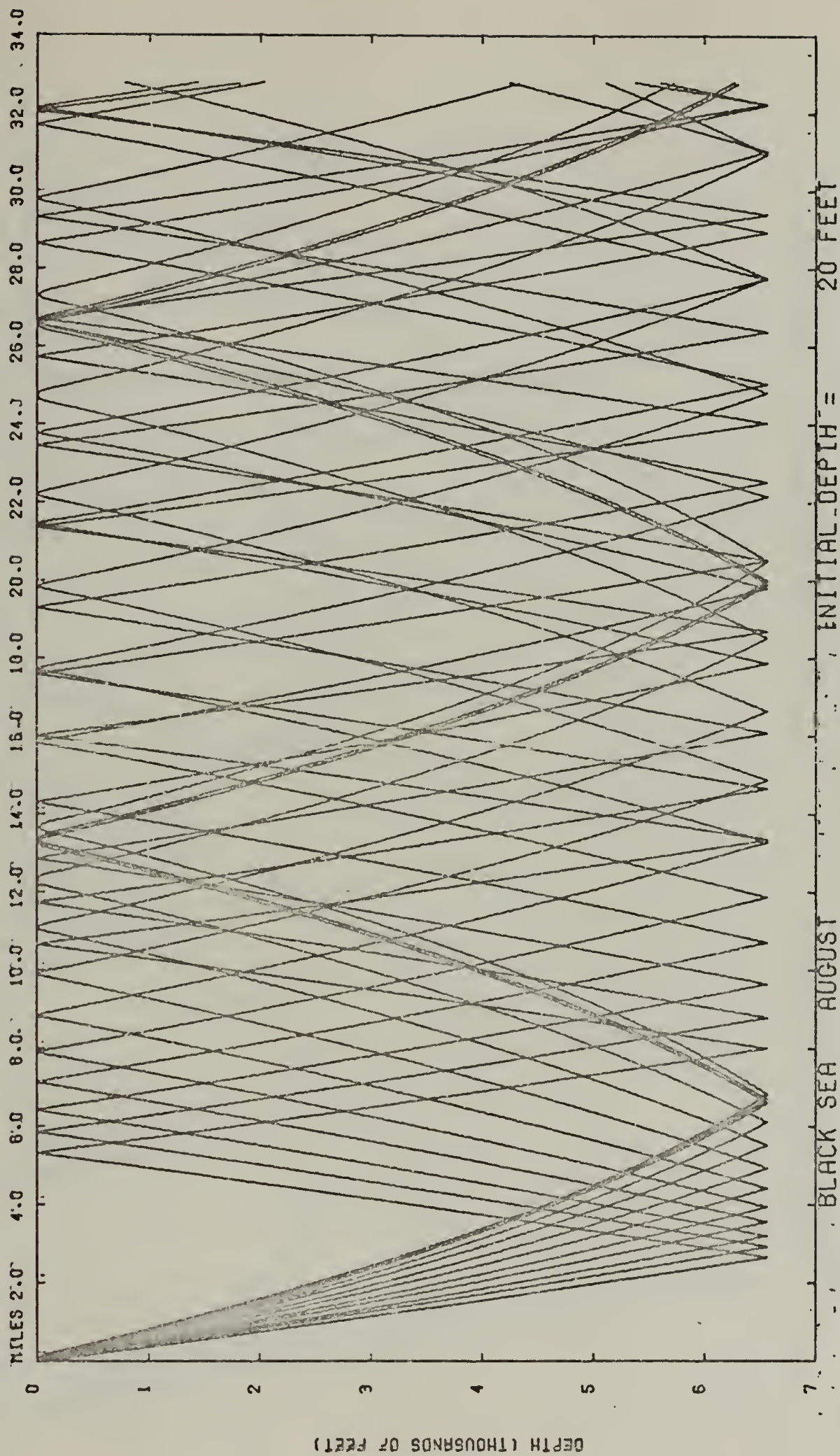


Figure 56. Ray Diagram in the Central Part of the Black Sea for August.





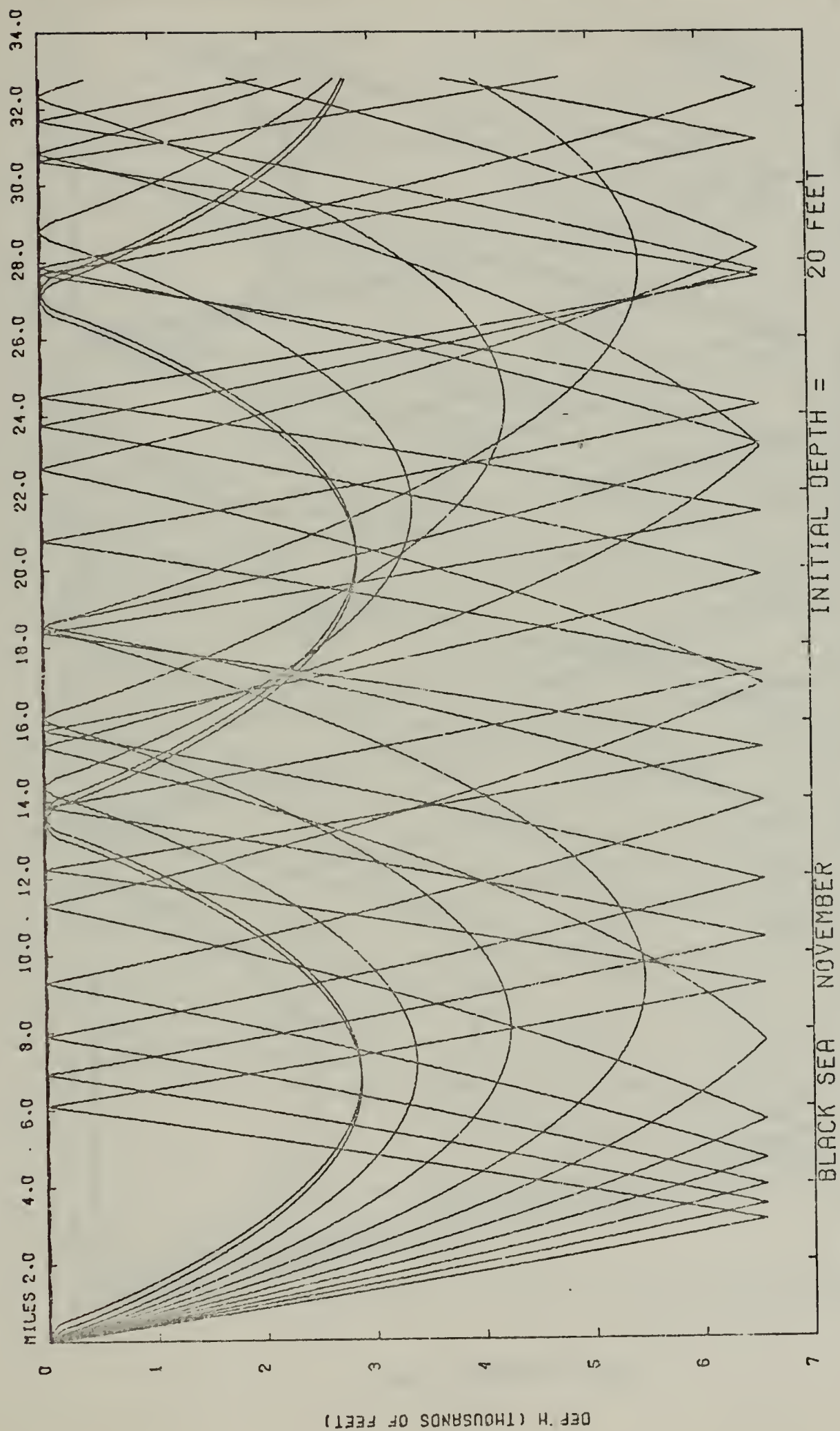


Figure 57. Ray Diagram in the Central Part of the Black Sea for November.



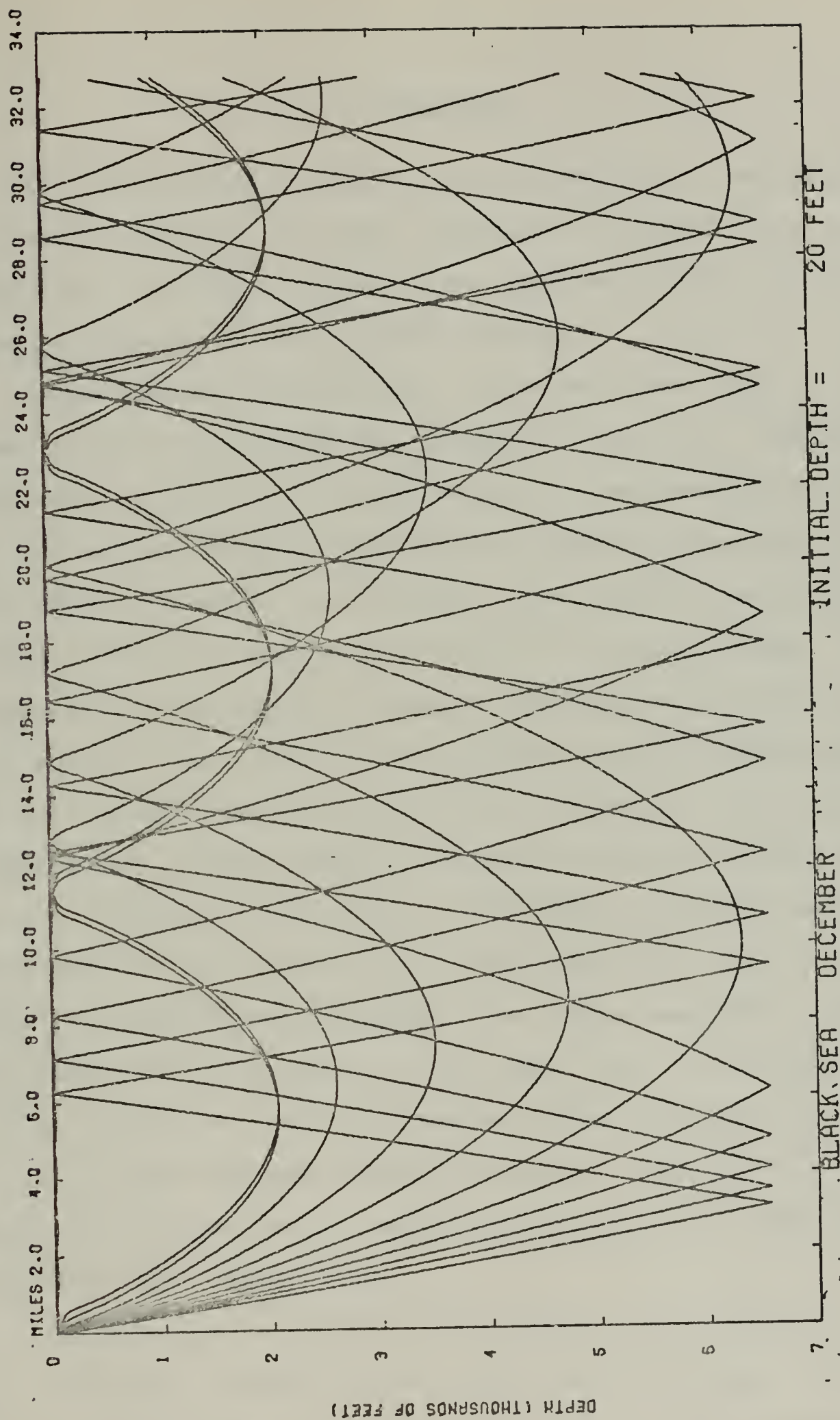


Figure 58. Ray Diagram in the Central Part of the Black Sea for December.





## VI. CONCLUSION

The propagation of sound in the Black Sea is dependent on several factors, the most important of which is the sound velocity structure. Another most important factor is the characteristics of the bottom sediments.

Large seasonal temperature variations occur only in the upper layer of the Black Sea (Figures 17 and 18). Maximum variation is seen at the surface and it decreases with depth. At the surface, maximum and minimum temperatures occur during the months of August and February. The temperature difference between these two months is  $17.07^{\circ}\text{C}$  at the sea surface. But, below 125 m, the maximum seasonal temperature variation is not greater than  $0.22^{\circ}\text{C}$ . The salinity variation with season in the central part of the Black Sea is not as important as temperature. Large seasonal salinity variations occur only in the vicinity of the coast. Therefore, the sound velocity structure in the central part of the Black Sea strictly depends upon the temperature variation. So, large amplitude sound velocity variations occur in the upper layer to a depth of 125 m. At the sea surface, maximum sound velocity variation is 56, 1 m/sec between summer and winter. Below 125 m, maximum variation is not more than 1 m/sec at the same depth for each month (Table VII).

The Black Sea exhibits a well defined sound channel at 50 - 75 meters caused by a cold intermediate layer. Therefore, a convergence zone occurs during the months of May,



November and December at which time sound velocity near the bottom exceeds that near the surface. The range of rays comprising the convergence zones during these three months were found from ray diagrams (Figures 53, 57 and 58). According to these diagrams, the maximum and minimum convergence zone widths are 22, 564 yd in May and 10,148 yd in November.

At very low frequencies, sound ceases to be trapped in the mixed layer or in any sound channel. This occurs when the frequency approaches the cutoff frequency. These cutoff frequencies in the Black Sea were computed and were presented in Table X. According to these results, high cutoff frequency is seen during the month of July when the surface duct is thin and the surface roughness is small due to low mean wind speeds. Therefore, the minimum useful sonar frequency must be higher than 5,558.92 Hz to cover all seasons.

Little is known about the bathymetry and the distribution of bottom sediments, and the physical properties of bottom sediments are not known for the Black Sea. For this reason, the bottom reflectivity and critical angles were calculated using several assumptions. These assumptions were given in Chapter IV. According to Arkhangel'skiy, the central part of the Black Sea is mostly covered with gray clay and mud. Therefore very poor bottom reflective conditions exist. From earlier calculation, the bottom critical angles range from  $69^{\circ} 40'$  to  $73^{\circ} 19'$  (Table IX). So, any sound ray striking the bottom with an angle less than critical will be partly



reflected. These reflection coefficients were given in Table IX.

Finally, monthly ray diagrams were given in Figures 51 through 58. It can be seen from these figures, that very unique sound propagation occurs in the central part of the Black Sea during the summer (July-August). The reason is a strong surface negative velocity gradient. No refracted surface reflected sound propagation is seen for the  $-2$  to  $+20^\circ$  rays and all rays that leave the source between these angles are reflected from the bottom, resulting in a large shadow zone formation in the summer (Figures 55 and 56).



## Appendix A

### COMPUTATION OF SOUND VELOCITY

The computation of sound velocity in the sea depends on the physical properties of sea water (temperature, salinity, and pressure).

In some cases, the sound velocity profile for a particular area of the sea is determined from the temperature and salinity versus depth measurement through the use of existing tables such as those of Matthews. However for this thesis, Wilson's equation is used to compute the sound velocities [19]. The component equations are shown below:

$$V = 1449.14 + V_T + V_P + V_S + V_{STP}$$

$$V_T = 4.5721T - 4.4532 \times 10^{-2}T^2 - 2.6045 \times 10^{-4}T^3 \\ + 7.9851 \times 10^{-6}T^4$$

$$V_P = 1.60272 \times 10^{-1}P + 1.0268 \times 10^{-5}P^2 \\ + 3.5216 \times 10^{-9}P^3 - 3.3603 \times 10^{-12}P^4$$

$$V_S = 1.39799 (S-35) + 1.69202 \times 10^{-3} (S-35)^2$$





$$\begin{aligned}
V_{STP} = & (S-35) (-1.1244 \times 10^{-2} T + 7.711 \times 10^{-7} T^2 + 7.7016 \times 10^{-5} P) \\
& - 1.2943 \times 10^{-7} P^2 + 3.1580 \times 10^{-8} PT + 1.5790 \times 10^{-9} PT^2) \\
& + P (-1.8607 \times 10^{-4} T + 7.4812 \times 10^{-6} T^2 + 4.5283 \times 10^{-8} T^3) \\
& + P^2 (-2.5294 \times 10^{-7} T + 1.8563 \times 10^{-9} T^2) + P^3 (-1.9646 \times 10^{-10} T)
\end{aligned}$$

Where,

$V$  = Velocity of sound in meters per second

$V_T$  = Velocity for temperature influence

$V_P$  = Velocity for pressure influence

$V_S$  = Velocity for salinity influence

$V_{STP}$  = Velocity for interaction of temperature,  
salinity and pressure influence

The entering arguments and their units and ranges are shown below:

Temperature	Degrees centigrade	$-4 < T < 30$
Salinity	Parts per mille	$0 < S < 37$
Pressure	Kilogram per square centimeter	$1 < P < 1000$

The computer program was used to compute sound velocity profiles for given station. And the profiles of sound velocity versus depth are drawn by means of a subroutine (CALL DRAW). The main program listing is shown in Appendix B.



# APPENDIX B

## COMPUTATION OF SOUND VELOCITY

```

THIS PROGRAM COMPUTES SOUND VELOCITY IN THE SEA WATER
ACCORDING TO WILSON'S EQUATION
DEPTH OF SEA WATER
TEMPERATURE OF SEA WATER
SALINITY OF SEA WATER
PRESSURE OF SEA WATER
DENSITY OF SEA WATER
SV(100), SVP(100), P(100), SVT(100), SVS(100),
STP(100), SPVL(100), SX(100), Z(100)
REAL LABEL/4H /
REAL*8 ITITL2(12)
REAL*8 ITITL2(12)
DO 50 I=1,17
READ(5,40) D(I), T(I), S(I)
FORMAT(3F10.2)
CONTINUE
WRITE(6,75)
FORMAT(11,4X, 'DEPTH', 6X, 'TEMP.', 4X, 'SAL.', 6X, 'SOVEL.', 30X,
17 '(METER)', 4X, '(DEG C)', 3X, '(ppt)', 5X, '(MPS)', 3X, '//)
DO 100 I=1,17
P(I)=(1025+2.5E-7*D(I))*D(I)+1.03
SVT(I)=VELOCITY FOR TEMPERATURE INFLUENCE
SVT(I)=4.5721*T(I)**2-2.6045E-4*T(I)**3
1+7.9851E-6*T(I)**4
SVT(I)=VELOCITY FOR PRESSURE INFLUENCE
SVT(I)=1.60272E-1*P(I)**2+3.5216E-9*P(I)**3
1-3.3603E-12*P(I)**4
SVS(I)=VELOCITY FOR SALINITY INFLUENCE
SVS(I)=1.39799*(S(I)-35.)+1.69202E-3*(S(I)-35.)**2
STP(I)=VELOCITY FOR INTERACTION OF TEMPERATURE, SALINITY
AND PRESSURE INFLUENCE
STP(I)=(S(I)-35.)*(-1.1244E-2*T(I)+7.7711E-7*T(I)**2
1+7.7015E-9*T(I)**2+3.1580E-8*P(I)*T(I)
2+1.5790E-6*T(I)**2+4.5283E-8*T(I)**3)
3+7.4812E-2*(-2.5294E-10*T(I))
4+P(I)**3*(-1.9646E-10*T(I))
5+P(I)**3*VELOCITY OF SOUND IN THE SEA WATER
SOVEL(I)=1449.14+SVT(I)+STP(I)
WRITE(6,80) I, T(I), S(I), SOVEL(I)
FORMAT(32X, F5.0, 5X, F5.2, 5X, F6.1)
CONTINUE
DO 100 I=1,17

```







## LIST OF REFERENCES

1. Caspers, H., "Black Sea and Sea of Azov," In Treatise on Marine Ecology and Paleoecology, V. 1, p. 801-802, 30 December 1957. ✓
2. Goncharov, V. P., Yemel'yanova, L. P., Mikhaylov, O. V., and Tsyplev, Yu. I., "Areas and Volumes of the Mediterranean and the Black Sea," Oceanology, V. 5, No. 6, p. 38-43, 1965.
- ① 3. Caspers, H., "Black Sea and Sea of Azov," In Treatise on Marine Ecology and Paleoecology, V. 1, p. 808, 827-829 30 December 1957.
4. Novitsky, V. P., Vertical Structure of Water and General Features of Water Circulation in the Black Sea, paper presented at U.S. Naval Oceanographic Office, Trans. 405, 1968.
5. Filippov, D. M., "The Cold Intermediate Layer in the Black Sea," Oceanology, V. 5, No. 4, p. 47-51, 1965.
6. Vladimirtsev, Yu. A., "An Investigation of Mixing Processes in the Black Sea," Okeanologiya, V. 1, No. 6, p. 976-982, 1961.
7. Neumann, G., The Black Sea on Oceanographic Summary, paper presented at U.S. Naval Oceanographic Office, Trans. 139, 1961.
8. Weyl, P. K., Oceanography on Introduction to the Marine Environment, p. 206, Wiley, 1970.
9. Liebermann, L. N., "Reflection of Sound from Coastal Sea Bottom," The Journal of the Acoustical Society of America, V. 20, No. 3, p. 305-309, May 1948.
10. Nafe, J. E., and Drake, C. L., Physical Properties of Marine Sediments, paper presented at Lamont Geological Observatory (Columbia University) Contribution No. 598, 1961.
11. Kinsler, L. E. and Frey, A. R., Fundamentals of Acoustics, 2nd Ed., p. 145, Wiley, 1962.
12. Kinsler, L. E. and Frey, A. R., Fundamentals of Acoustics, 2nd Ed., p. 144, Wiley, 1962.





13. Urlick, R. J., Principles of Underwater Sound for Engineers,  
p. 187-189, McGraw-Hill, 1967.
14. Urlick, R. J., Principles of Underwater Sound for Engineers,  
p. 216, McGraw-Hill, 1967.
15. Urlick, R. J., Principles of Underwater Sound for Engineers,  
p. 125, McGraw-Hill, 1967.
16. The Chief of Naval Operations Specification NAVAIR  
50-1C-51, Components of the 1000-Mb. Winds of the  
Northern Hemisphere, 1 September 1966.
17. Zenkovich, V. P., Morphology and Dynamics of the Soviet  
Coast of the Black Sea, paper presented at U.S. Naval  
Oceanographic Office, Trans. 141, 1962.
18. Barkovskaya, M. G., Regularities in the Distribution of  
Bottom Sediments on the Shelf of the Soviet Coast of  
the Black Sea, paper presented at U.S. Naval  
Oceanographic Office, Trans. 250, 1965.
19. Wilson, W. D., "Equation for the Speed of Sound in Sea  
Water," The Journal of the Acoustical Society of  
America, V. 32, No. 10, p. 1357, October 1960.
20. Urlick, R. J., Principles of Underwater Sound for Engineers,  
p. 195, McGraw-Hill, 1967.



# INITIAL DISTRIBUTION LIST

	No. Copies
1. Library, Code 0212 Naval Postgraduate School Monterey, California 93940	2
2. Department of Oceanography, Code 58 Naval Postgraduate School Monterey, California 93940	3
3. Dr. W. W. Denner Department of Oceanography Naval Postgraduate School Monterey, California 93940	5
4. Dr. R. S. Andrews Department of Oceanography Naval Postgraduate School Monterey, California 93940	1
5. Deniz Kuvvetleri Komutanligi Personel Egitim Sb. Mudurlugu Ankara, Turkey	1
6. Dz. Kuv. Seyir ve Hidrografi Dairesi Bsk. Cubuklu, Istanbul Turkey	2
7. Istanbul Teknik Universitesi Taskisla, Istanbul Turkey	1
8. Orta-Dogu Teknik Universitesi Ankara, Turkey	1
9. Dz. Yzb. Yavuz Ergengil Muhtesip Iskender Mah. Akseki Cad. No. 24 Fatih, Istanbul - Turkey	5
10. Defense Documentation Center Cameron Station Alexandria, Virginia 22314	2



## DOCUMENT CONTROL DATA - R &amp; D

(Security classification of title, body of abstract and indexing annotation must be entered when the overall report is classified)

1. ORIGINATING ACTIVITY (Corporate author) Naval Postgraduate School Monterey, California 93940		2a. REPORT SECURITY CLASSIFICATION Unclassified	
		2b. GROUP	
3. REPORT TITLE THE SOUND PROPAGATION CONDITIONS IN THE BLACK SEA			
4. DESCRIPTIVE NOTES (Type of report and, inclusive dates) Master's Thesis; September 1971			
5. AUTHOR(S) (First name, middle initial, last name) Yavuz Ergengil Lieutenant, Turkish Navy			
6. REPORT DATE September 1971	7a. TOTAL NO. OF PAGES 120	7b. NO. OF REFS 20	
8a. CONTRACT OR GRANT NO.		9a. ORIGINATOR'S REPORT NUMBER(S)	
b. PROJECT NO.			
c.		9b. OTHER REPORT NO(S) (Any other numbers that may be assigned this report)	
d.			
10. DISTRIBUTION STATEMENT Approved for public release; distribution unlimited.			
11. SUPPLEMENTARY NOTES		12. SPONSORING MILITARY ACTIVITY Naval Postgraduate School Monterey, California 93940	
13. ABSTRACT <p>The sound propagation conditions in the central part of the Black Sea were investigated. Profiles of temperature and salinity were generated by averaging data from the U.S. National Oceanographic Data Center over monthly periods. Wilson's equation was used to compute sound velocities and a digital computer program provided plots of sound velocity versus depth and selected ray trace diagrams.</p> <p>Seasonal temperature, salinity and sound velocity variations are found only in the upper layer of the Black Sea. Below 125 m, seasonal variations are insignificant.</p> <p>A well defined sound channel exists in the Black Sea that is caused by a cold intermediate layer. Therefore, a seasonal convergence zone is observed during the months of May, November and December.</p> <p>Finally, bottom reflectivity was calculated by Rayleigh's formula and surface backscattering strength was calculated according to Schulkin and Shaffer.</p>			





KEY WORDS	LINK A		LINK B		LINK C	
	ROLE	WT	ROLE	WT	ROLE	WT
Temperature Salinity Sound velocity Ray diagrams Black Sea sound propagation conditions						













130759

Thesis  
E5668  
c.1

Ergengil

130759

The sound propaga-  
tion conditions in the  
Black Sea.

16 JUN 72

4 AUG 73

5 SEP 73

18 OCT 74

21 JAN 77

30 JUL 81

2 AUG 88

8/10/75

BINDERY

20741

22542

22542

22754

24838

26403

80002

Thesis  
E5668  
c.1

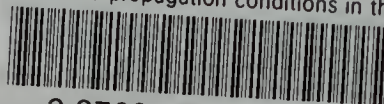
Ergengil

130759

The sound propaga-  
tion conditions in the  
Black Sea.

thesE5668

The sound propagation conditions in the



3 2768 002 06205 1

DUDLEY KNOX LIBRARY